

Multi-physics analysis of electric vehicles (EV) powertrain

-
System interactions in EV traction motor design

Dr Sara Roggia

Senior Design Engineer, Motor Design Limited

Sara.Roggia@motor-design.com

Dr Matteo Iacchetti

Senior Lecturer, The University of Manchester

matteo.iacchetti@manchester.ac.uk

Motor Design Ltd (MDL) Motor Design Limited

Motor-CAD Software

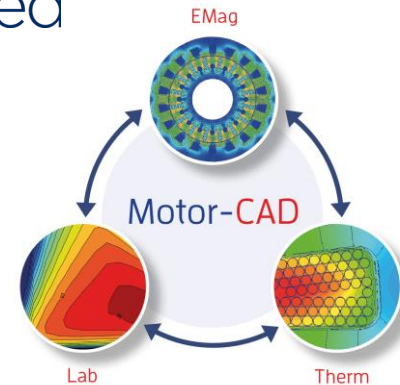
- Develop Motor-CAD software for electric motor design
- High level of customer support and engineering know-how
- Motor design software is developed by motor engineers

Consultancy

- Design, analysis & training

Research

- Involved in collaborative government/EU funded research projects:
 - **Concept_e** – Prototype Electric vehicle development with Jaguar Land Rover (JLR)
 - **HVEMS** – High Volume E-Machines Manufacturing Supply Make-Like-Production prototyping facility in the UK with JLR
 - **Tevva** – Design of SRM motors for Trucks
 - **ReFreeDrive** – Rare Earth Traction motors with improved performance and lower cost (Induction and Reluctance Motors)
 - **ELETAD** – Helicopter electric tail rotor



Motor Design Limited & The University of Manchester

➤ Collaborate with universities worldwide to develop electric machine modelling techniques and create validation data

- The University of Manchester (UK)
- The University of Warwick (UK)
- The University of Nottingham (UK)
- University of Bristol (UK)
- University of Cassino (IT)



➤ Collaboration with **The University of Manchester (UoM)**

Collaborative research to model mechanical stress in electrical machines due to high speed effects



The University of Manchester



Introduction

- Development of an electric vehicle (EV) powertrain is a complex systems problem
- Achieving an optimal system design requires evaluation of many different concepts and topologies as well as detailed understanding of the system interactions
- These interactions are typically cross specialism or discipline, involve different teams and often require multi-physics analysis
- Design and simulation tools are crucial to evaluating different design topologies as well as identifying and understanding important system interactions

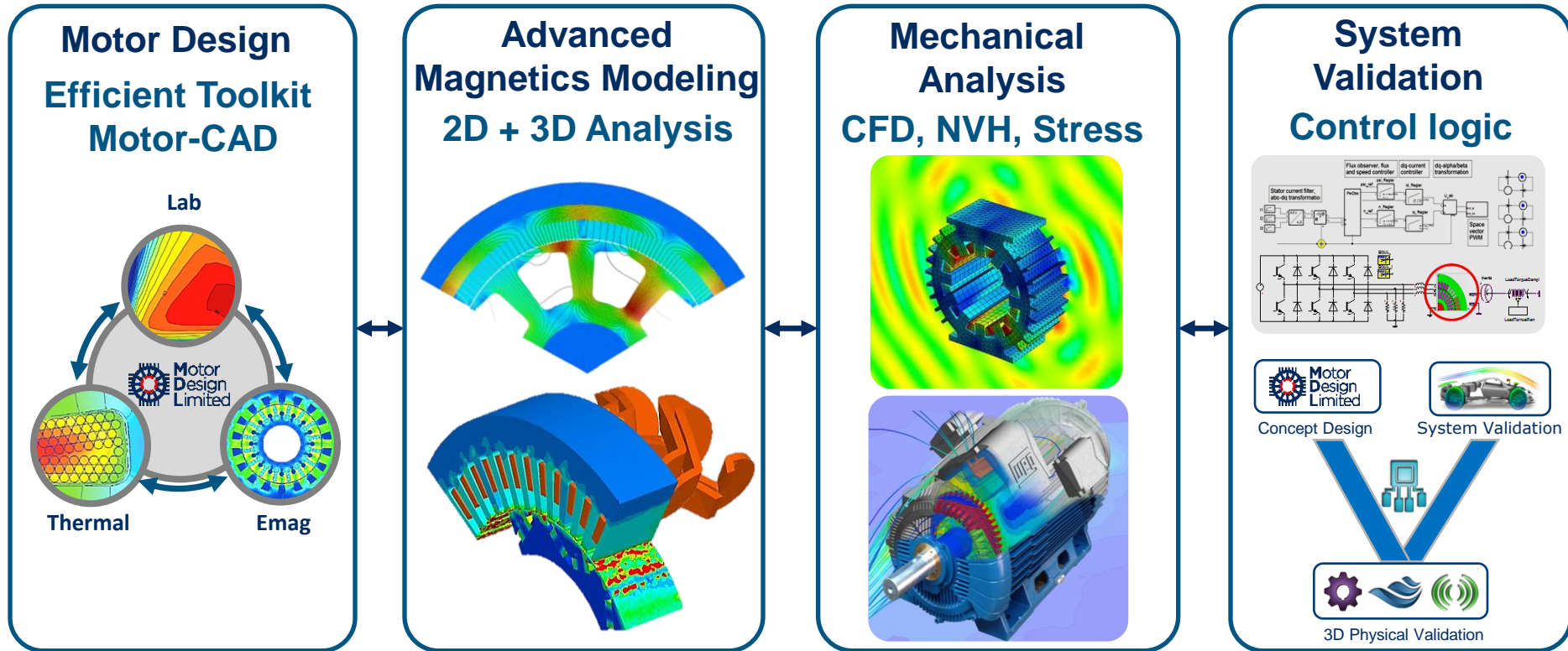


Motor
Design
Limited

MANCHESTER
1824
The University of Manchester

ICEM
International Conference on Electrical Machines

Improved System Design Workflow



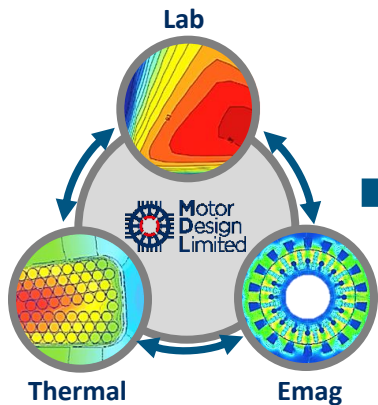
Design

Analysis

Operation

Improved System Design Workflow

Motor Design Efficient Toolkit Motor-CAD



Multi-Physics Analysis of E-Machines Over the Full Torque/Speed Operating Envelope

- Integrated software for motor performance analysis

Motor-CAD:

- **EMag:** 2D FEA electromagnetic analysis and loss calculation
- **Therm:** Network/FEA Thermal Analysis
- **Lab:** Fast prediction of efficiency maps and drive cycles

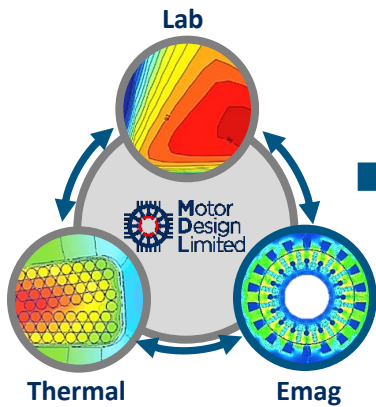
Design

Analysis

Operation

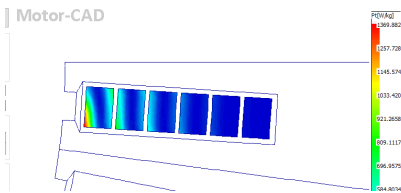
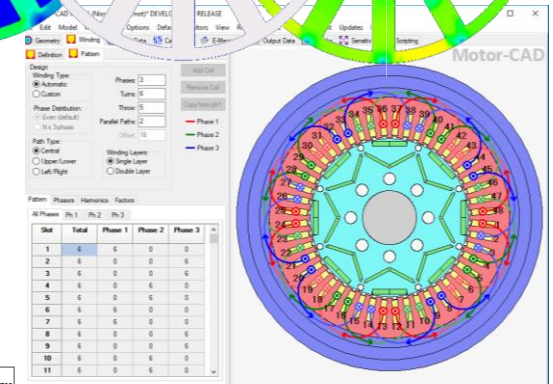
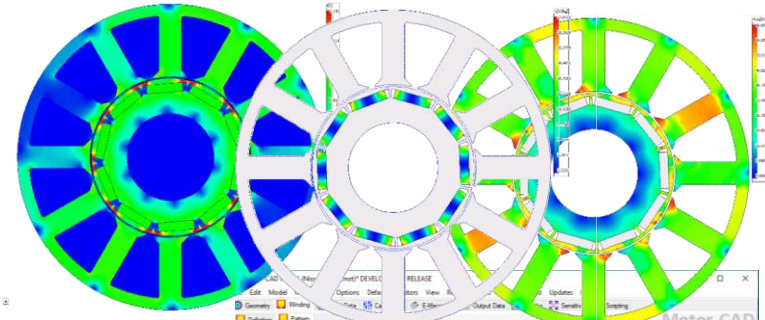
Improved System Design Workflow

Motor Design Efficient Toolkit Motor-CAD

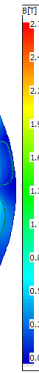
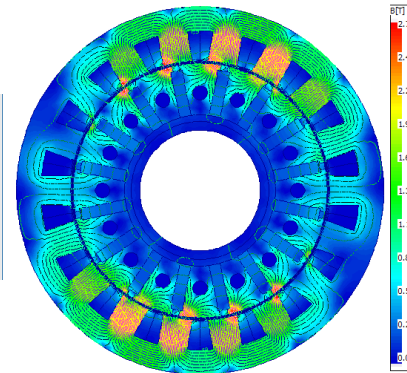


Motor-CAD EMag

- Motor Types:
 - BPM (inner & outer rotor)
 - Induction
 - Synchronous reluctance
 - Switched reluctance
 - Synchronous wound field
- Very fast and easy to set-up a design and do complex analysis
- Comprehensively validated



Winding eddy current loss



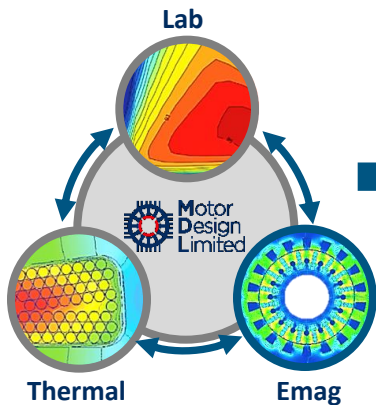
Design

Analysis

Operation

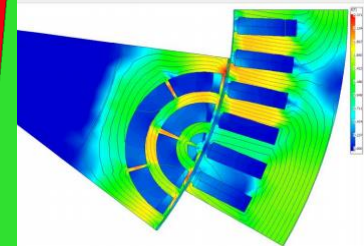
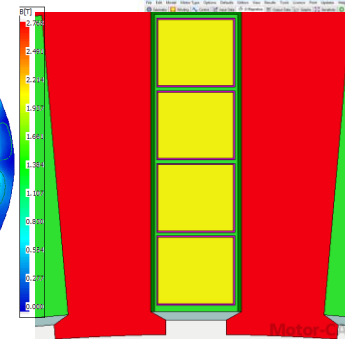
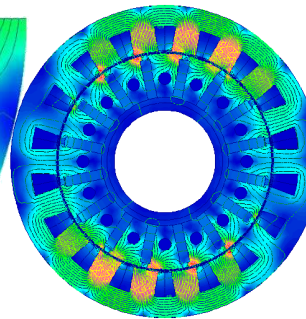
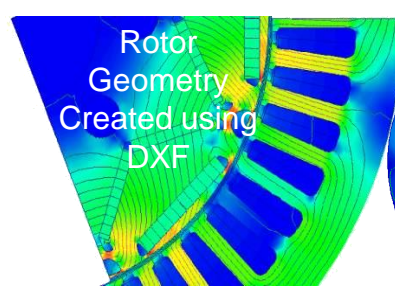
Improved System Design Workflow

Motor Design Efficient Toolkit Motor-CAD

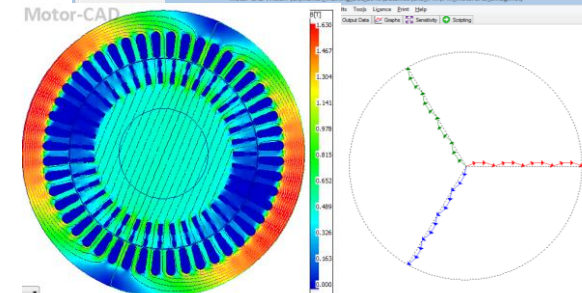
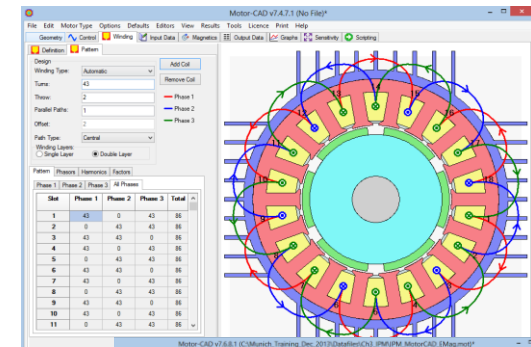


Motor-CAD EMag

- Extensive range of parametrised templates geometries with additional flexible DXF or script based geometry definition
- Fast 2D FEA transient electromagnetic solver combined with analytical models
- Analysis of losses including AC winding losses & magnet eddy currents
- Standard or custom winding designs



Rotor Geometry Created using Script



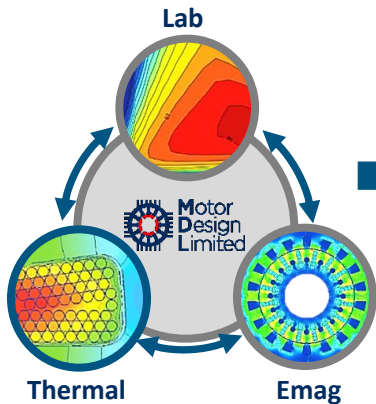
Design

Analysis

Operation

Improved System Design Workflow

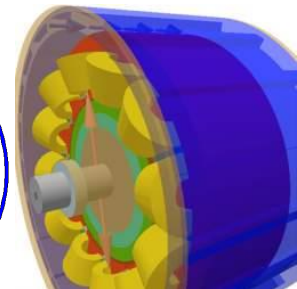
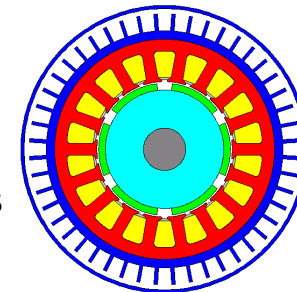
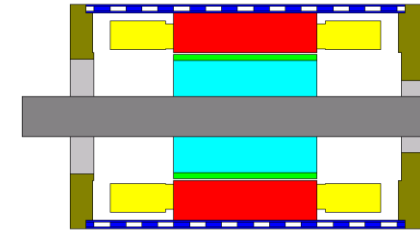
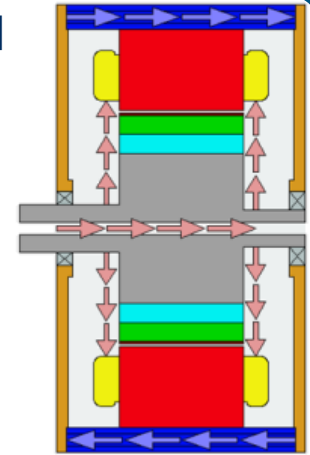
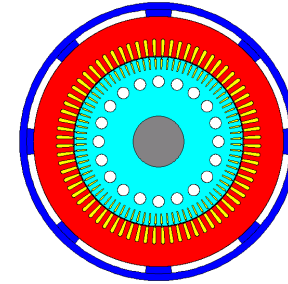
Motor Design Efficient Toolkit Motor-CAD



Motor-CAD Therm: Cooling Types Investigated

Motor-CAD includes models for an extensive range of cooling types:

- TENV: Totally enclosed non-ventilated (Natural convection from housing)
- TEFC: Totally enclosed fan cooled (Forced convection from housing)
- Through ventilation
- TE with internal circulating air (Internal air circulating path, water jacket as heat exchanger)
- Open end-shield cooling
- Water jackets (Axial or circumferential)
- Submersible cooling
- Wet rotor & wet stator cooling
- Spray cooling (e.g. Oil spray cooling of end windings)
- Direct conductor cooling (e.g. Slot ducts with oil)



Design

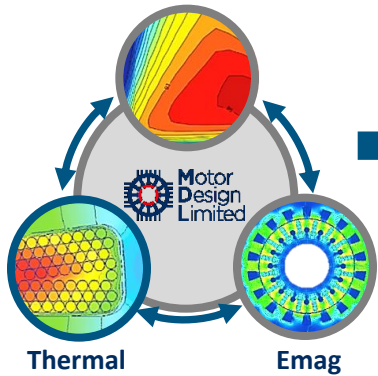
Analysis

Operation

Improved System Design Workflow

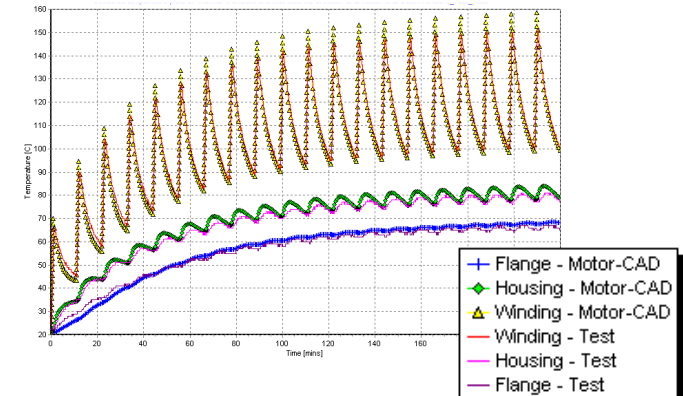
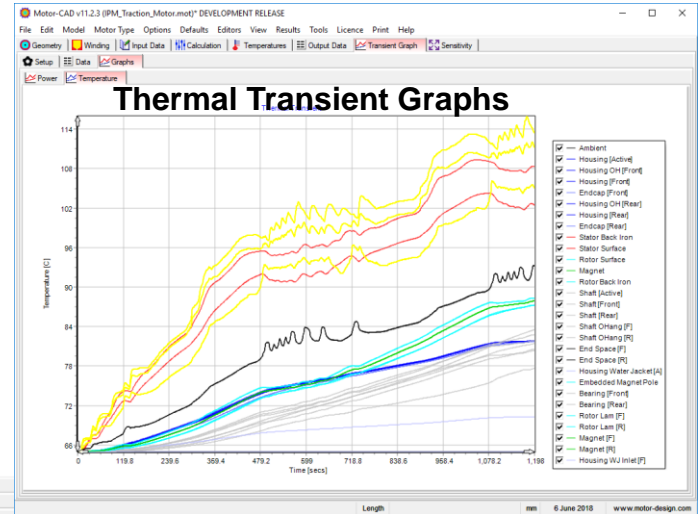
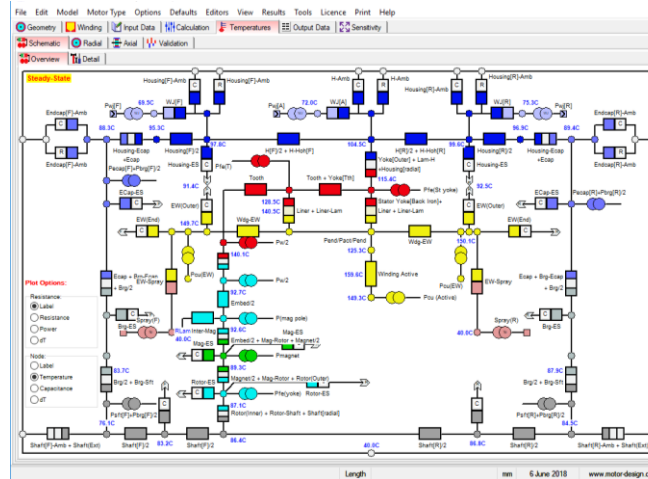
Motor Design Efficient Toolkit Motor-CAD

Lab



Motor-CAD Therm: Steady-State & Transient Thermal Analysis

- Calculation of steady-state or transient thermal performance
- Temperature rises over a complex duty cycle can be solved rapidly and analysed iteratively during the design process



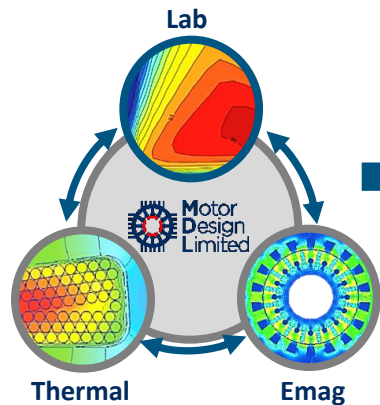
Design

Analysis

Operation

Improved System Design Workflow

Motor Design Efficient Toolkit Motor-CAD

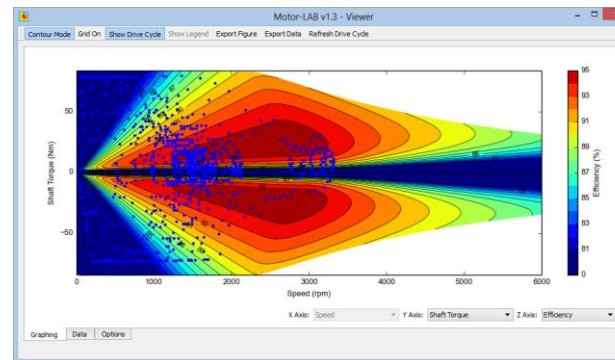


Motor-CAD Lab: Virtual Testing Laboratory

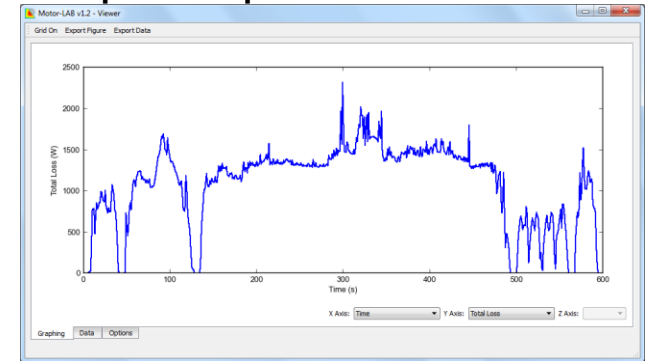
Virtual testing including fast calculation of Efficiency Maps/Losses and Duty Cycle Analysis

- Very fast and accurate prediction of the motor electromagnetic and thermal performance over the full torque/speed envelope by use of intelligent loss algorithms
- Automated calculation of optimum phase advance angle for maximum torque/amp or maximum efficiency control
- Suited to applications such as traction applications that have complex duty cycle loads

Efficiency map with drive cycle overlaid



Loss vs Time calculated from efficiency map to be input into thermal model



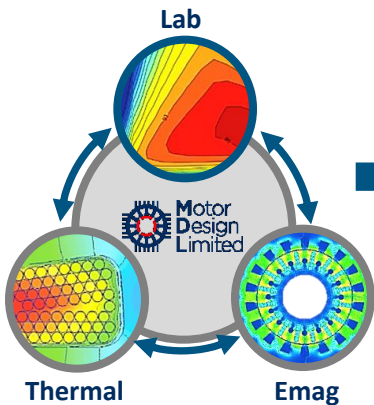
Design

Analysis

Operation

Improved System Design Workflow

Motor Design Efficient Toolkit Motor-CAD



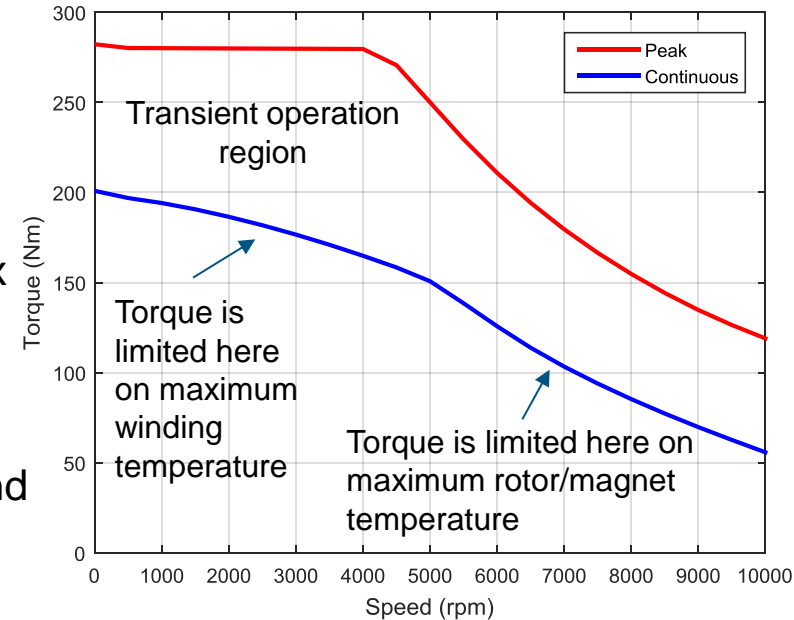
Motor-CAD Lab: Electromagnetic and Thermal Limited Envelope

Peak torque envelope

- Maximum torque/amp or maximum efficiency control

Continuous torque envelope

- Co-simulations between electromagnetic model (via flux linkage and loss maps) with thermal model
- Maximum torque at different speeds for a limited winding and rotor temperature
- Thermal transient for a set amount of time that gives a certain maximum winding temperature



This is output matches how electric motors are typically specified. It is very useful to compare these curves for different design variations.

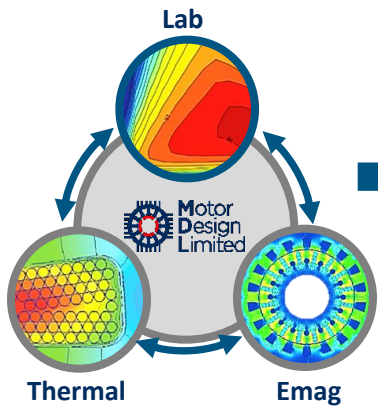
Design

Analysis

Operation

Improved System Design Workflow

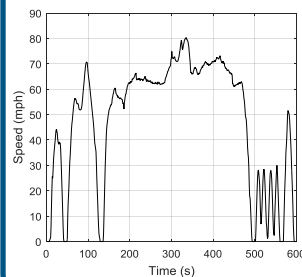
Motor Design Efficient Toolkit Motor-CAD



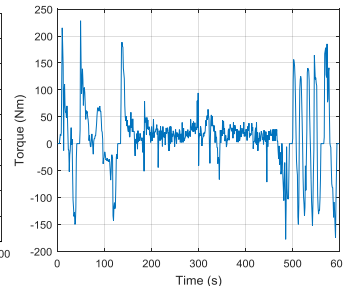
Motor-CAD Lab: Dynamic Operations

- The operation of these machines is very dynamic and considerations of performance across the full torque/speed operating envelope are required
- Modelling tools need to support this, Motor-CAD is a unique solution on the market for this type of analysis
- It allows machine efficiency to be optimised over standard operating cycles and sized for a worst-case cycle, giving minimum system size and cost

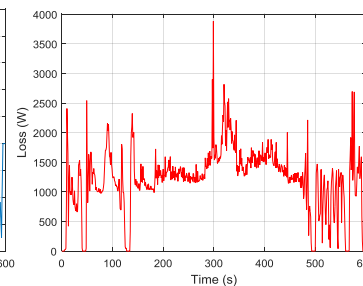
Vehicle Speed
Profile



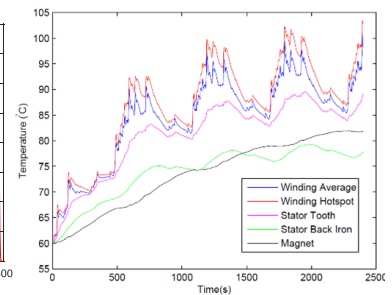
Motor/Generator:
Time vs Torque vs
Speed



Motor/Generator:
Loss vs Time



Motor/Generator:
Temperature Vs
Time



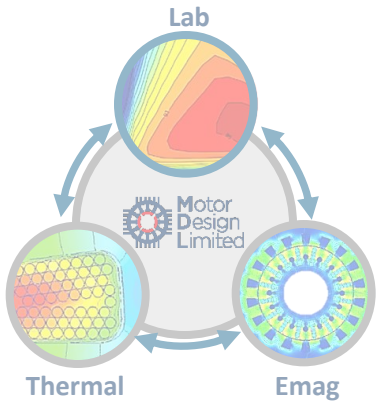
Design

Analysis

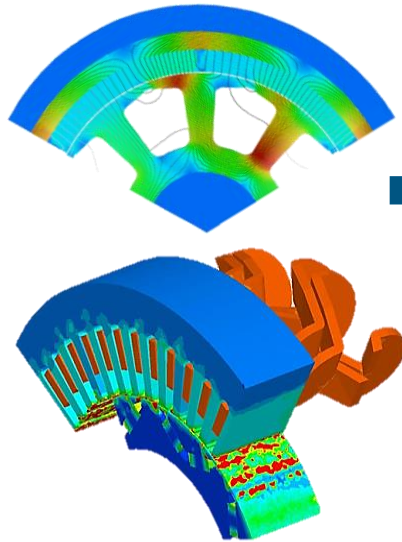
Operation

Improved System Design Workflow

Motor Design
Efficient Toolkit
Motor-CAD



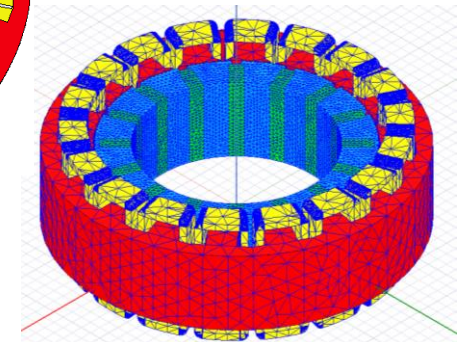
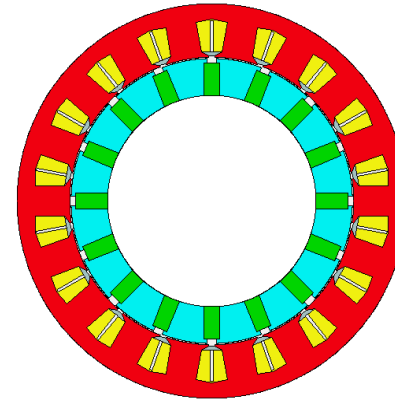
Advanced
Magnetics Modeling
2D + 3D Analysis



Export Model for 3D Simulations

Partnership with Ansys provides coupling to high power numerical simulation

- 3D FEA for analysis of end-effects with Ansys Maxwell



3D leakage effects can be important and could worsen motor performance

Design

Analysis

Operation

Improved System Design Workflow

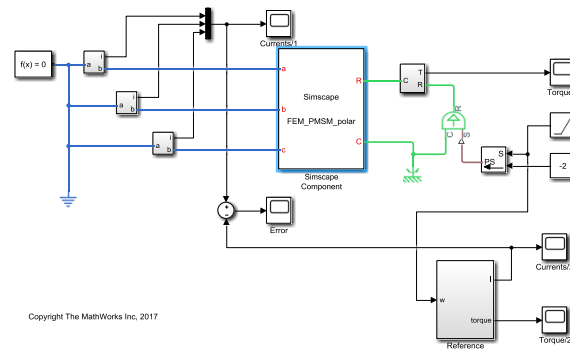
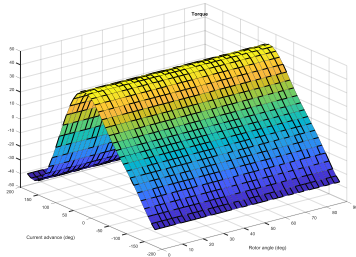
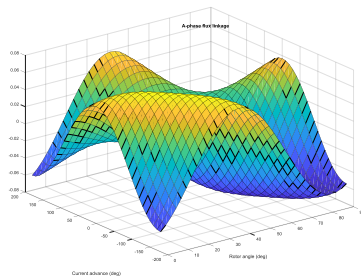
System Simulations

Vehicle thermal system behaviour

- Co-simulation with GT-Suite

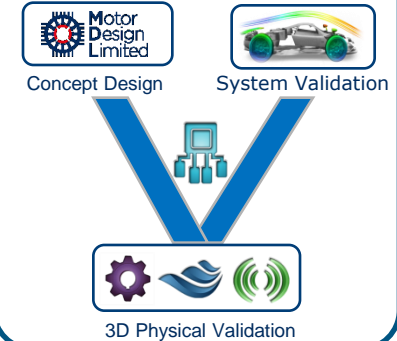
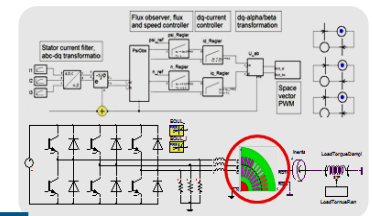
Combined inverter and motor behaviour

- Model export to Simulink Simscape mapping of motor attributes that take in account non-linear motor behaviour



Motor Model Implementation in Simulink Environment

System Validation Control logic



Design

Analysis

Operation

Improved System Design Workflow

Coupled e-machine and inverter modelling

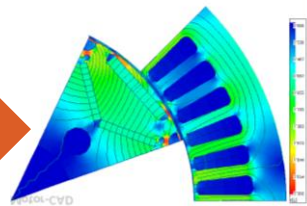
Motor behaviour considering

- Time harmonics in current waveform
- L_d , L_q , λ_m model with saturation and positional variation

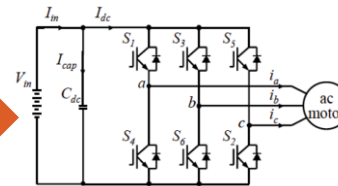
I_d , I_q
input
demand



Input current
waveform – initially
ideal

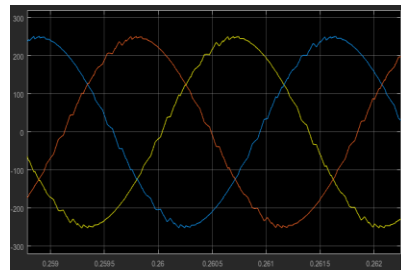


Calculate
 $L_d(\theta)$, $L_q(\theta)$, $\lambda_m(\theta)$



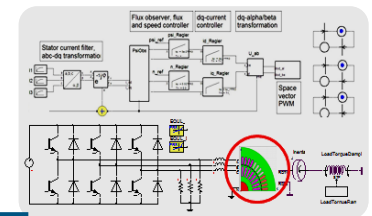
Simulate inverter circuit
including DC link and
control loops using
calculated motor
inductances

Convergence loop



Feed updated current waveforms back into FEA simulation

System Validation Control logic



Concept Design



System Validation



3D Physical Validation

Design

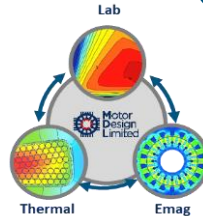
Analysis

Operation

Tutorial Overview

Motor Design

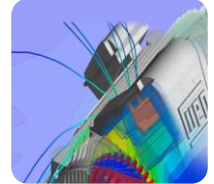
Trade-off Analysis for a BEV traction application



1. eMachine Comparison - PM, IM, Sync
2. Windings Comparison - Hairpin vs Stranded
3. Cooling Comparison - Water Jacket, Internal Air and Oil Spray

Mechanical Analysis

NVH and Mechanical Stress



4. NVH Analysis - Behaviour of Motor + Gearbox
5. Mechanical Stress Analyses (Problem formulation and Solution)

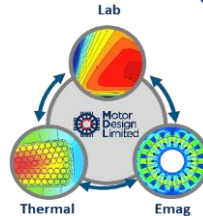
Design

Analysis

Tutorial Overview

Motor Design

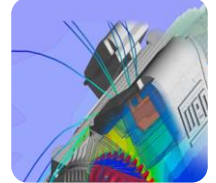
Trade-off Analysis for a BEV traction application



1. eMachine Comparison - PM, IM, Sync
2. Windings Comparison - Hairpin vs Stranded
3. Cooling Comparison - Water Jacket, Internal Air and Oil Spray

Mechanical Analysis

NVH and Mechanical Stress



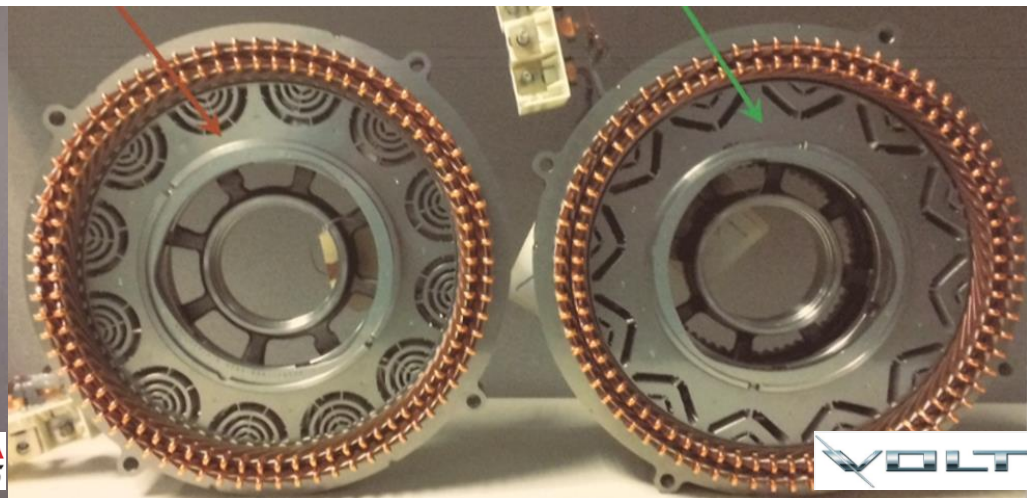
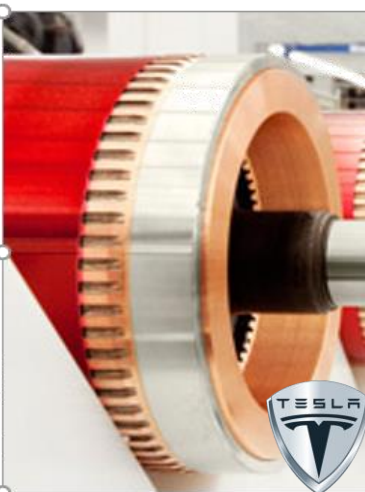
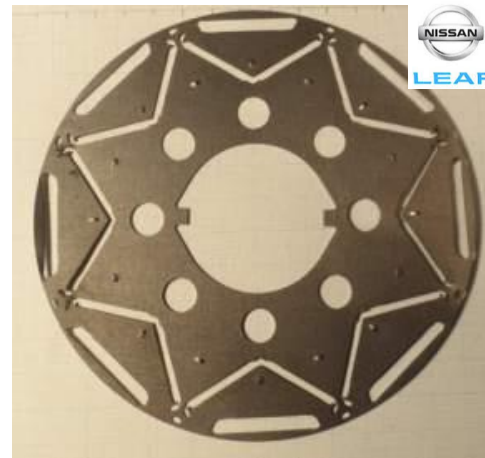
4. NVH Analysis - Behaviour of Motor + Gearbox
5. Mechanical Stress Analyses (Problem formulation and Solution)

Design

Analysis

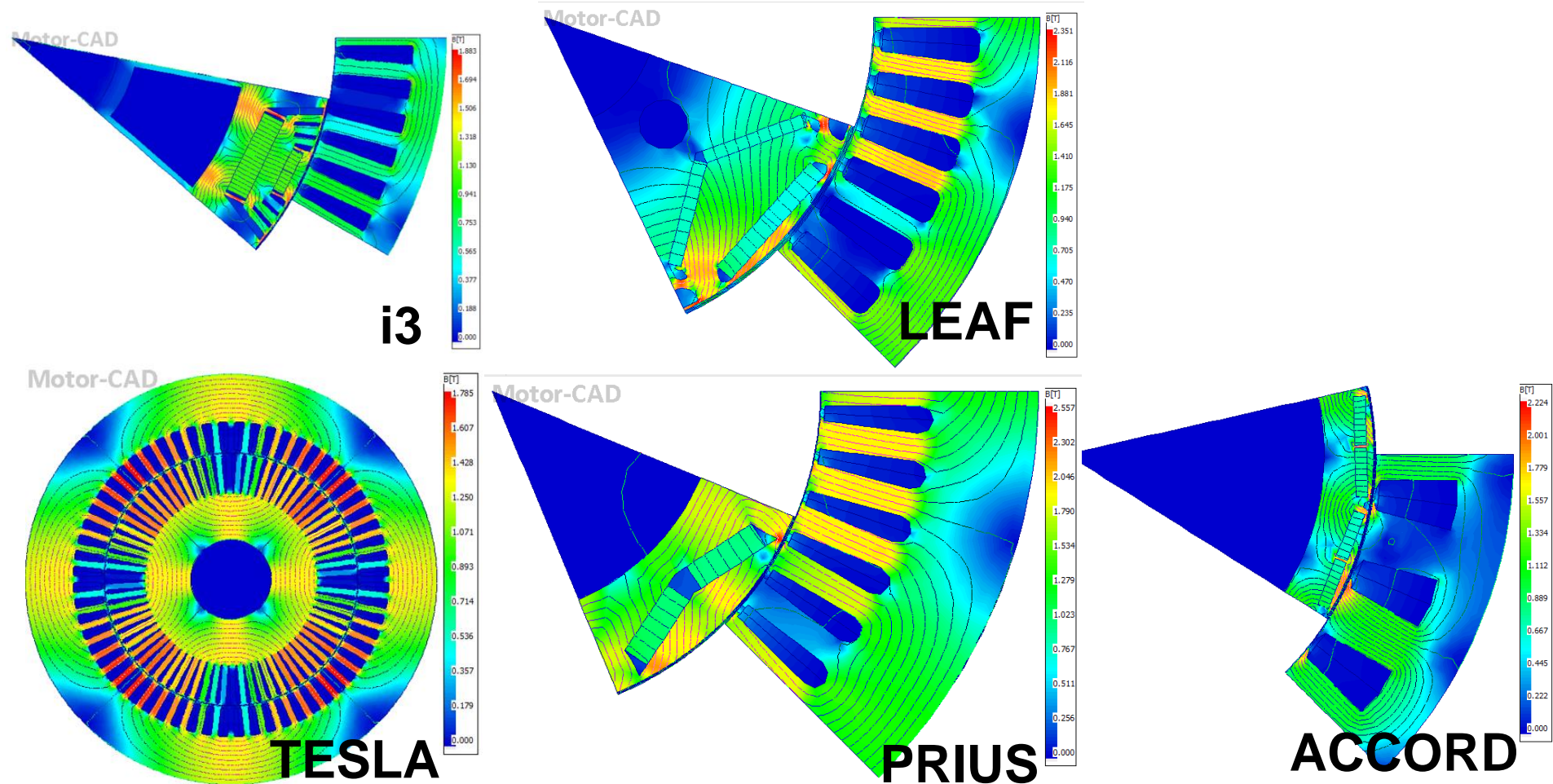
1. eMachine Comparison

Many motor types and topologies have been developed recently, as seen by the wide range of EV traction motor designs on the market



1. eMachine Comparison

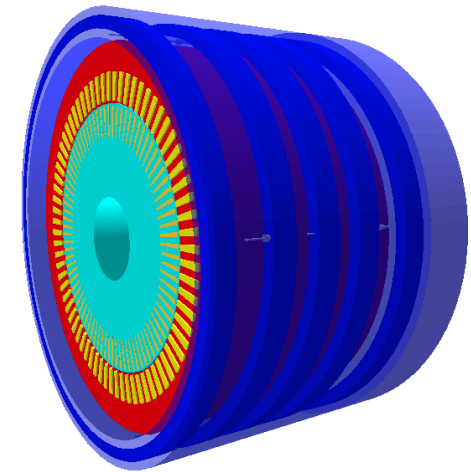
- Using published teardown data for Nissan LEAF motor
- Developed models to validate & demonstrate software tools for modelling traction applications



1. eMachine Comparison

Comparison of PM, IM and Sync traction machine types

- Same outer diameter
- Same peak performance requirements
- Different axial lengths
- Same water jacket cooling



Specifications

Peak Torque	350 Nm
Peak Power	150 kW
DC Link Voltage	400 Vdc
Max Current	500 Arms
Stator Outer Diameter	250 mm
Maximum speed	12,000 rpm

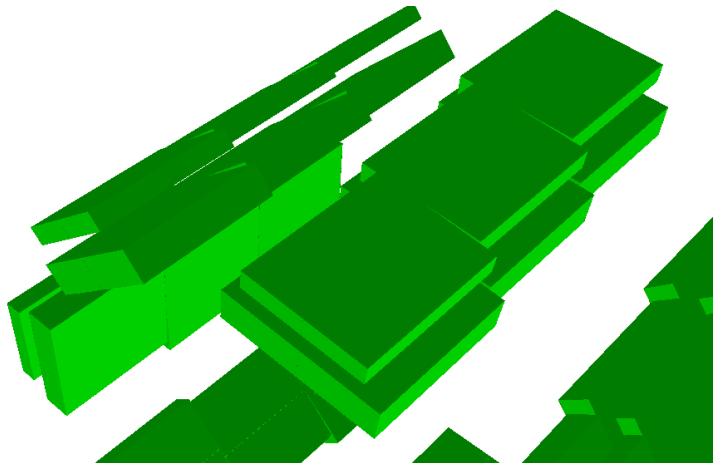
Cooling System

Inlet Temperature	65 degC
Coolant Flow Rate	6.5 l/min
Coolant	EGW 50/50

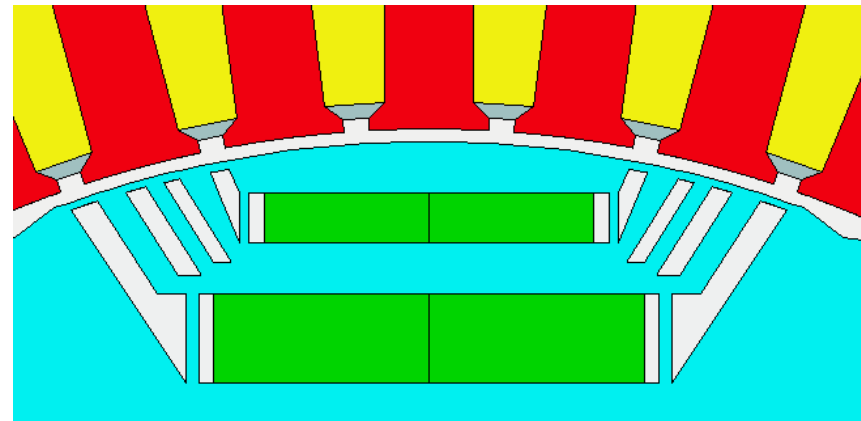
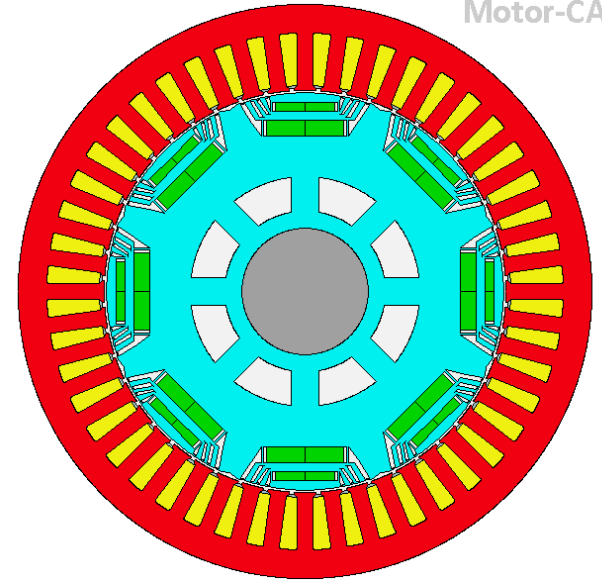
Cooling channels over active machine section only

Brushless PM machine

- 48 slot 8 pole IPM
- Double layer magnet – similar to BMW i3
- N42UH magnet
- M250-35A steel
- 250mm OD
- Multi-stranded stator windings
- Step skewed rotor on the market



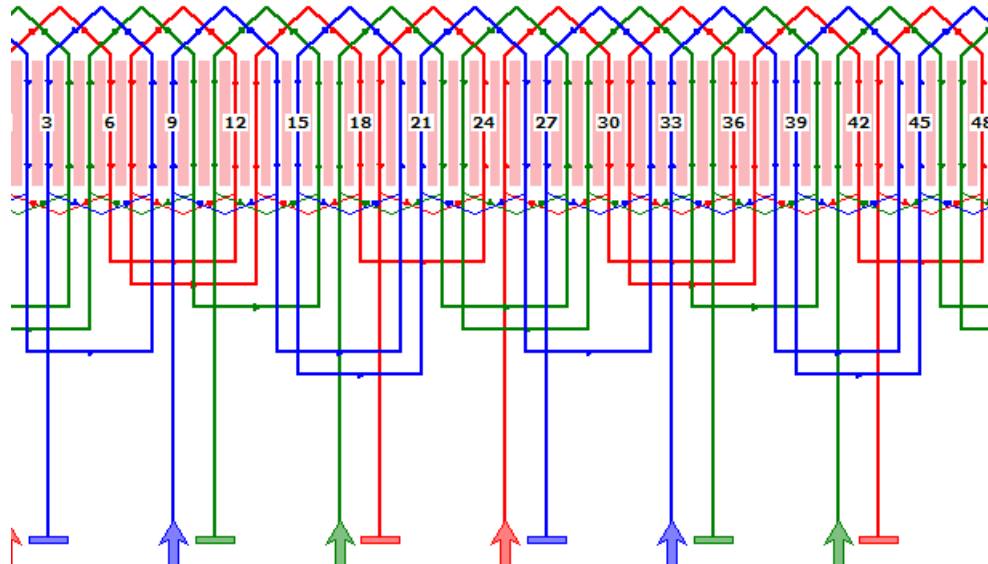
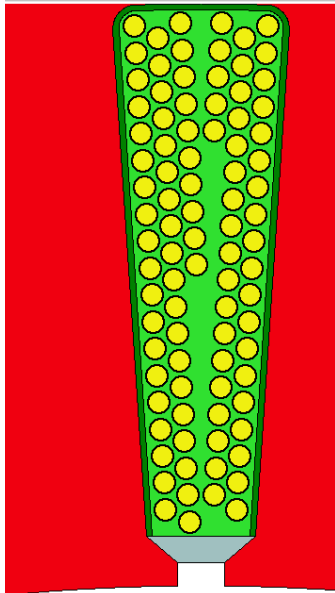
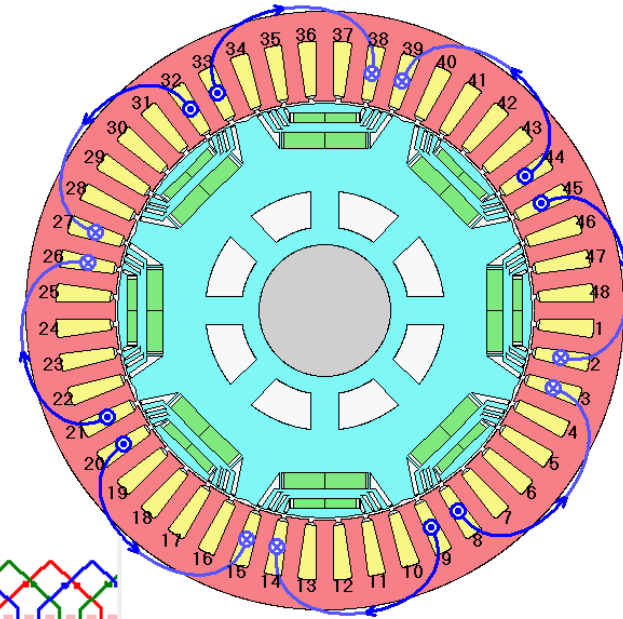
Motor-CAD



1. eMachine Comparison

Brushless PM machine

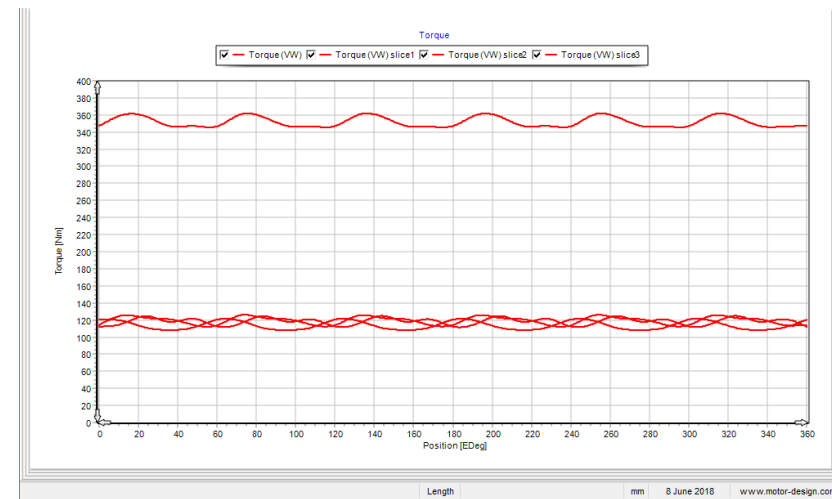
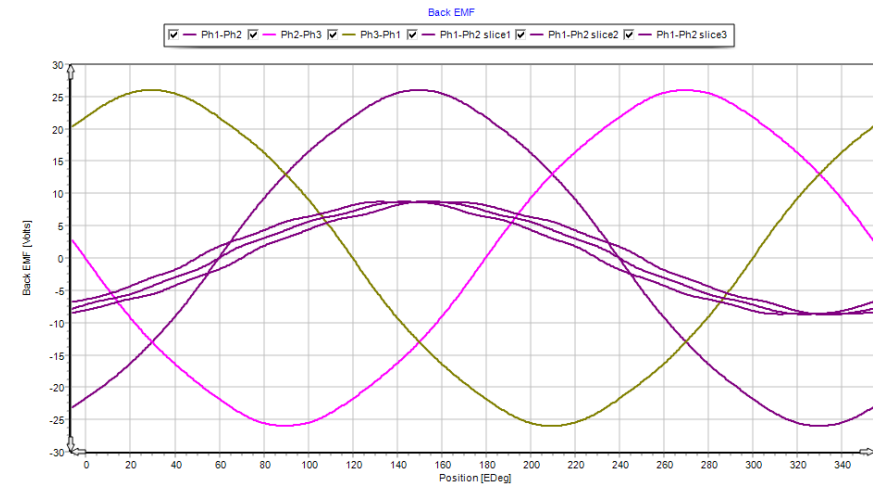
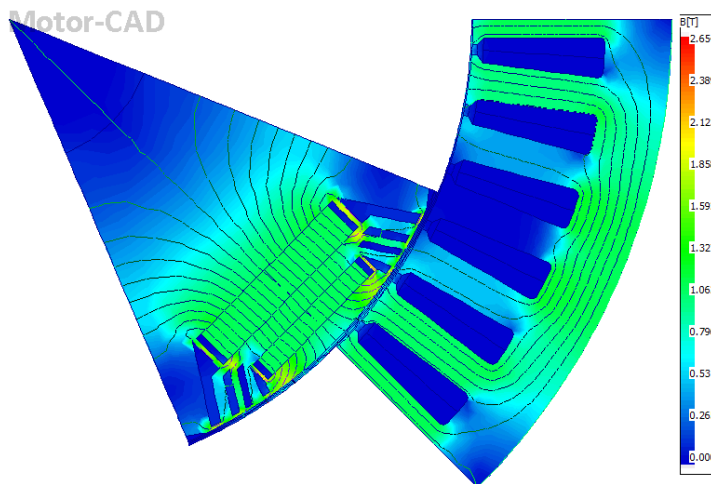
- Single layer winding
- Coil pitch - 5 slots
- 6 turns per coil, with 15 strands per turn
- 40% copper slot fill
- 2 parallel paths per phase



1. eMachine Comparison

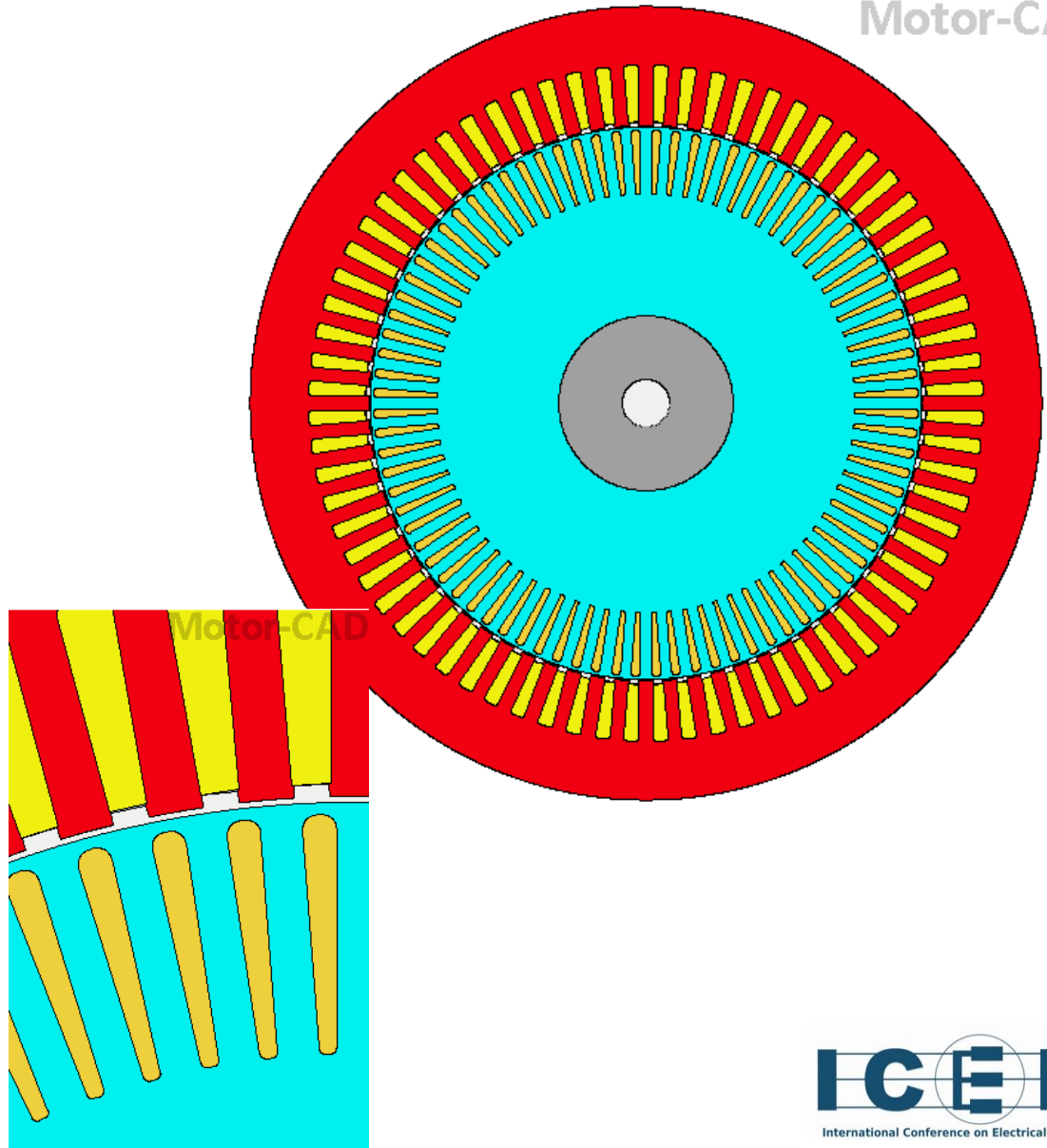
Brushless PM machine

- Back emf waveform at 500rpm
- 3 slices combine to give sinusoidal waveform
- Torque waveform at 350Nm
- 3 slices combine to minimise torque ripple
- Torque ripple = 4.4%



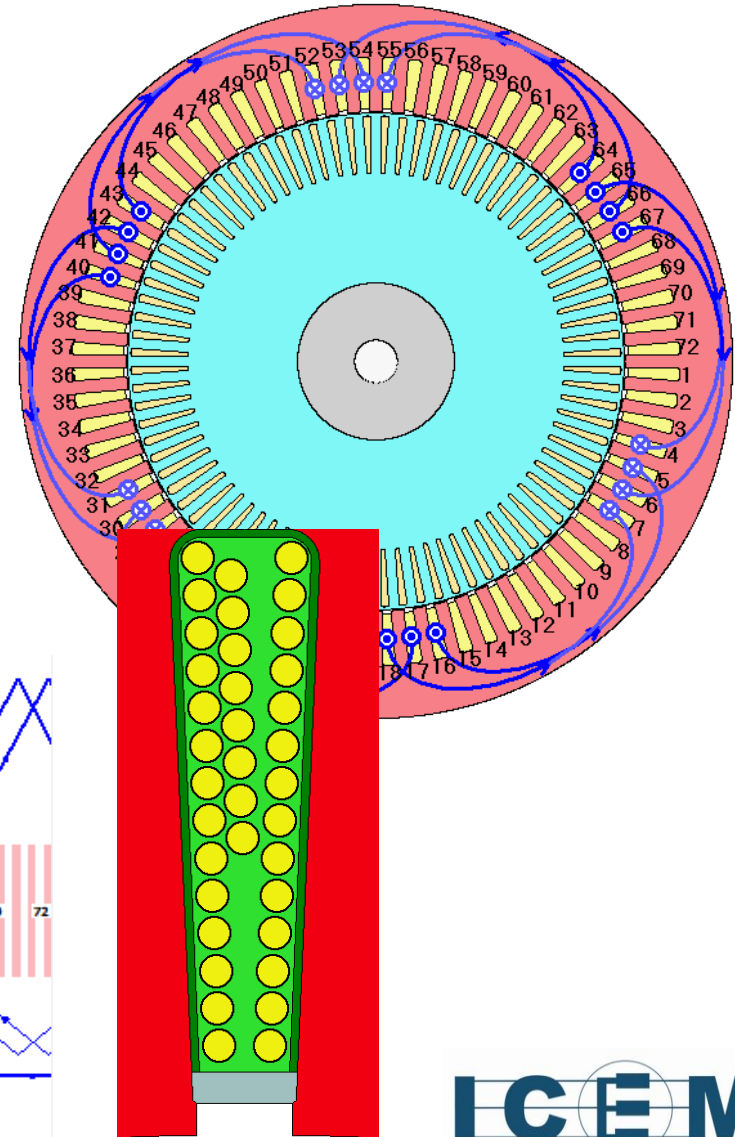
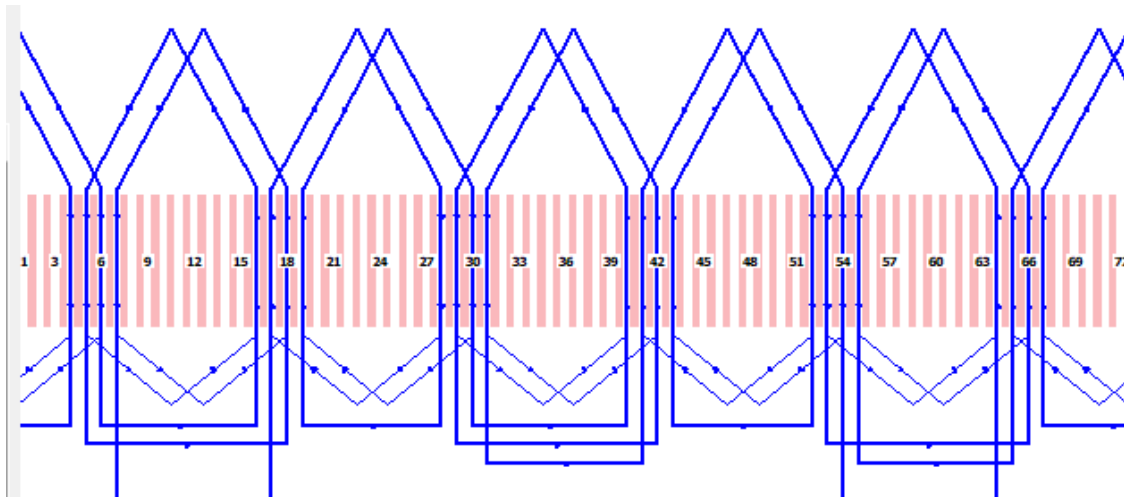
Induction machine (IM)

- 72 slot 84 bar
- 6 pole
- Copper rotor
- M250-35A
- 250mm OD
- Multi-stranded winding
- 5° mech rotor bar skew



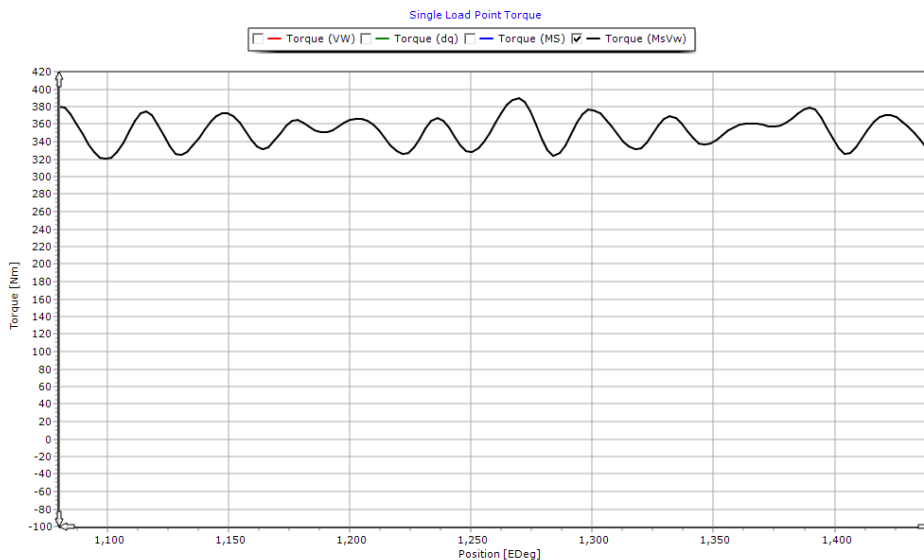
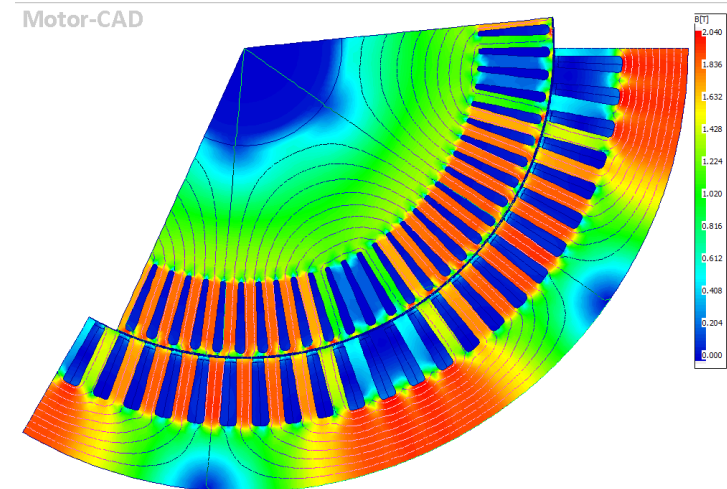
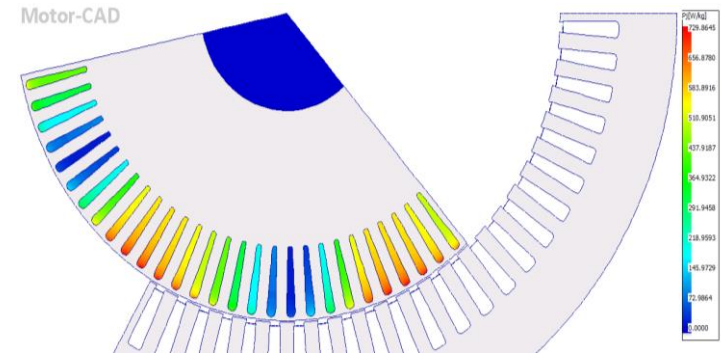
Induction machine (IM)

- Single layer winding
- Coil pitch - 11 slots
- 3 turns per coil, with 15 strands per turn
- 40% copper slot fill
- 2 parallel paths per phase



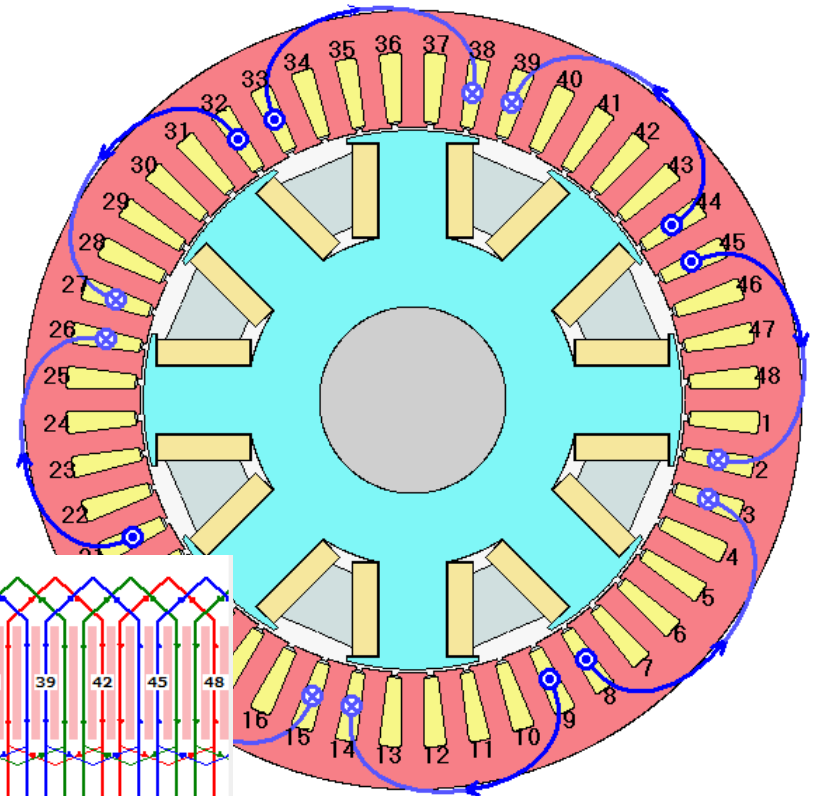
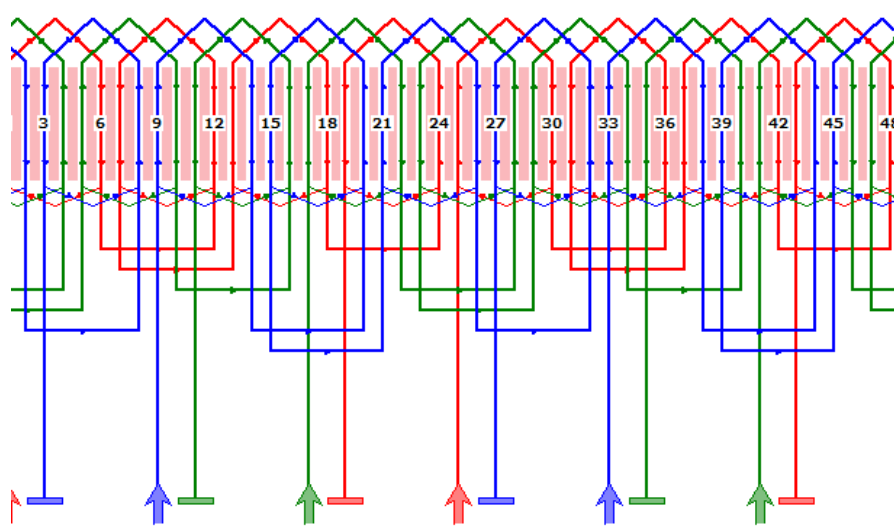
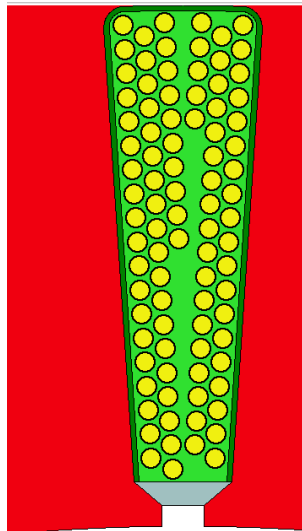
Induction machine (IM)

- Torque waveform, flux density and rotor bar eddy current density at 350Nm
- Solved with full transient solver inc. rotor rotation (e.g. space harmonics)
- 17% ripple but rotor bar skew isn't account for in this example



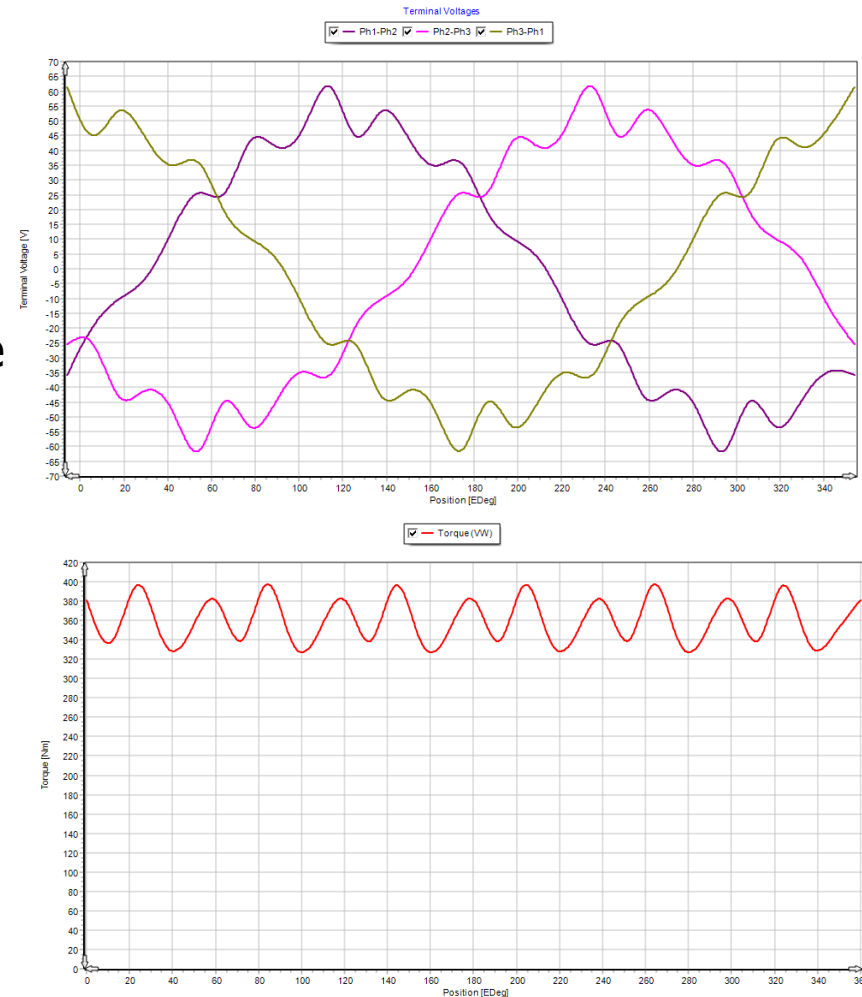
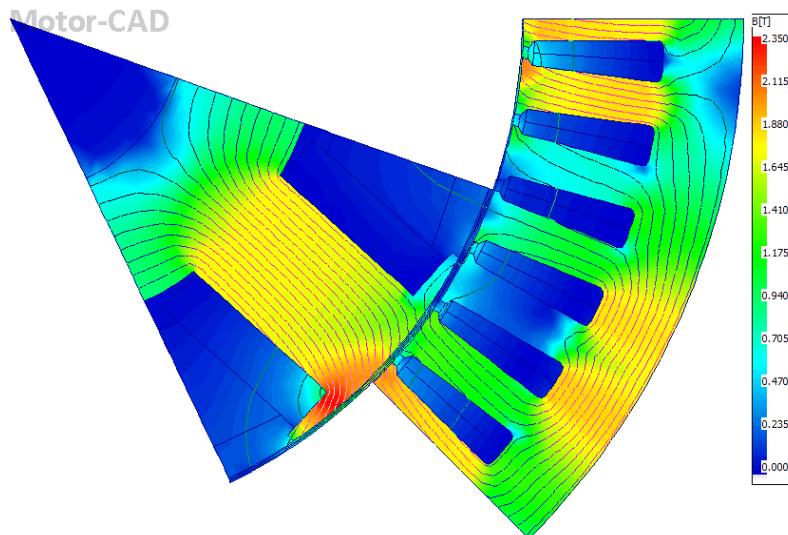
Wound Field Synchronous machine

- Single layer winding
- Coil pitch - 5 slots
- 6 turns per coil, with 15 strands per turn
- 40% copper slot fill
- 2 parallel paths per phase



Induction machine (IM)

- Torque and voltage waveform at 350Nm, 500rpm
- 17% torque ripple
- 12% THD on line-line terminal voltage waveform
- Difficult to reduce with WFSM as rotor skewing not feasible



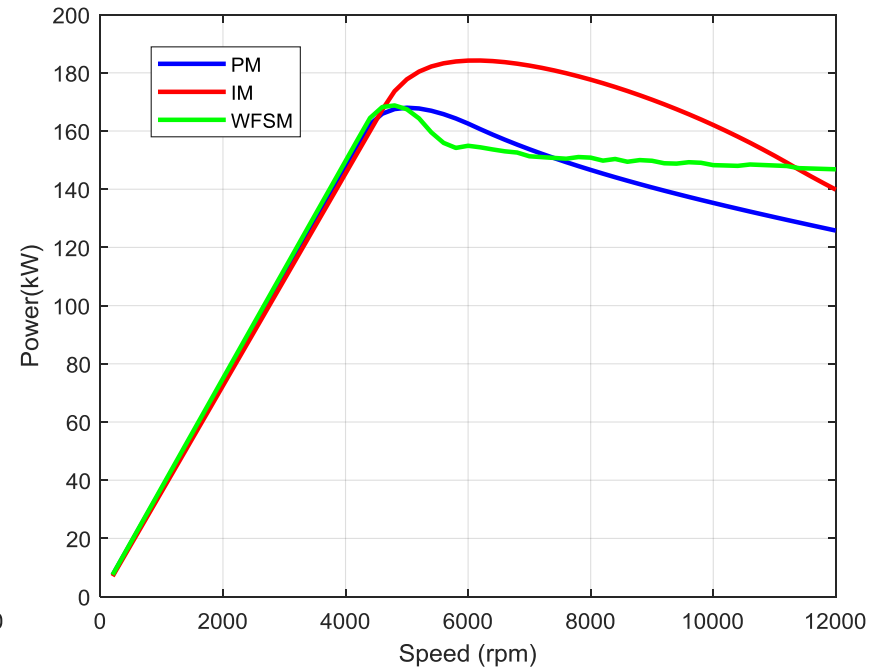
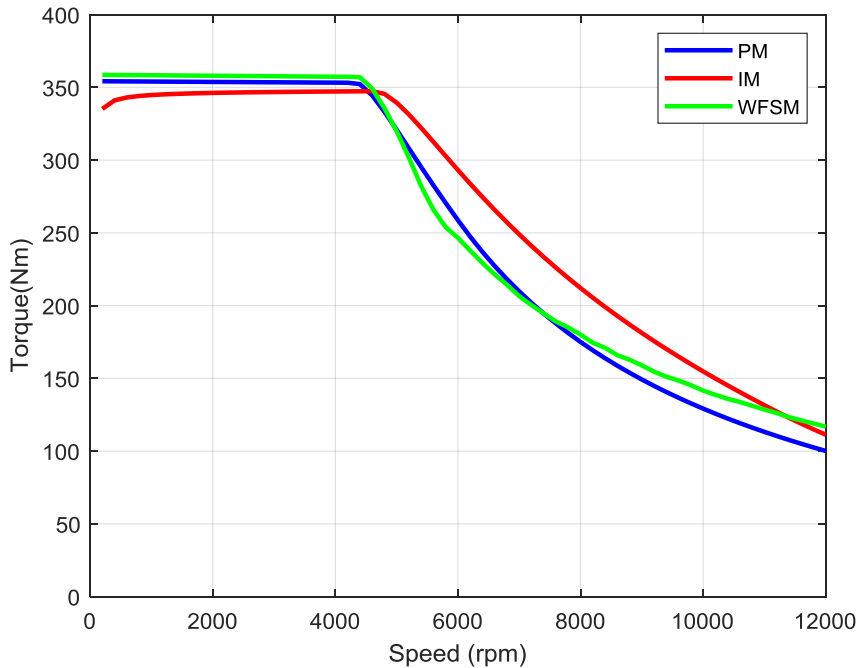
1. eMachine Comparison

- All machines designed for equivalent peak performance characteristic
- IM has longer end windings due to winding pattern

Dimensions	PM	IM	WFSM
Active length (mm)	100	120	120
End winding overhang (mm)	30	40	30
Total length (mm)	160	200	180
Weight	PM	IM	WFSM
Steel (kg)	26.1	33.4	28.17
Copper (kg)	5.05	13.7	8.5
Magnet (kg)	2.05	0	0
Total (kg)	33.2	47	36.7

Peak Performance Comparison

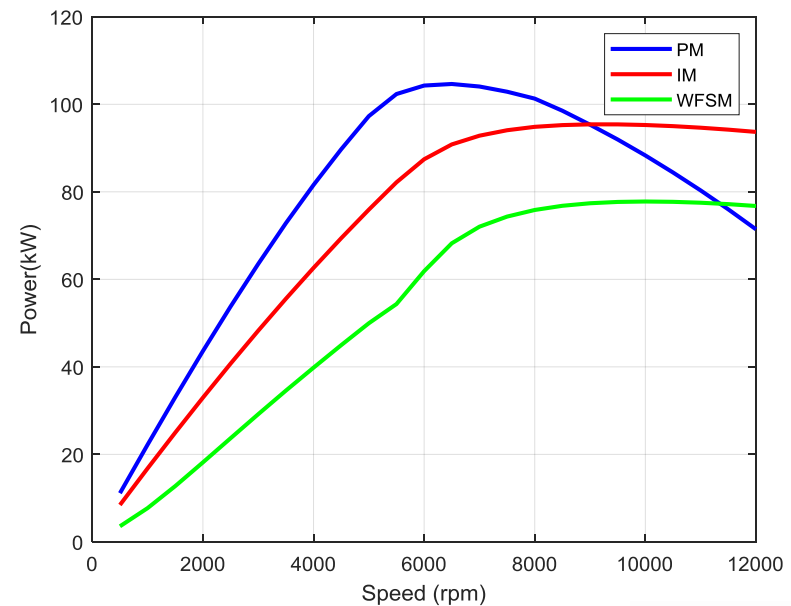
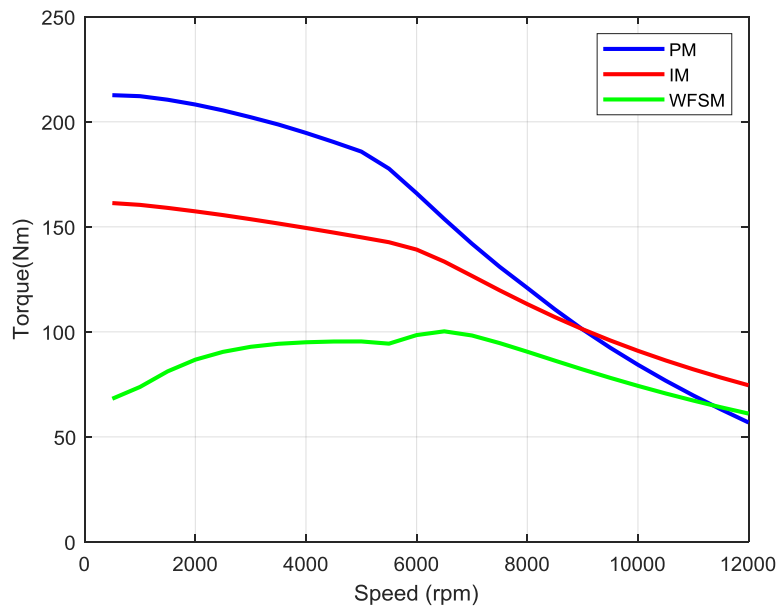
350Nm, 150kW Target



1. eMachine Comparison

Continuous Performance Comparison

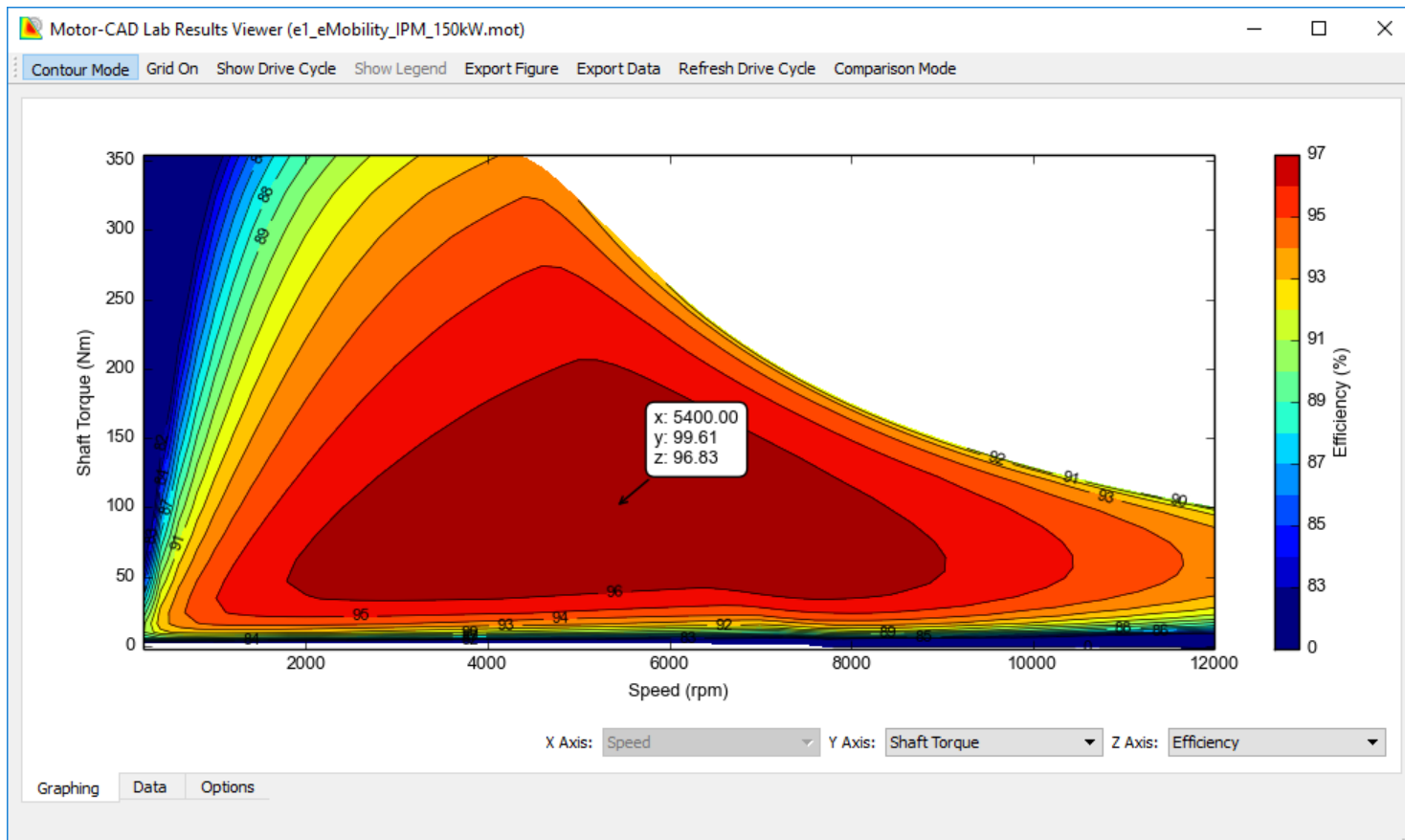
- Stator winding limited on 180°C hotspot
- PM - Magnet limit = 160 °C, IM Rotor Bar=220 °C, WFSM rotor winding hotspot =180 °C
- WFSM limited by rotor temperature, ideally requires rotor cooling



1. eMachine Comparison

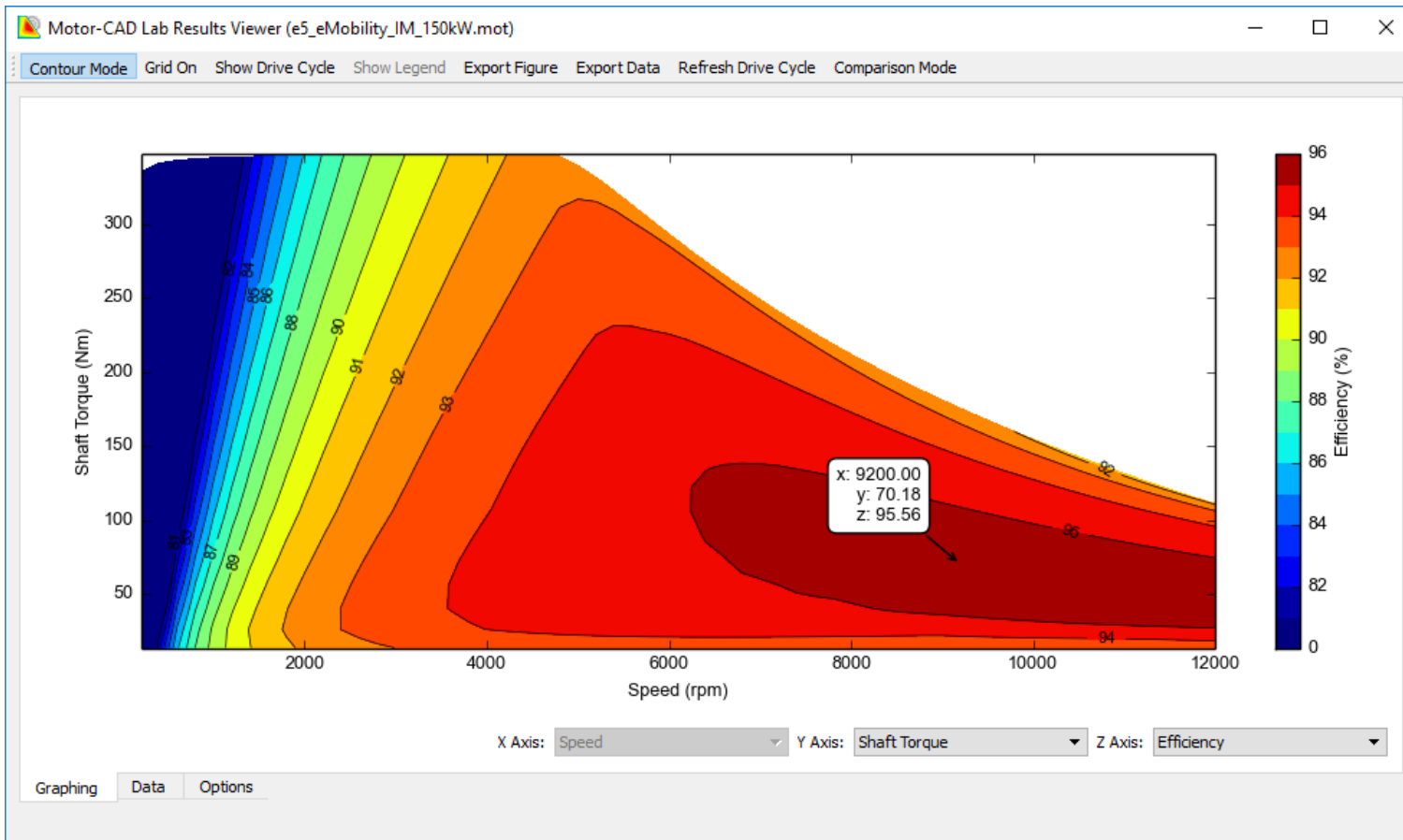
PM Machine Efficiency Map

- 96.8% peak efficiency
- Maximum efficiency region from 2-9krpm
- Large high efficiency region in typical drive cycle area



IM Machine Efficiency Map

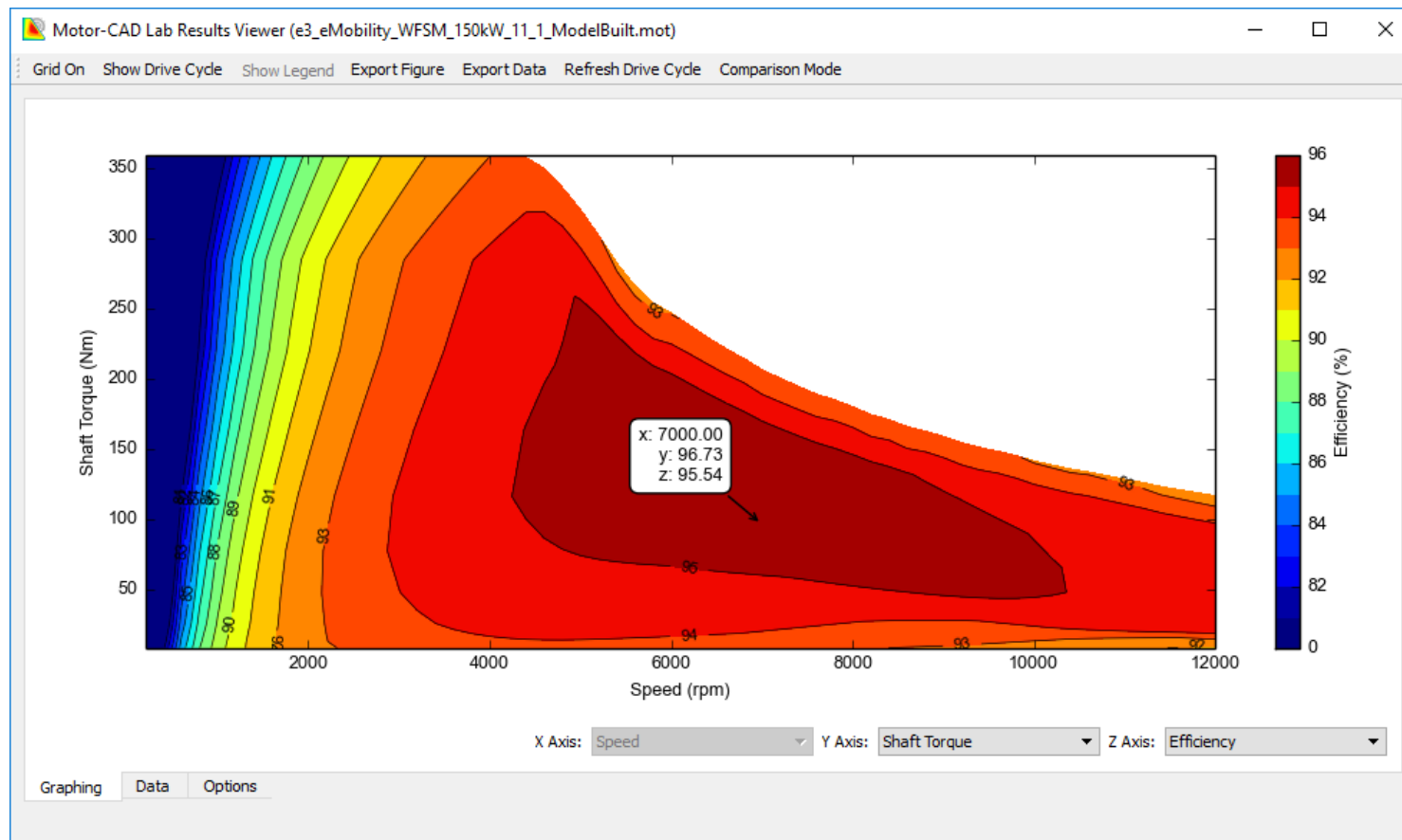
- 95.5% peak efficiency
- High efficiency region from 7-12krpm



1. eMachine Comparison

WFSM Machine Efficiency Map

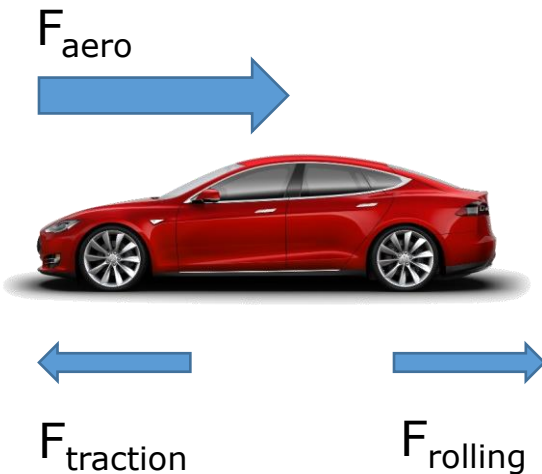
- 95.5% peak efficiency
- Maximum efficiency region from 5-10krpm
- High efficiency region at higher torque levels than PM or IM machine



1. eMachine Comparison

Energy Use over a Drive Cycle

- Simple kinematic model used with example EV vehicle parameters



Parameter	Value
Vehicle mass	1700 kg
Rolling resistance coefficient	0.0054
Air density	1.225 kg/m ³
Frontal area	2.81 m ²
Drag Coefficient	0.24
Wheel radius	0.35m
Mass correction factor	1.04
Gear ratio	10:1

$$F_{rolling} = k_r mg$$

$$F_{aero} = \frac{1}{2} \rho v^2 C_d A_f$$

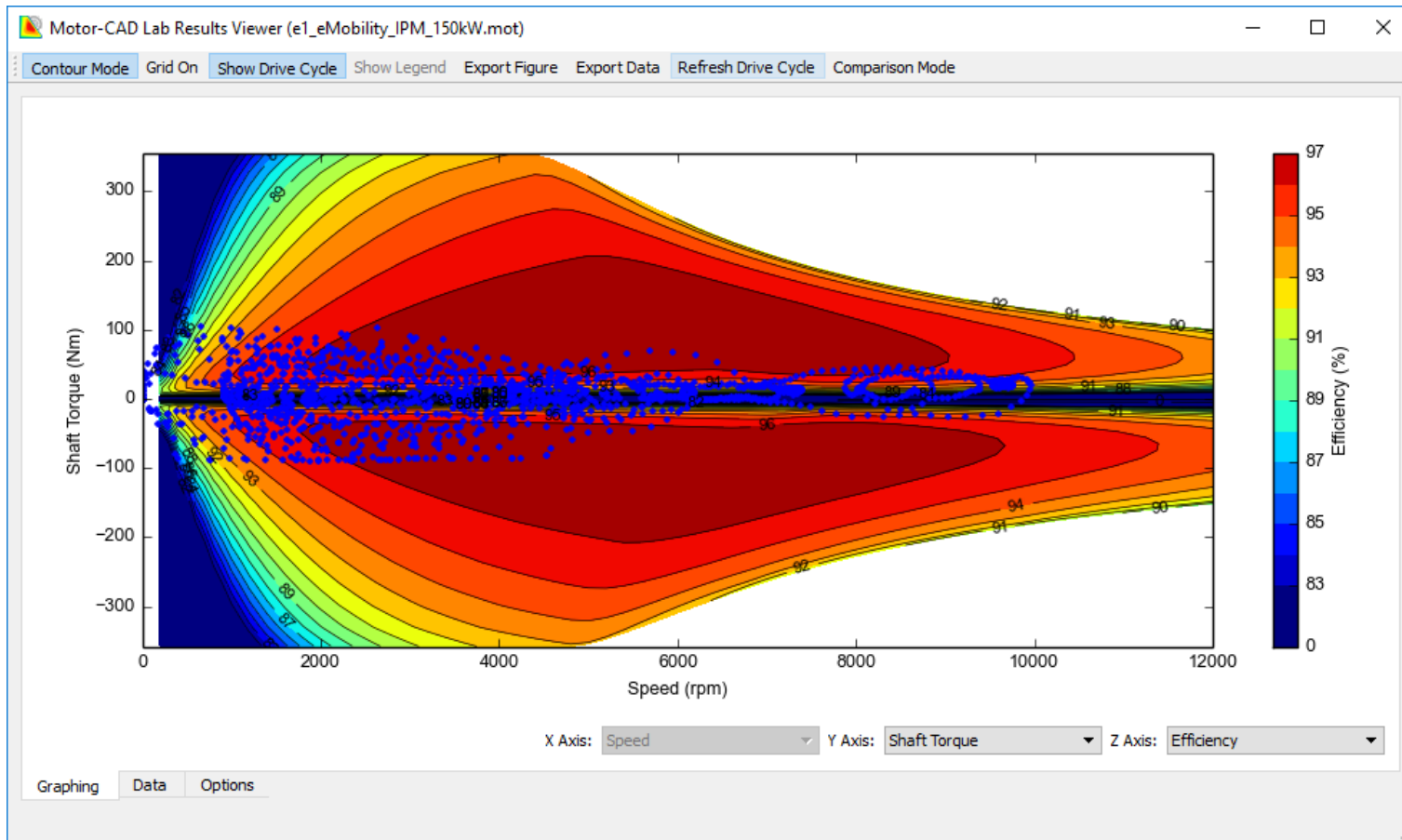
$$T_{motor} = k_{dem} \frac{F_{traction} \cdot r_\omega}{n_d}$$

$$\text{Acceleration of Vehicle} = \frac{(F_{traction} - F_{aero} - F_{rolling})}{m}$$

1. eMachine Comparison

Energy Use over a Drive Cycle

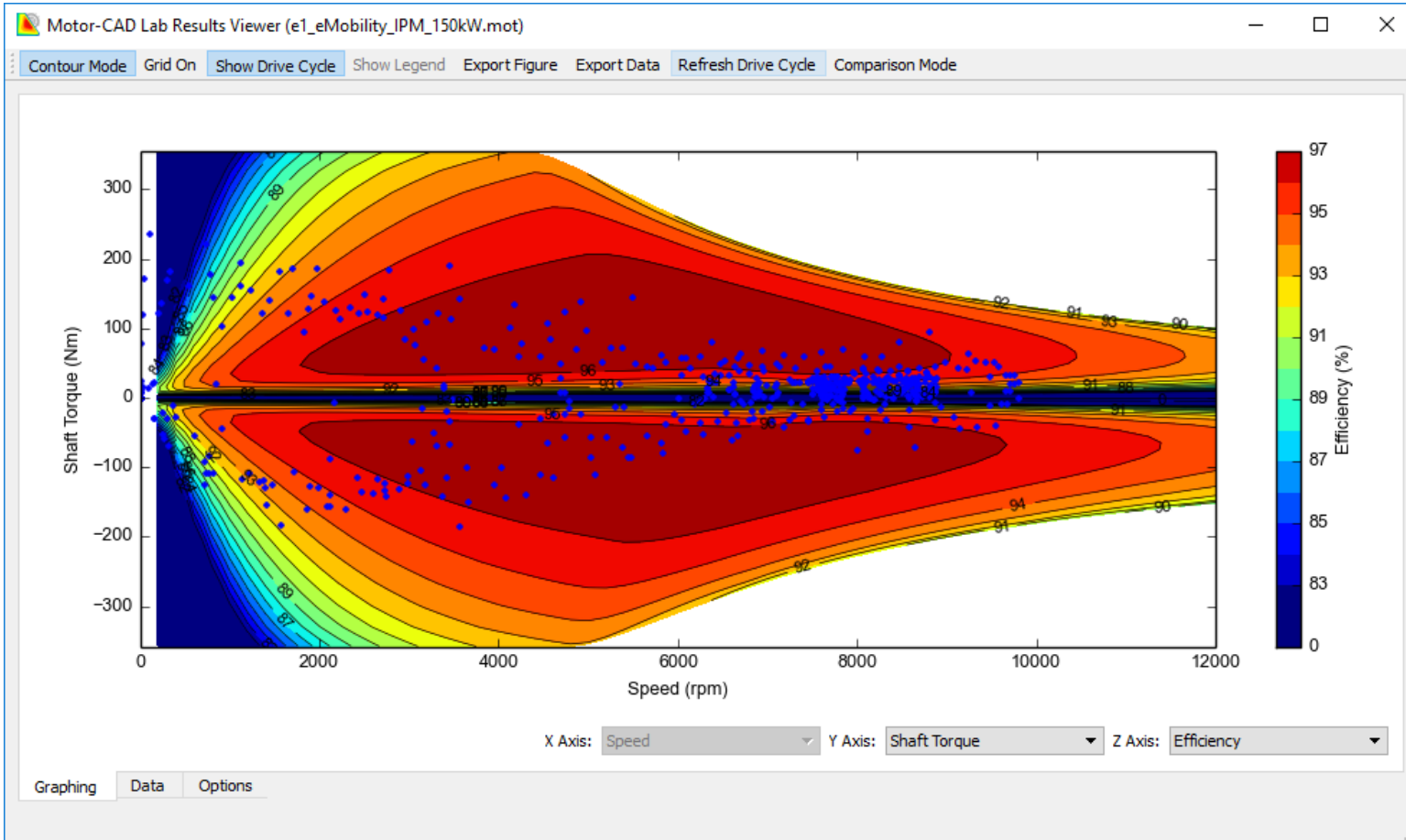
- WLTP Class 3 Drive Cycle



1. eMachine Comparison

Energy Use over a Drive Cycle

- US06 Drive Cycle



1. eMachine Comparison

Energy Use over a Drive Cycle

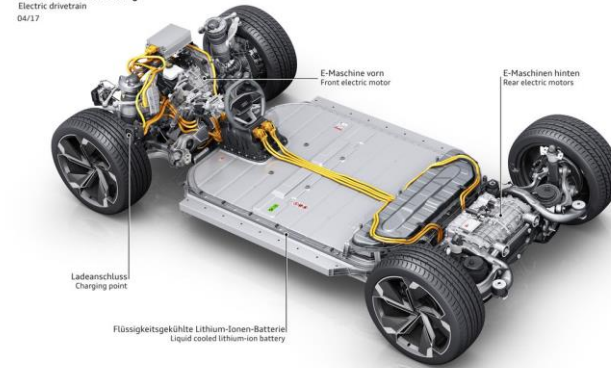
- Reduced efficiency = reduced range/increased battery size
- PM gives best efficiency over cycle

	IPM	IM	WFSM
Total Loss - WLTP	255.53Wh	310.25Wh	312.62Wh
Av. Efficiency - WLTP	94.32%	93.17%	92.79%
Total Loss - US06	176.09Wh	223.57Wh	214.9Wh
Av. Efficiency - US06	94.72%	93.39%	93.44%

Dual Motor Solution?

- Premium EVs are tending to adopt a dual motor topology, one on each axle
- For example, Jaguar i-pace, Audi e-tron, Tesla Model 3/S/X
- Could optimal efficiency and energy use be achieved by using the PM machine on the rear axle and IM machine on the front or vice versa?
- The IM machine could be optimised for higher speed, low torque cruising. While the PM machine could work well for low-medium speed operation and high torque operation
- Tesla have announced a version of the model 3 with this set-up

Audi e-tron Sportback concept
elektrischer Antriebsstrang
Electric drivetrain
04/17



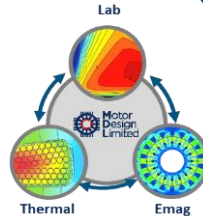
Summary

- PM machine offers improved efficiency and reduced mass/volume at higher cost
- Systems aspects, such as improved range or reduced battery mass for the same, with increased efficiency may mean that the PM motor gives the lowest overall system cost
- However the PM and IM machines show improved efficiencies at different areas of the map and if a dual motor configuration is used this could be advantageous
- The WFSM has similar performance to the IM however the thermal performance is very constrained on rotor temperature and really some rotor cooling system is required in this example

Tutorial Overview

Motor Design

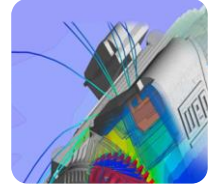
Trade-off Analysis for a BEV traction application



1. eMachine Comparison - PM, IM, Sync
2. Windings Comparison - Hairpin vs Stranded
3. Cooling Comparison - Water Jacket, Internal Air and Oil Spray

Mechanical Analysis

NVH and Mechanical Stress



4. NVH Analysis - Behaviour of Motor + Gearbox
5. Mechanical Stress Analyses (Problem formulation and Solution)

Design

Analysis

Stranded vs Hairpin

- Hairpin windings are growing in popularity and are used in the Gen2 GM volt and Toyota Prius MY17
- They offer advantages in manufacturing cost and performance repeatability
- However they also have some disadvantages
- The next section of the comparison looks at hairpin vs. stranded windings

Toyota Prius MY17

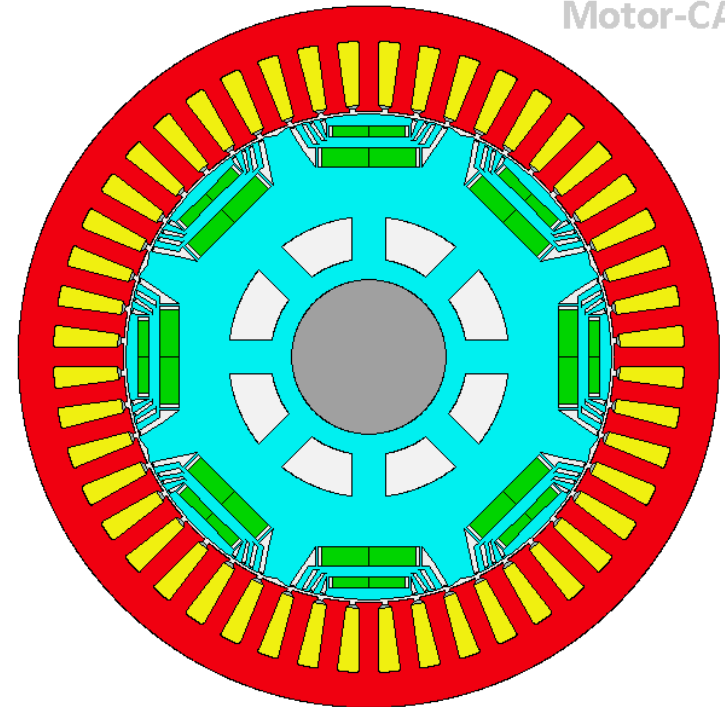
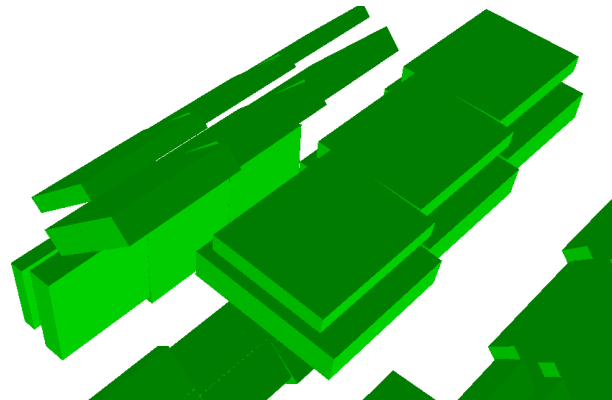


GM Volt

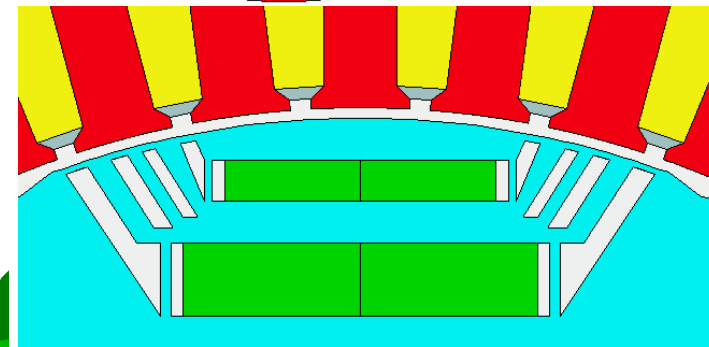


Stranded PM Machine

- Brushless PM machine
- 48 slot 8 pole IPM
- Double layer magnet – similar to BMW i3
- N42UH magnet
- M250-35A steel
- 250mm OD
- Multi-stranded stator windings
- Step skewed rotor
- 100mm axial length



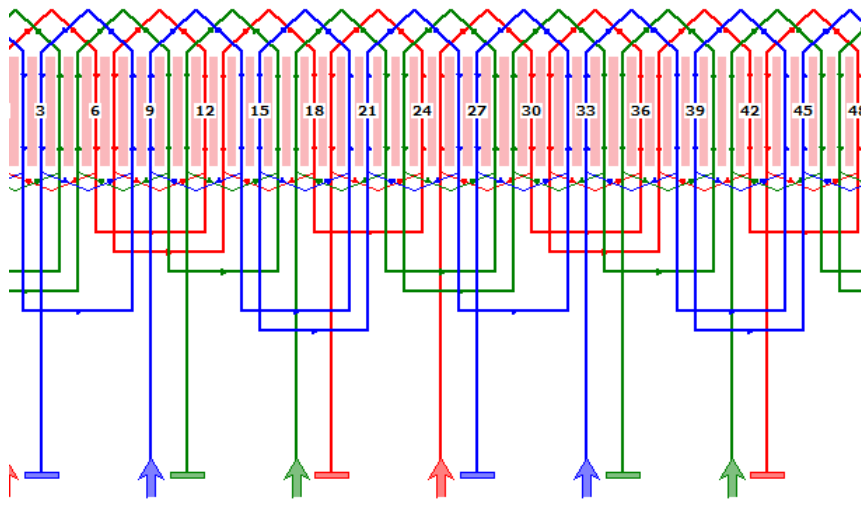
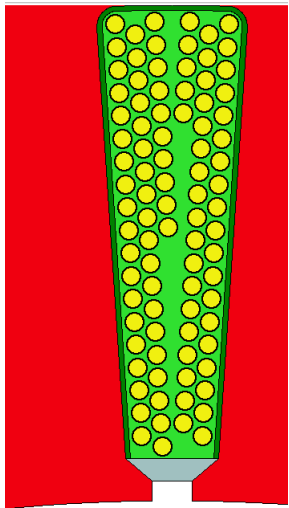
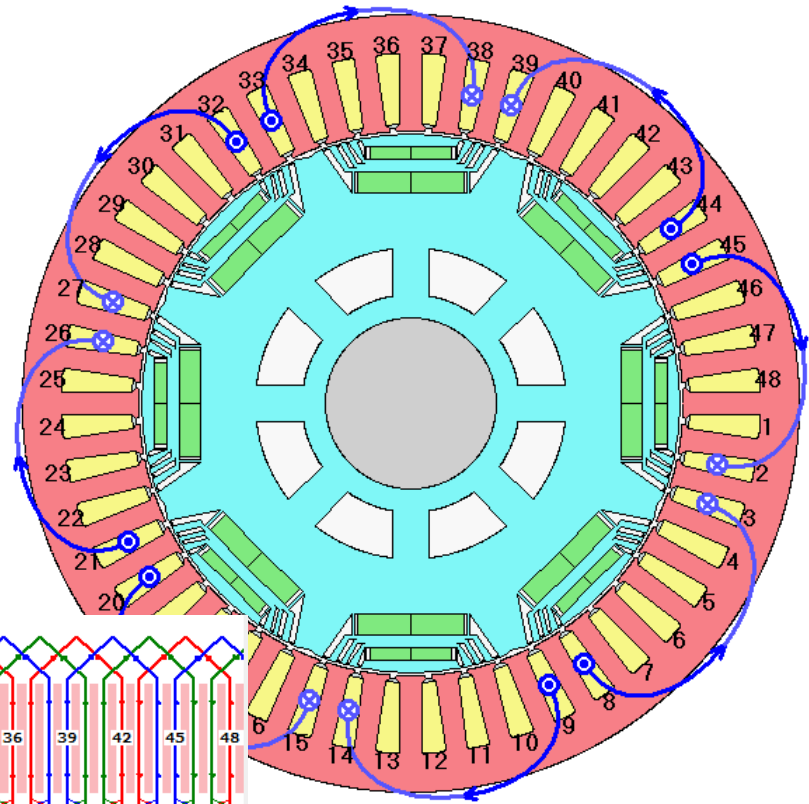
Motor-CAD



2. Winding Comparison

Stranded PM Machine

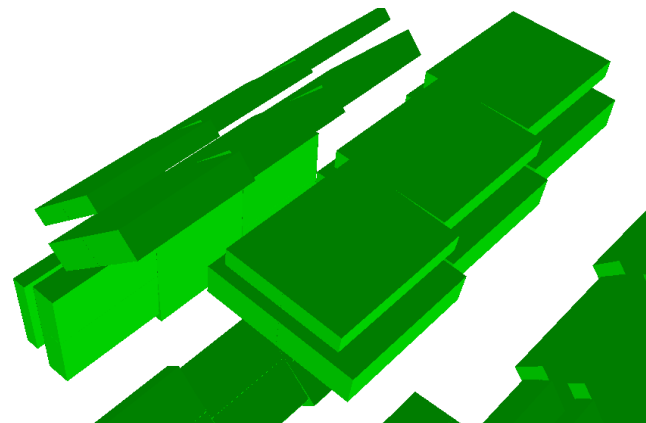
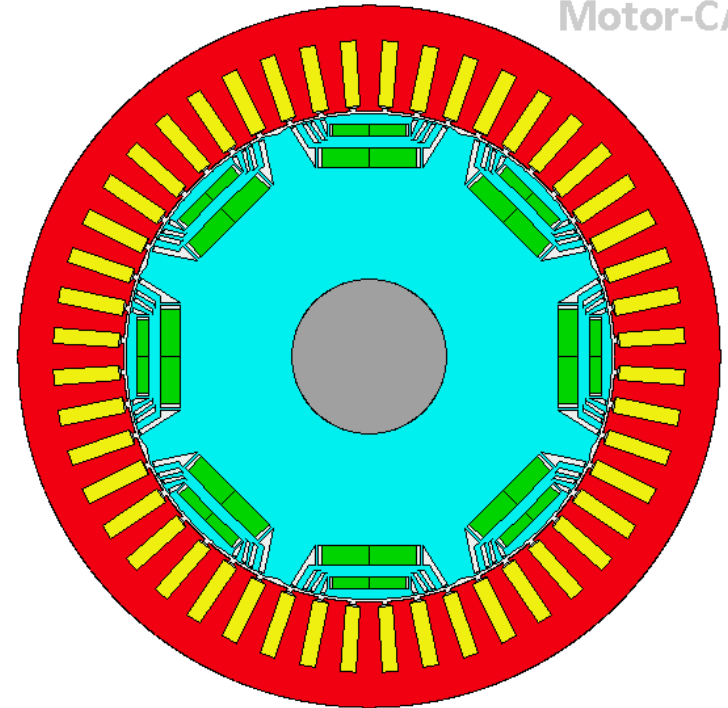
- Single layer winding
- Coil pitch - 5 slots
- 6 turns per coil, with 15 strands per turn
- 40% copper slot fill
- 2 parallel paths per phase



Hairpin PM Machine

- Brushless PM machine
- 48 slot 8 pole IPM
- Double layer magnet – similar to BMW i3
- N42UH magnet
- M250-35A steel
- 250mm OD
- **Multi-stranded stator windings**
- Step skewed rotor
- 100mm axial length

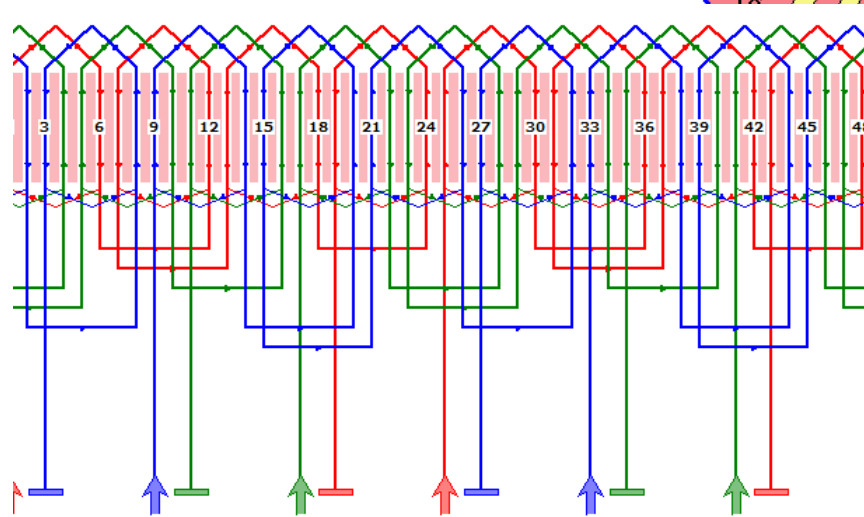
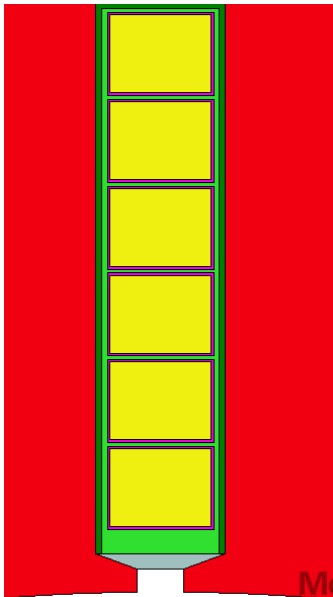
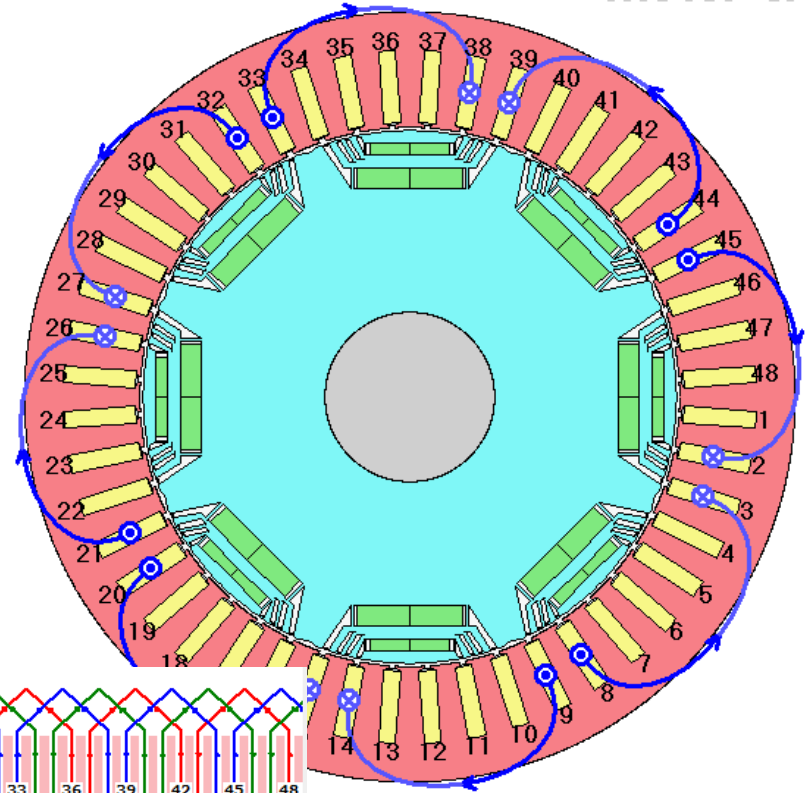
Motor-CAD



2. Winding Comparison

Hairpin PM Machine

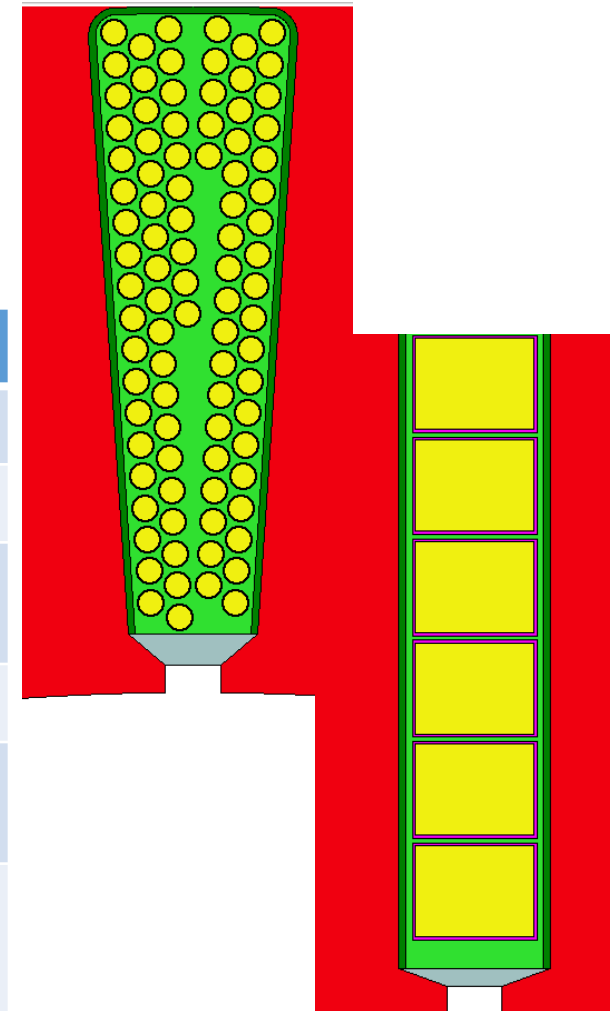
- Single layer winding
- Coil pitch - 5 slots
- 6 turns per coil
- 2 parallel paths per phase



2. Winding Comparison

- CSA of the slot is slightly lower with the hairpin
- Slot fill factor is higher giving lower resistance
- Higher AC loss but lower DC loss with hairpin

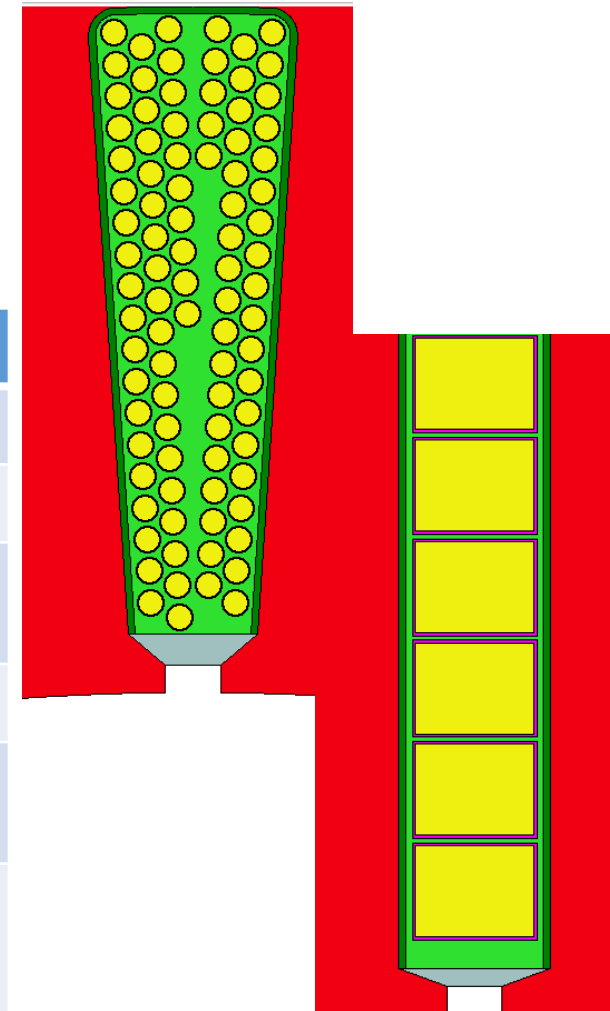
	Stranded	Hairpin
Copper Fill Factor	0.4	0.65
Slot Cross Sectional Area	145.7mm ²	130.9mm ²
Conductor Cross Sectional Area	58.29mm ²	85.14mm ²
Phase resistance	0.0113Ω	0.00773Ω
DC winding loss @ 100Nm, 8000rpm	1239W	873.6W
AC winding loss @ 100Nm, 8000rpm	596.4W	1069W
Combined winding loss @100N, 8000rpm	1835W	1942W



2. Winding Comparison

- CSA of the slot is slightly lower with the hairpin
- Slot fill factor is higher giving lower resistance
- Higher AC loss but lower DC loss with hairpin

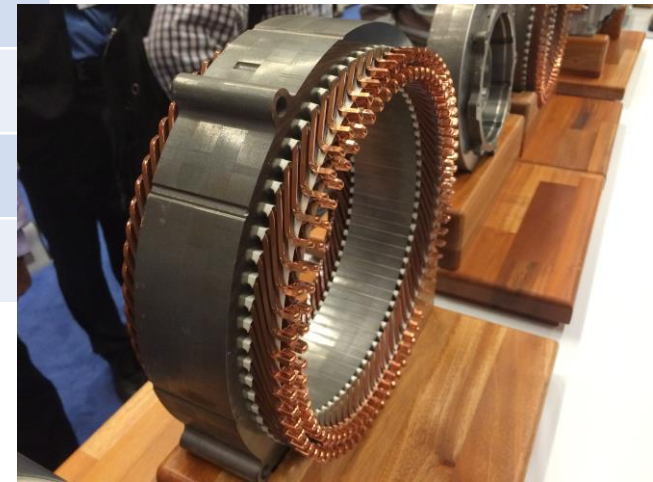
	Stranded	Hairpin
Copper Fill Factor	0.4	0.65
Slot Cross Sectional Area	145.7mm ²	130.9mm ²
Conductor Cross Sectional Area	58.29mm ²	85.14mm ²
Phase resistance	0.0113Ω	0.00773Ω
DC winding loss @ 100Nm, 8000rpm	1239W	873.6W
AC winding loss @ 100Nm, 8000rpm	596.4W	1069W
Combined winding loss @100N, 8000rpm	1835W	1942W



2. Winding Comparison

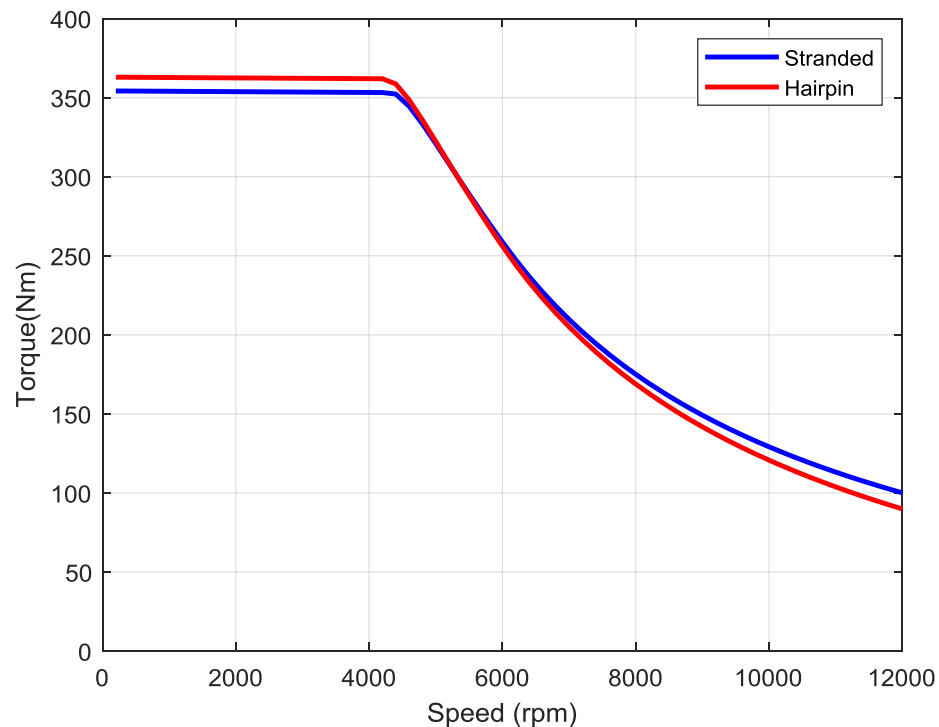
- Hairpin end windings are more compact on one end due to joins

Dimensions	Stranded	Hairpin
Active length	100mm	100mm
End winding overhang	30mm	25mm - Avg
Total length	160mm	150mm
Weight	Stranded	Hairpin
Steel	26.1kg	26.1kg
Copper	5.05kg	7.36kg
Magnet	2.05kg	2.05kg
Total	33.2kg	35.5kg



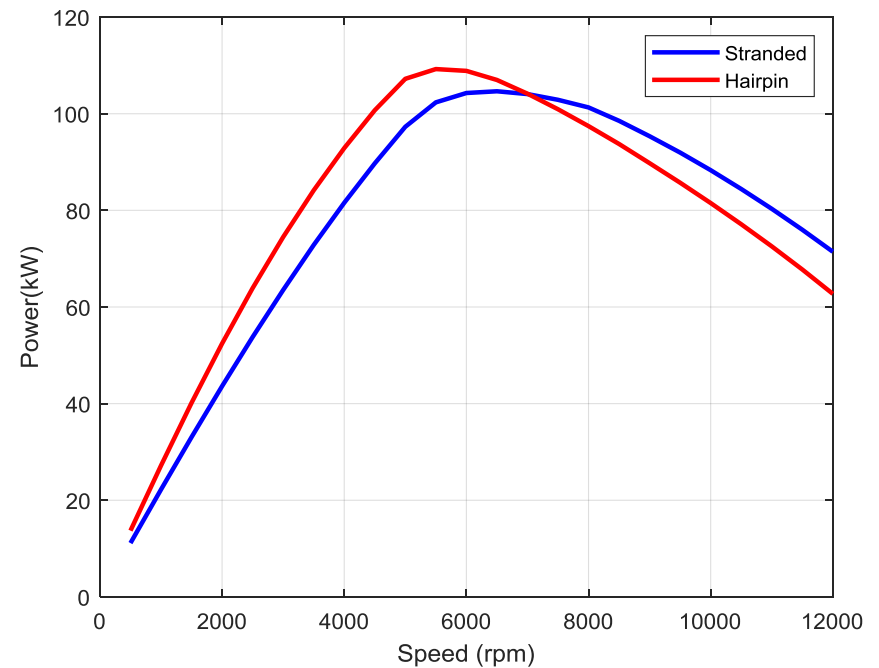
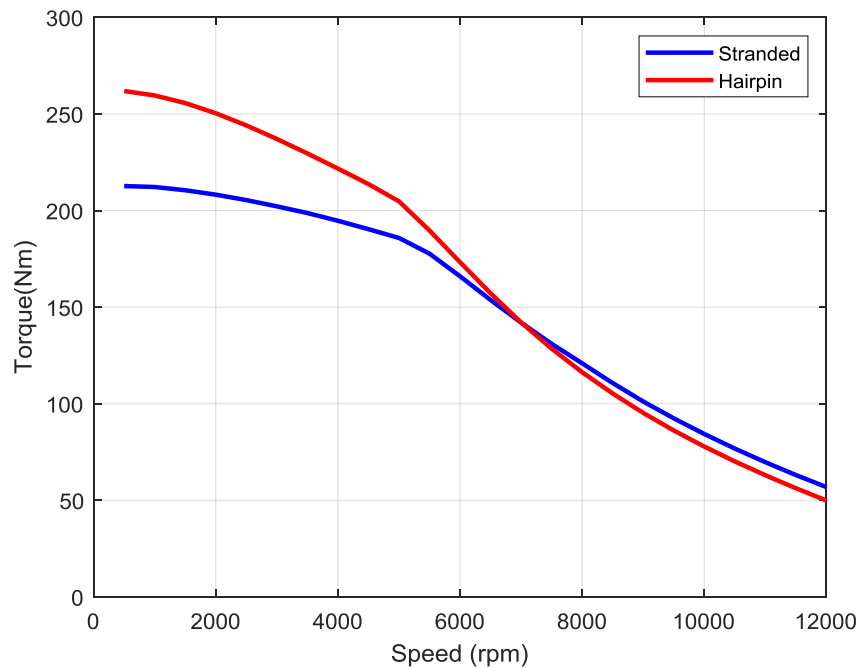
Peak Performance Comparison

- Similar peak performance characteristics
- Difference due to slight change in stator slot shape and increased losses at higher speed for the hairpin machine



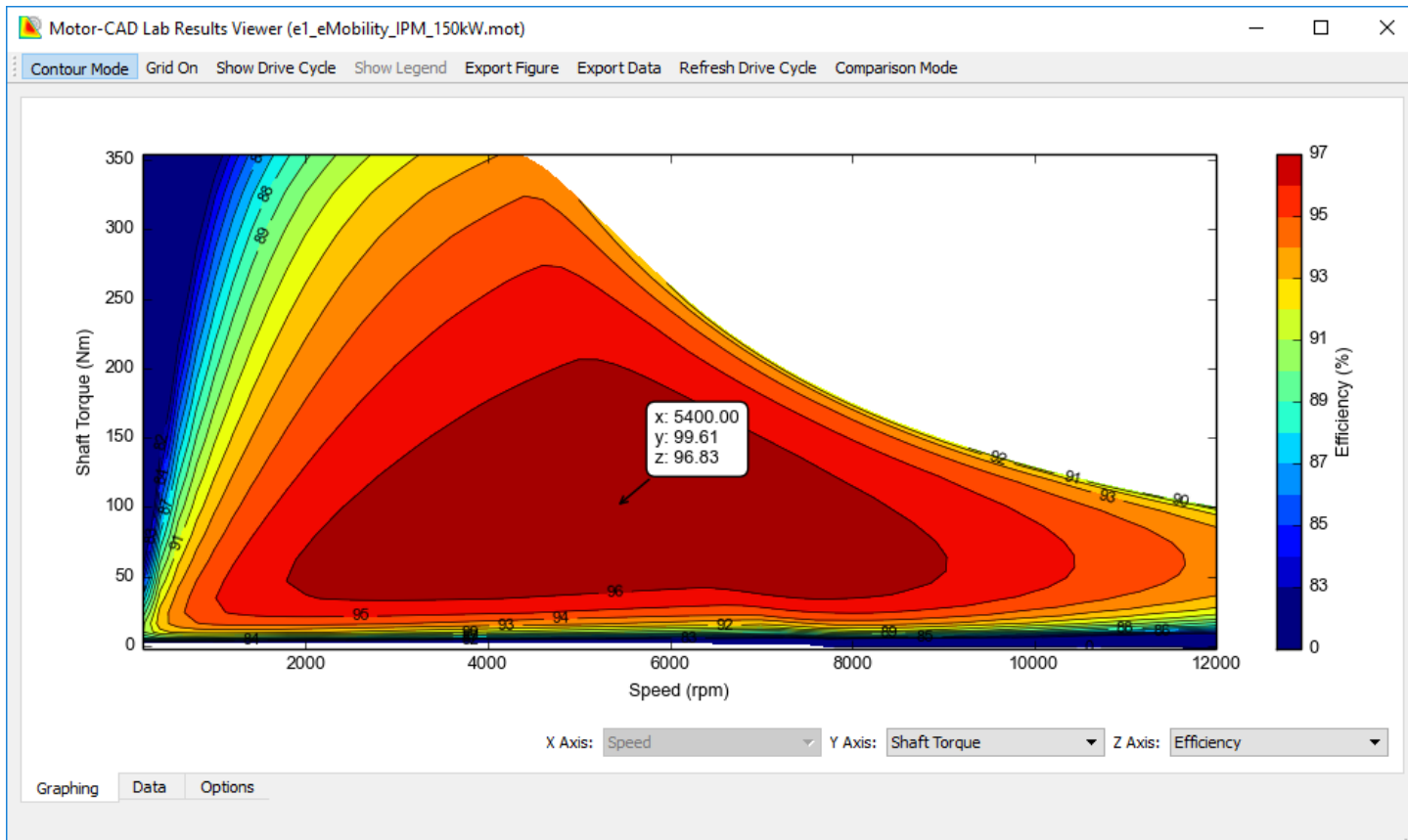
Continuous Performance Comparison

- Hairpin gives improve continuous torque at low speed but reduced at higher speeds



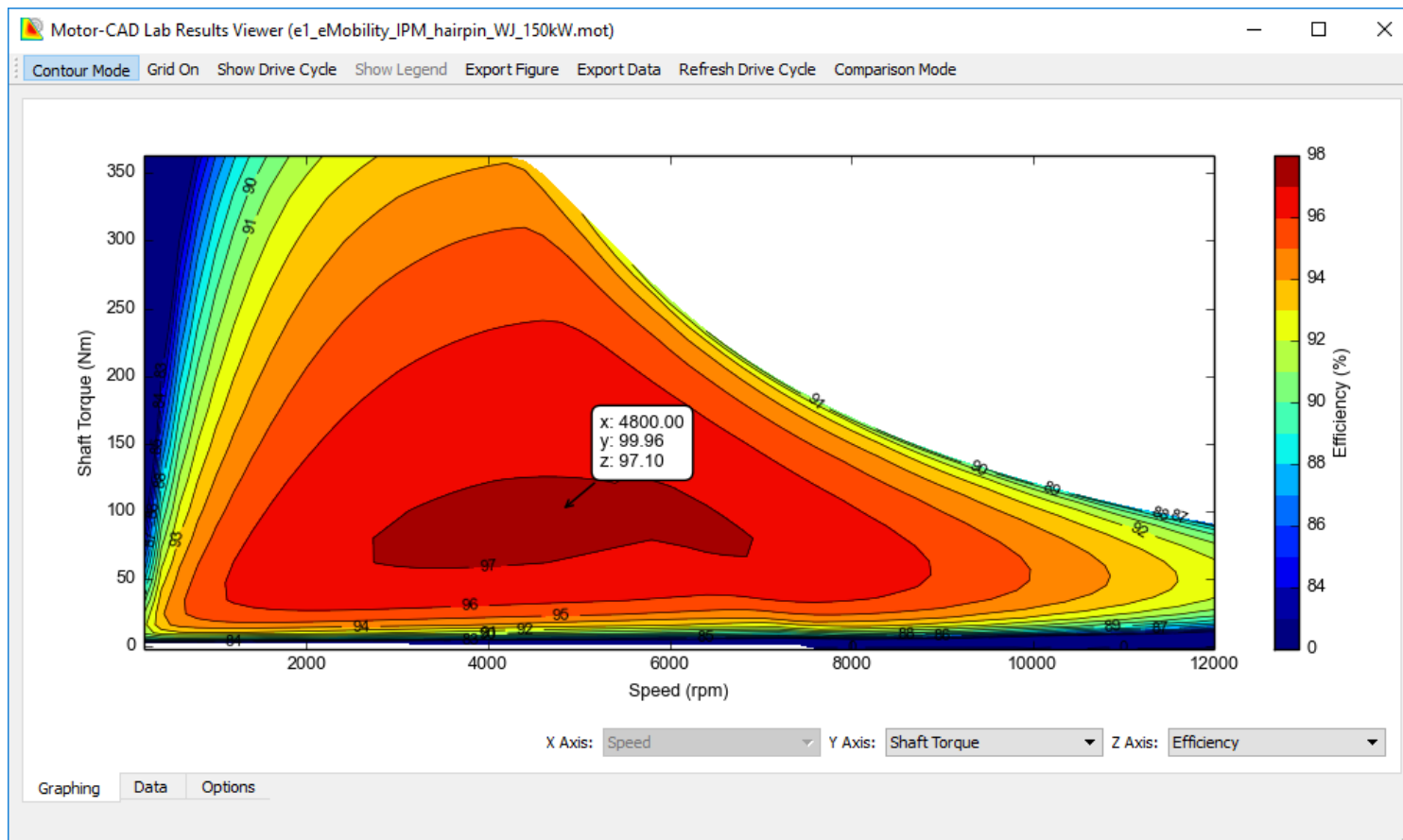
Stranded Windings Efficiency Map

- 96.8% peak efficiency
- Maximum efficiency region from 2-9krpm
- Large high efficiency region in typical drive cycle area



Hairpin Windings Efficiency Map

- Higher peak efficiency than stranded machine
- However efficiency at higher speeds is worse



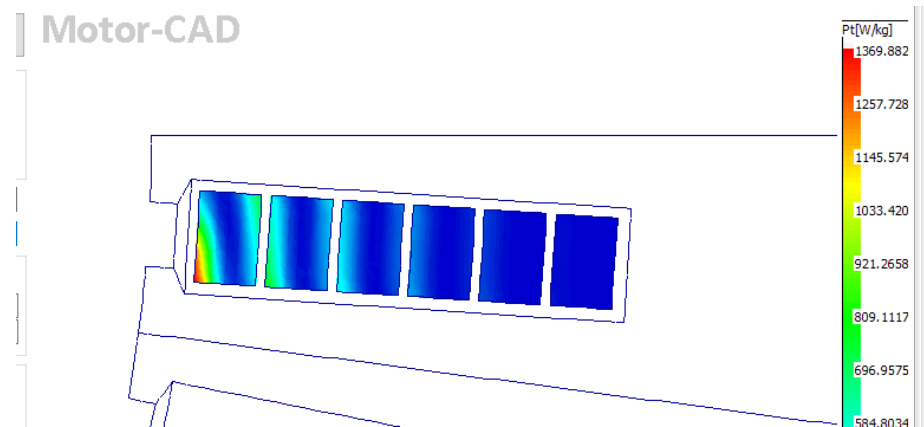
Energy use over drive cycles

- Over both cycles the hairpin machine offers improved efficiency over the stranded design

	Stranded IPM	Hairpin IPM
Total Loss - WLTP	255.53Wh	241.24Wh
Av. Efficiency - WLTP	94.32%	94.62%
Total Loss - US06	176.09Wh	165.31Wh
Av. Efficiency - US06	94.72%	95.03%

Summary

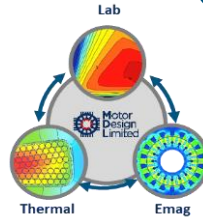
- Hairpin machine shows generally improved performance across the performance range
- However AC losses at higher speeds have the potential to create issues in performance and should be considered from an early stage in the design process.
- Over both cycles the hairpin machine offers improved efficiency over the stranded design



Tutorial Overview

Motor Design

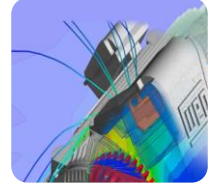
Trade-off Analysis for a BEV traction application



1. eMachine Comparison - PM, IM, Sync
2. Windings Comparison - Hairpin vs Stranded
3. **Cooling Comparison - Water Jacket, Internal Air and Oil Spray**

Mechanical Analysis

NVH and Mechanical Stress



4. NVH Analysis - Behaviour of Motor + Gearbox
5. **Mechanical Stress Analyses (Problem formulation and Solution)**

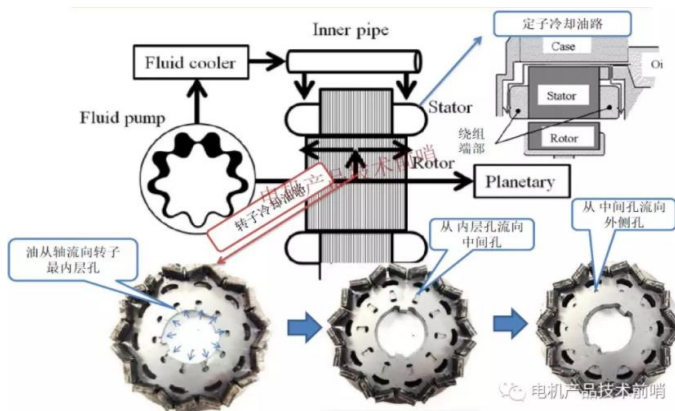
Design

Analysis

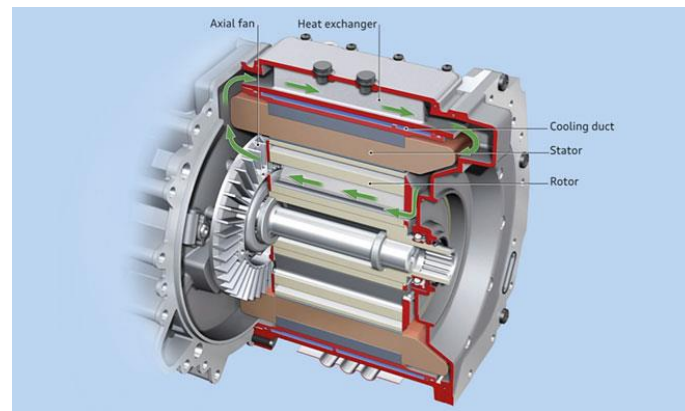
Cooling Systems

Using the IPM hairpin machine we will compare three different cooling methods

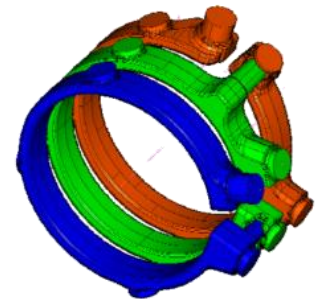
- 1) Water jacket, e.g. Nissan Leaf, BMW i3
- 2) Water jacket + Internal Air, e.g. Zytec traction machine, BMW 2225xe series
- 3) Oil spray cooling, e.g. Toyota Prius



3)



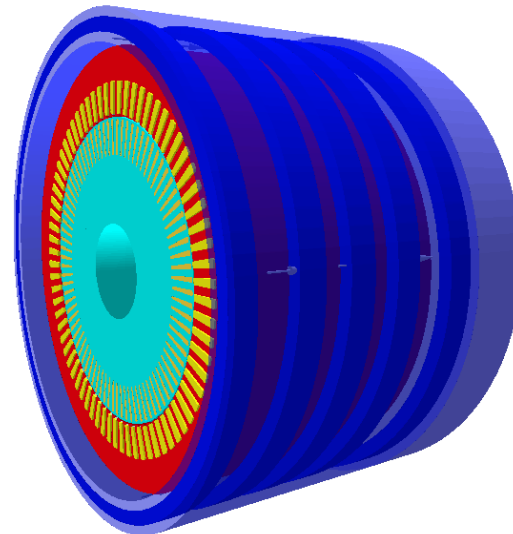
2)



1)

Water Jacket Cooling System

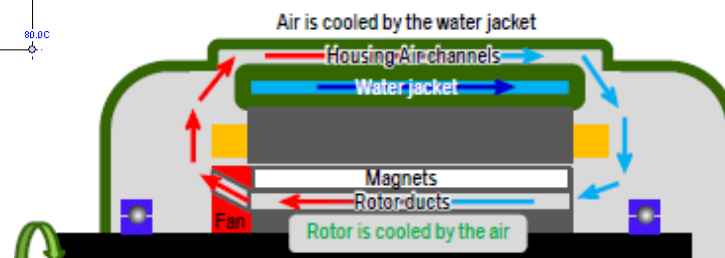
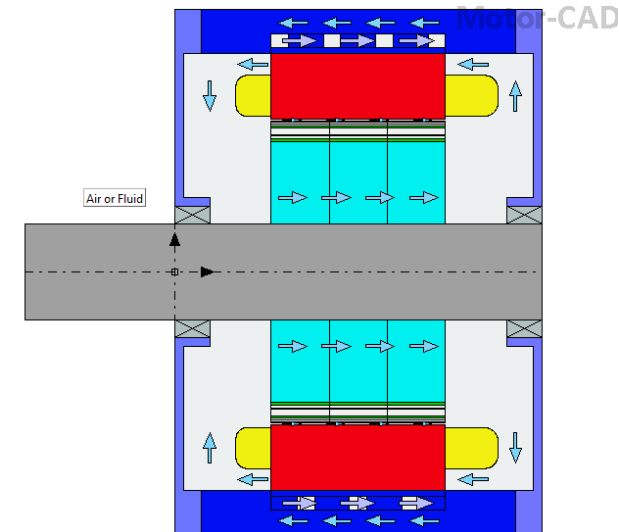
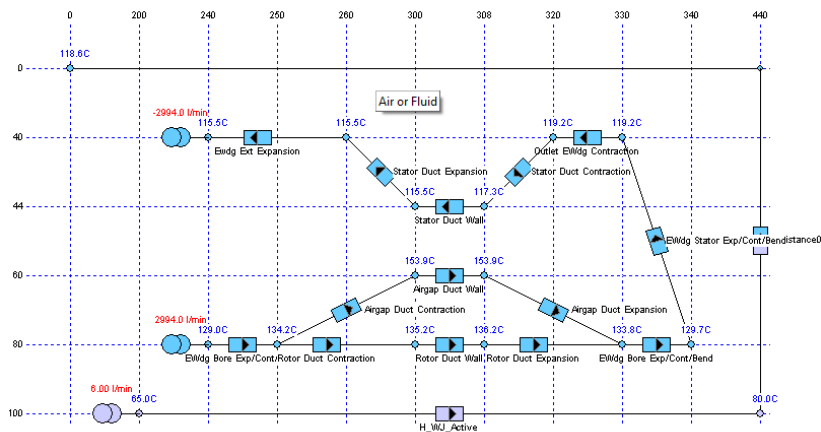
- Spiral water jacket
- 65 degC inlet temperature
- 6.5 l/min coolant flow rate
- EGW 50/50 coolant
- Cooling channels over active machine section only



3. Cooling System Comparison

Water Jacket + Air Cooling System

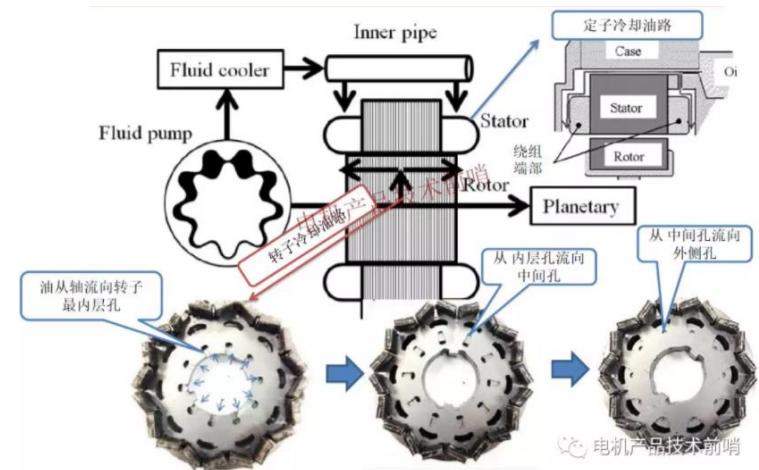
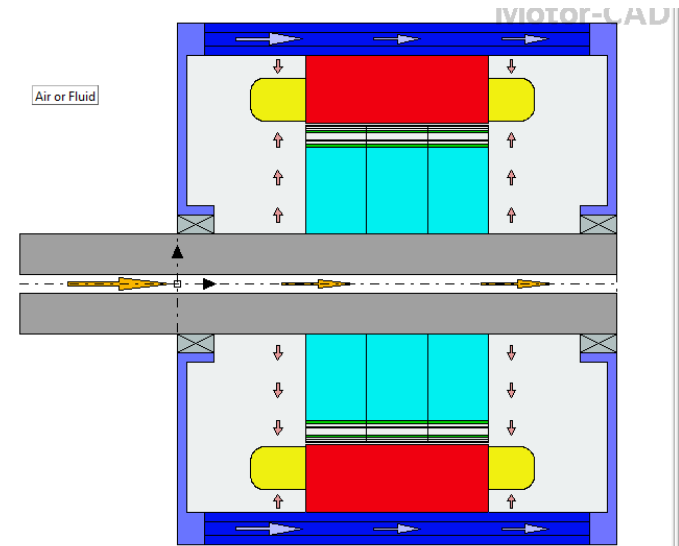
- Air is blown through the duct in the rotor and airgap by a fan
- This air is then recirculated through the housing to use this as a heat exchanger
- The system is sealed and enables rotor cooling



“The innovative traction motor of the BMW 225xe active tourer”, Advanced E-Motor Tech 2017, Dr.-Ing. A. Huber

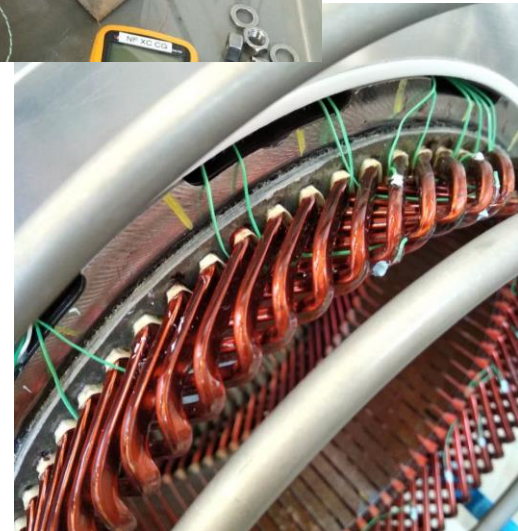
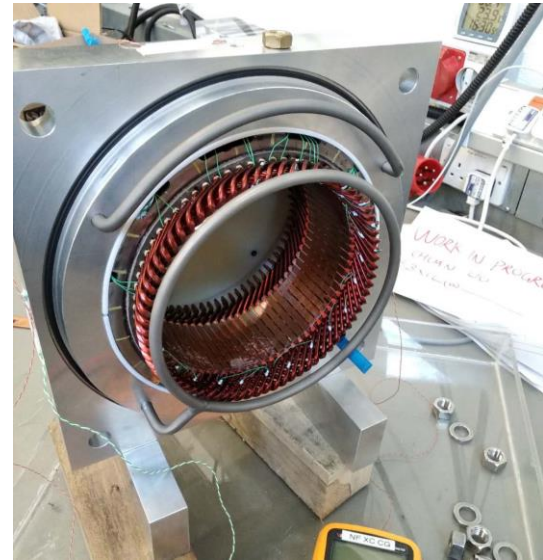
Oil Spray Cooling

- Oil passed through the shaft and thrown from the shaft onto the inner end winding surface using centrifugal force
- Oil tubes also run over the stator active section and drip oil over the outer surface of the end windings
- A sump collects the oil and passes through a heat exchanger.
- A flow rate of 4 l/min is assumed for the shaft oil and 8 l/min for the stator oil cooling with a 80°C inlet temperature
- This approach is potentially cheaper as it allows the oil cooling system to be shared with the transmission



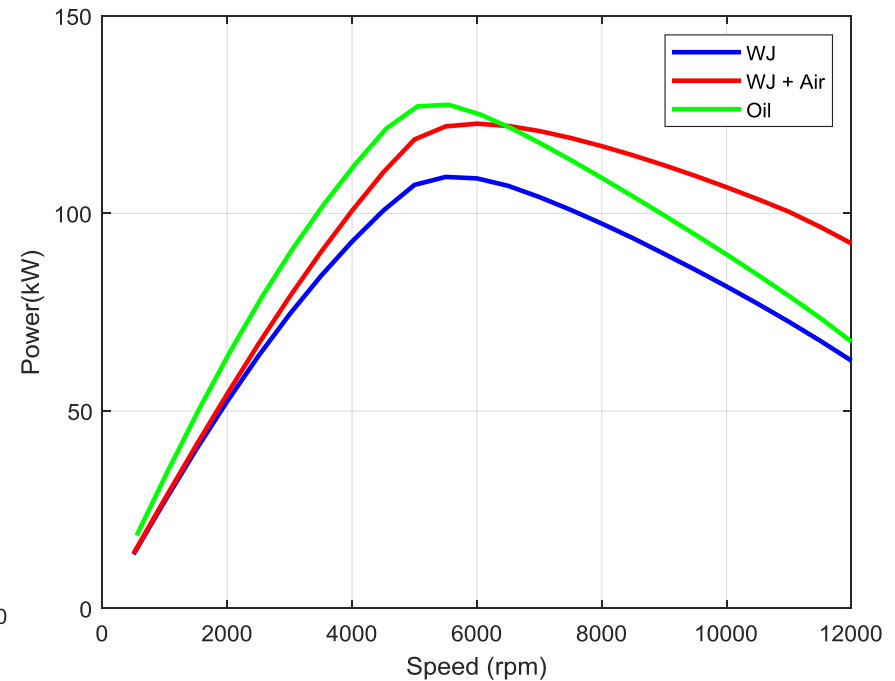
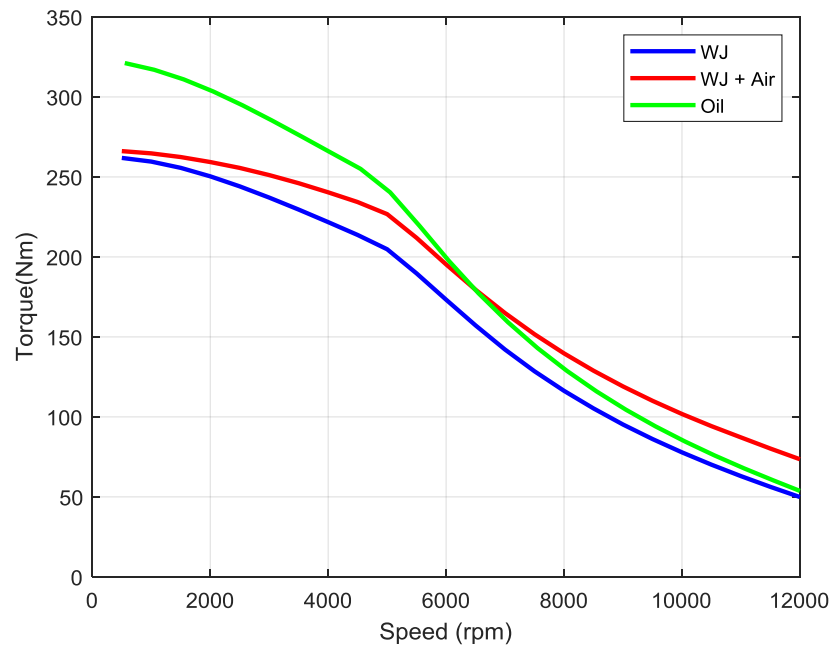
Modelling Oil Spray Cooling

- Correlations calculate heat transfer of surfaces based on surface area and oil flow rate, velocity and temperature
- Users need to define the flow path of the oil from the nozzle
- We are undertaking various research projects to test oil cooled machines, visualise the oil distribution and develop correlated models
- The types of flow investigated include, axial jets, oil drip, oil mist and oil thrown from rotor using centrifugal forces



Continuous Performance Comparison

- Oil gives best heat transfer
- At higher speeds the air cooling offer the most benefit as the internal flow rate is related to the shaft speed



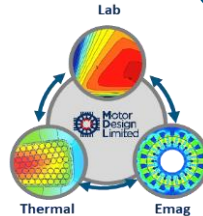
Summary

- It is tempting to draw generalised conclusions from these sort of studies but it **is often a mistake** to do so
- Small variations in the specifications and constraints can result in large differences in design decisions
- **System design is very iterative** and many different topologies and design decision need to be evaluated during the system optimisation
- On many occasions the **technical trade-offs** need to be weighed **against** other concerns such as **risk**
- Using state of the art software, motor design variations can be studied very quickly and easily enabling an optimal motor design and system configuration

Tutorial Overview

Motor Design

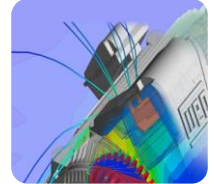
Trade-off Analysis for a BEV traction application



1. eMachine Comparison - PM, IM, Sync
2. Windings Comparison - Hairpin vs Stranded
3. Cooling Comparison - Water Jacket, Internal Air and Oil Spray

Mechanical Analysis

NVH and Mechanical Stress



4. NVH Analysis - Behaviour of Motor + Gearbox
5. Mechanical Stress Analyses - Problem formulation and Solution

Design

Analysis

4. NVH Analysis

NVH Behaviour of Motor + Gearbox

- NVH response has typically been left to the latter stages of the design process
- This can be expensive particularly if the motor and gearbox have acceptable NVH characteristics in isolation but problems occur when they are coupled
- Here we compare two interior PM motors for an EV traction application
- Consider the combined NVH response of the motor & gearbox

Motor Specification

Two interior PM (IPM) machines have been designed to meet the given specification

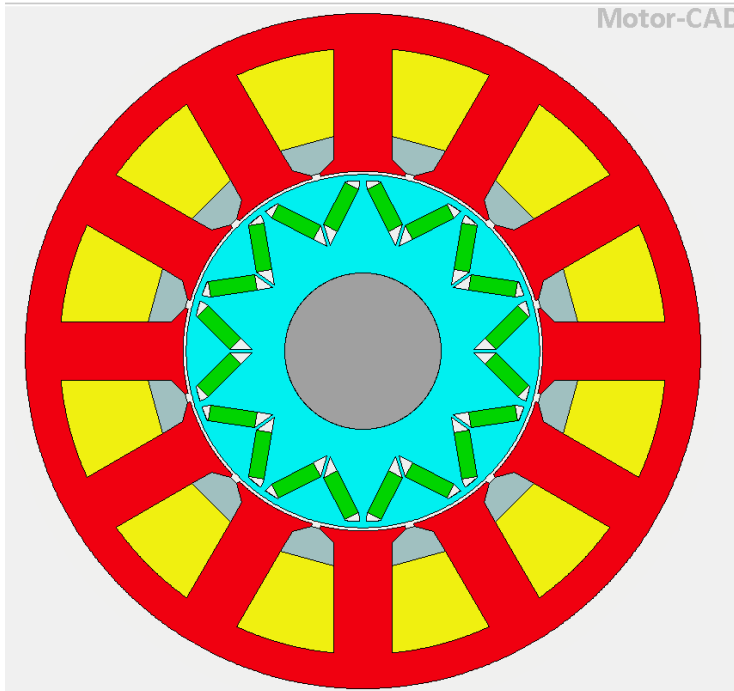
- 12 slot 10 pole design
- 12 slot 8 pole design

Same stator OD & axial length

Specification	
Peak Torque	160Nm
Peak Power	70kW
DC Link Voltage	400Vdc
Continuous Torque	80Nm
Stator Outer Diameter	216mm
Cooling system	TENV
Maximum speed	12,000rpm

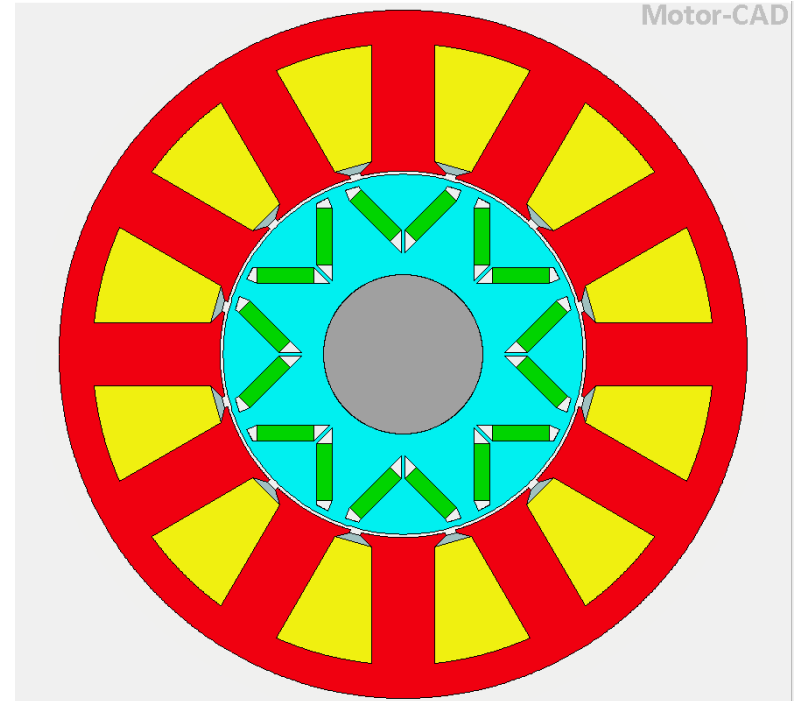
4. NVH Analysis

12 slot 10 pole



12 slot 10 pole machines have some favourable characteristics however they are well known for NVH issues

12 slot 8 pole



12 slot 8 pole (1.5 slots per pole) machines are a commonly used topology but can exhibit high levels of torque ripple and voltage harmonics

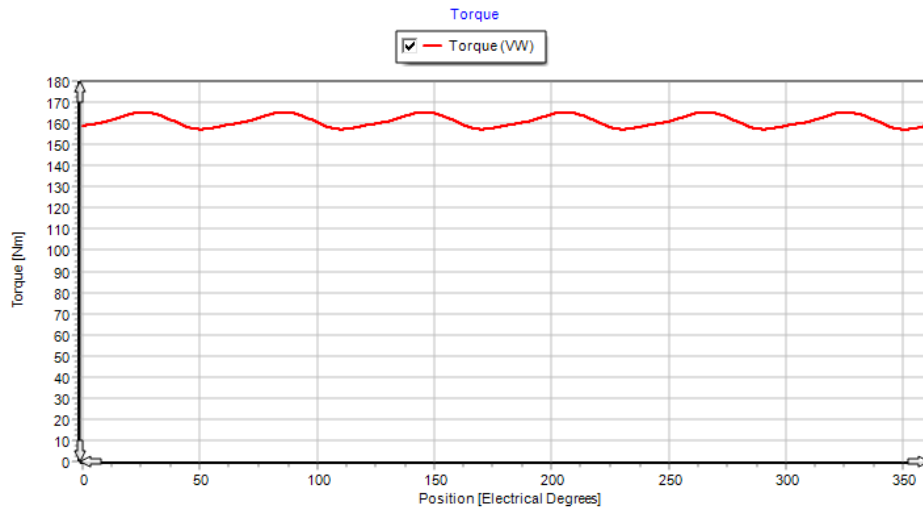
4. NVH Analysis

Design Comparison – Torque Ripple Low Speed

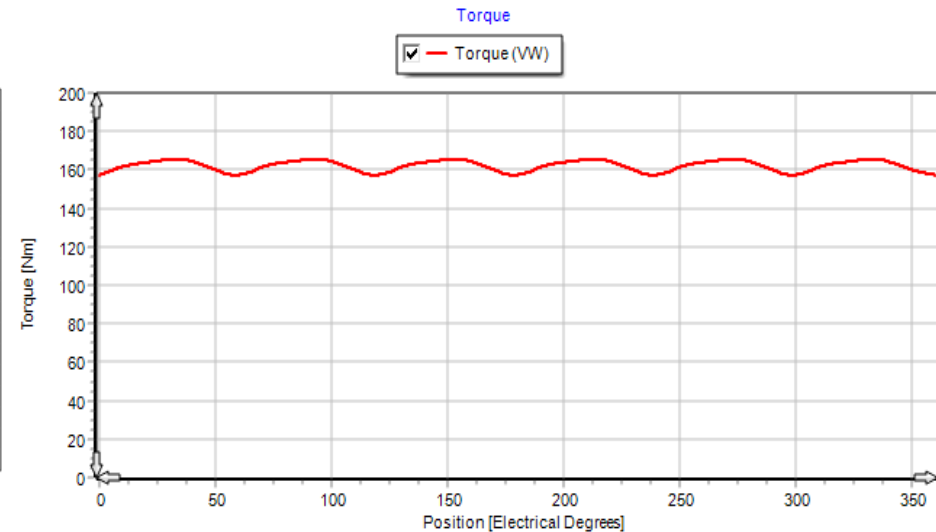
160Nm, 500rpm:

12/10 – 4.78% ripple

12/8 – 4.81% ripple



12 slot 10 pole



12 slot 8 pole

4. NVH Analysis

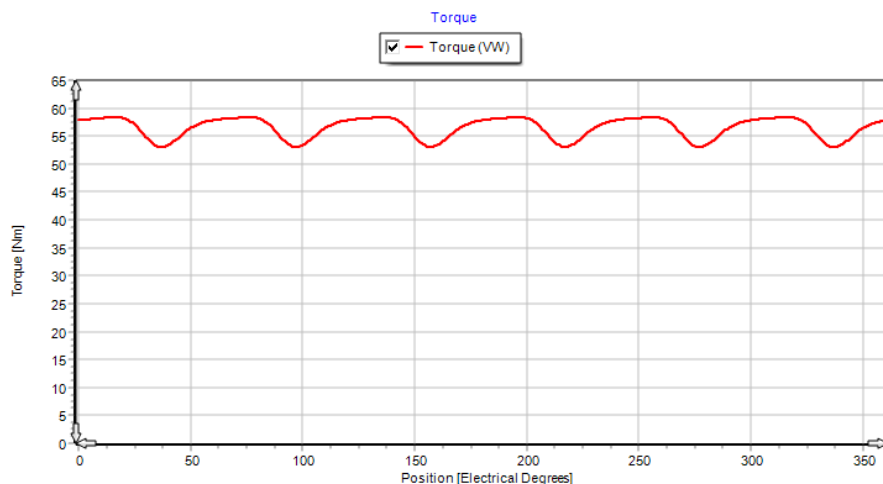
Design Comparison – Torque Ripple High Speed

60Nm, 12,000rpm:

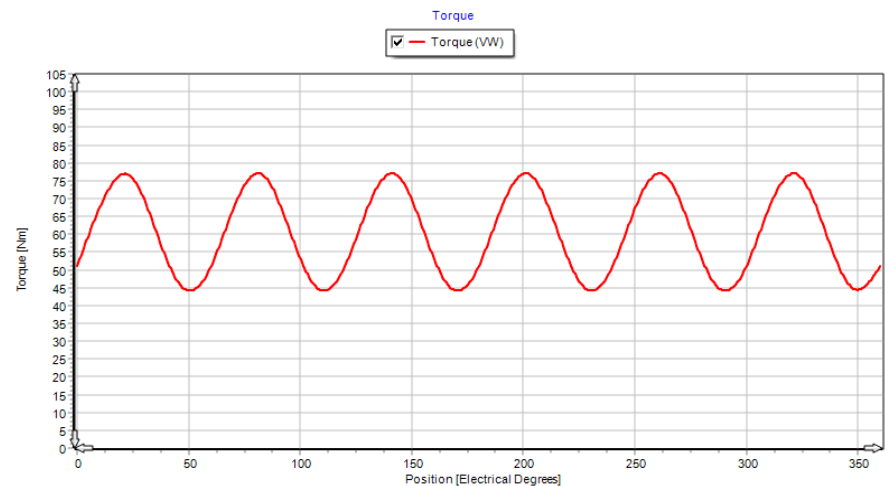
12/10 – 9.1% ripple

12/8 – 51% ripple

Torque ripple at higher speeds is larger for the 12/8 design



12 slot 10 pole

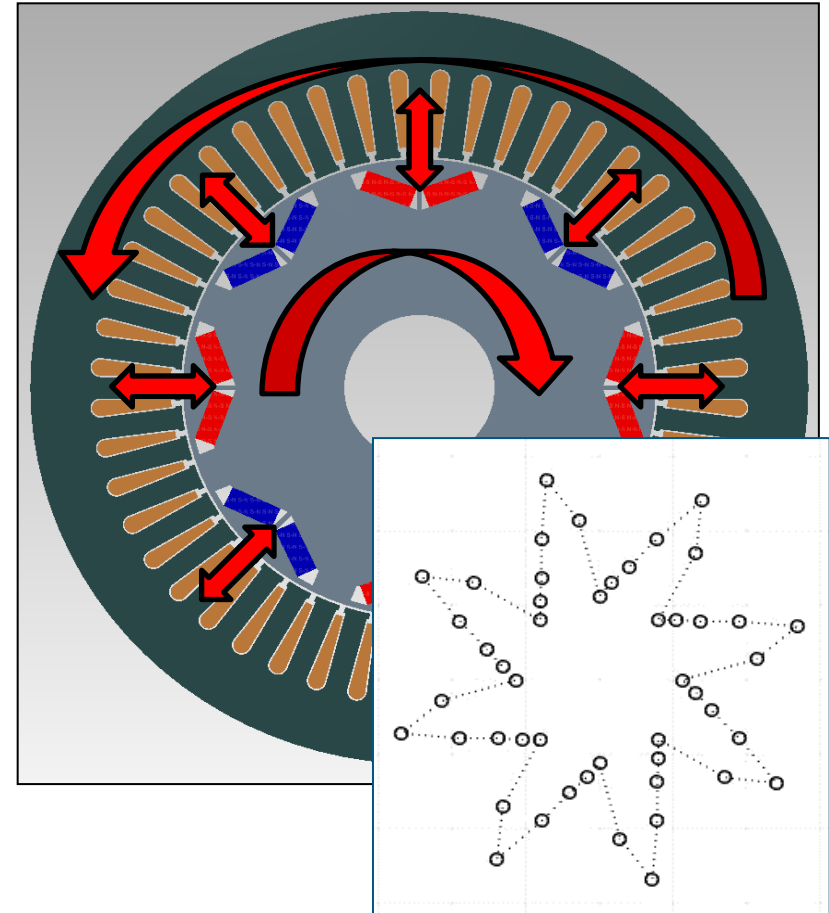


12 slot 8 pole

Motor noise mechanisms

- 1) Torque ripple
 - Equal and opposite torque on rotor and stator
- 2) Radial forces
 - Act between rotor and stator
 - Forces on rotor cancel out

Forces on stator generate complex force shapes

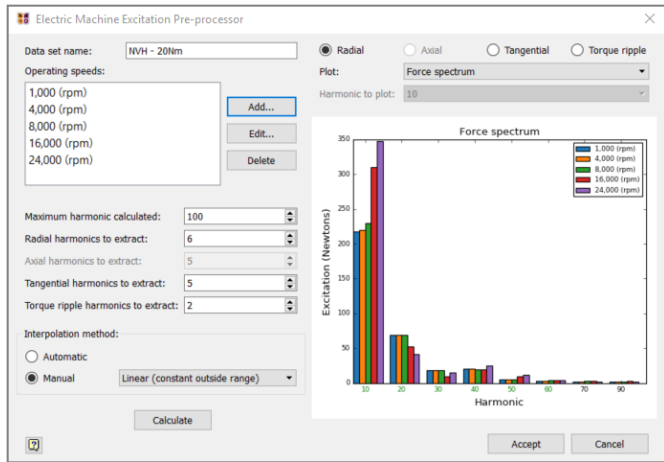


Analysis 4. NVH Analysis

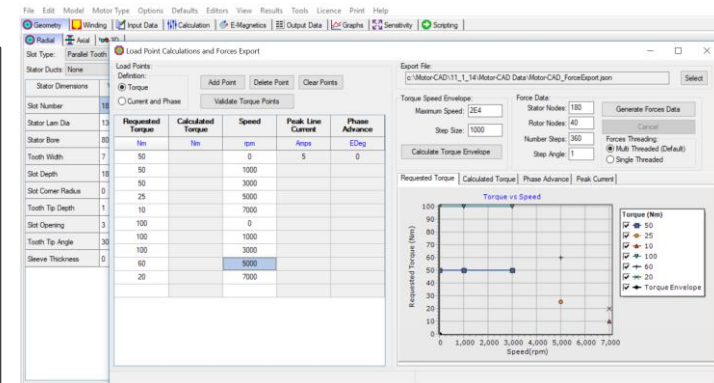
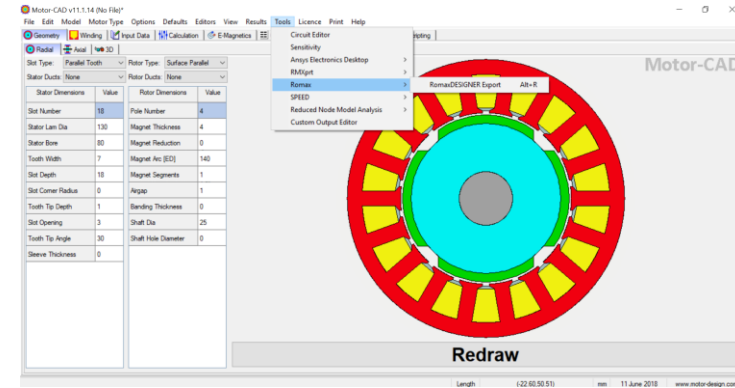
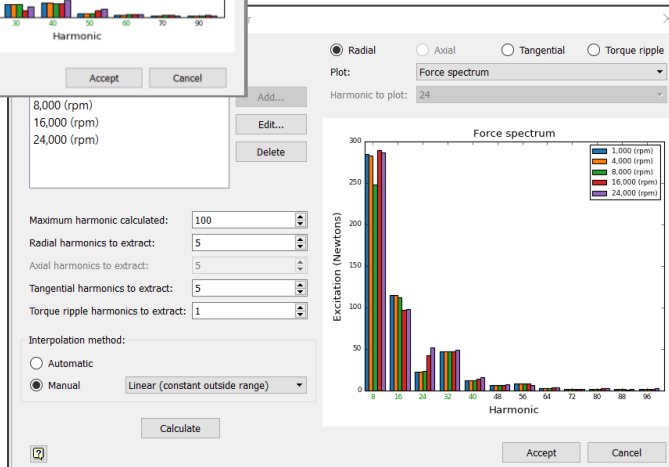
Import machine excitations into RomaxDesigner

- Radial Force excitations are of similar magnitude, fundamental is highest for both motors
- 12/10 has slightly higher fundamental (10th Harmonic) in field weakening (at high speed)

12/10 excitation data



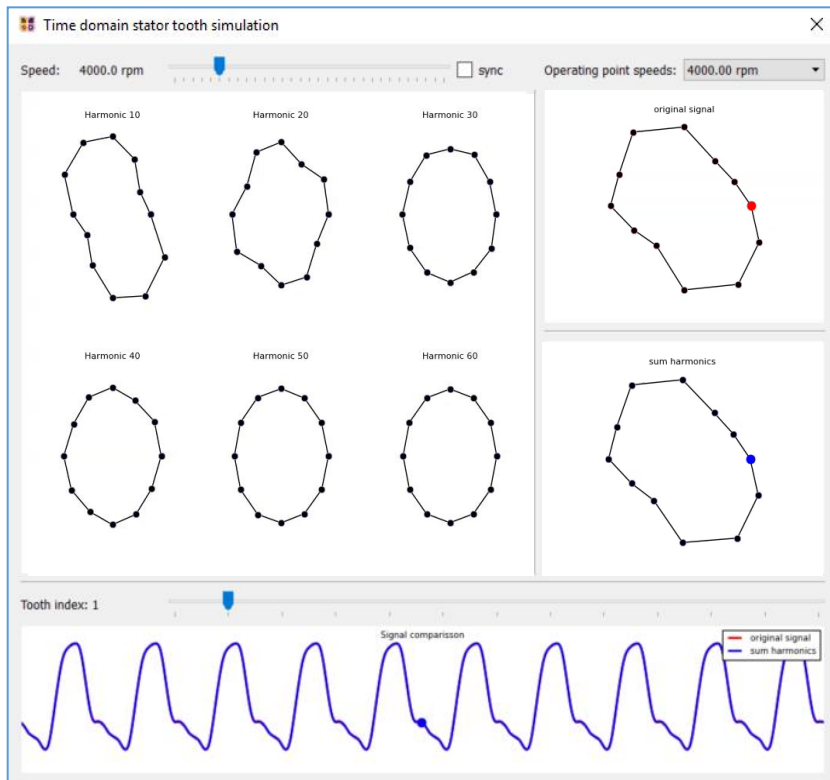
12/8 excitation data



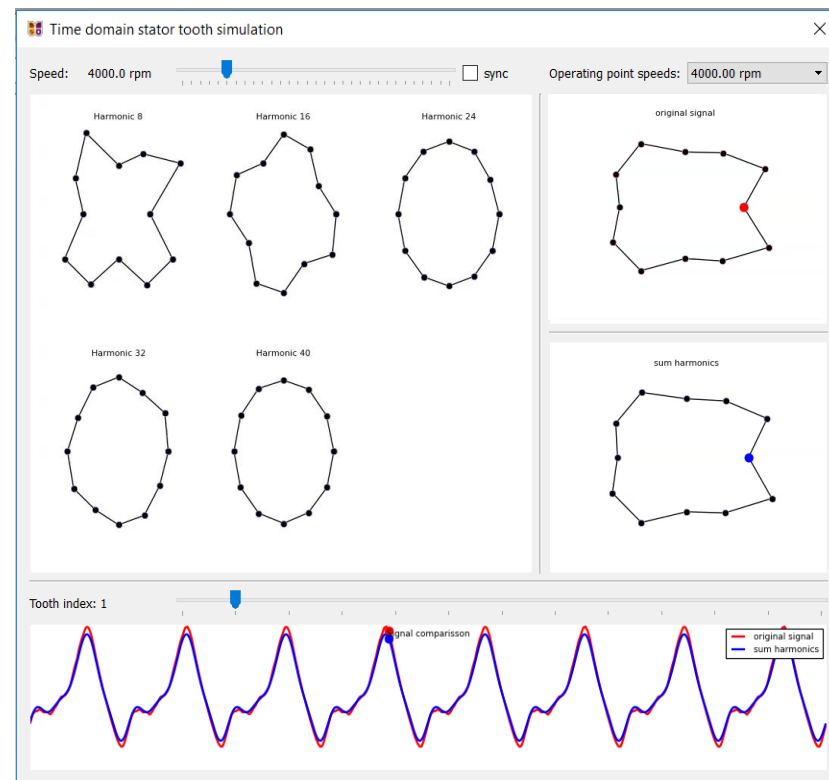
4. NVH Analysis

Imported excitation data – 12/10 vs. 12/8

12/10 excitation data



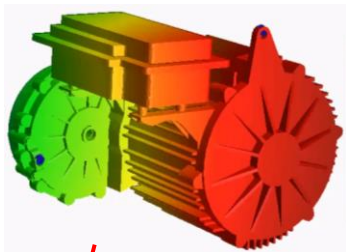
12/8 excitation data



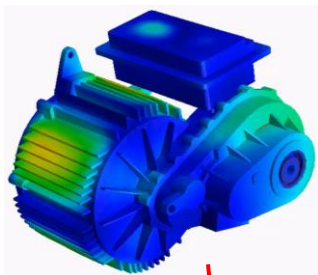
Analysis 4. NVH Analysis

Comparison of machine response

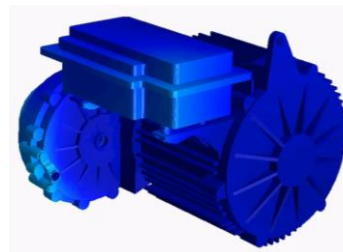
10th harmonic radial
128 rpm



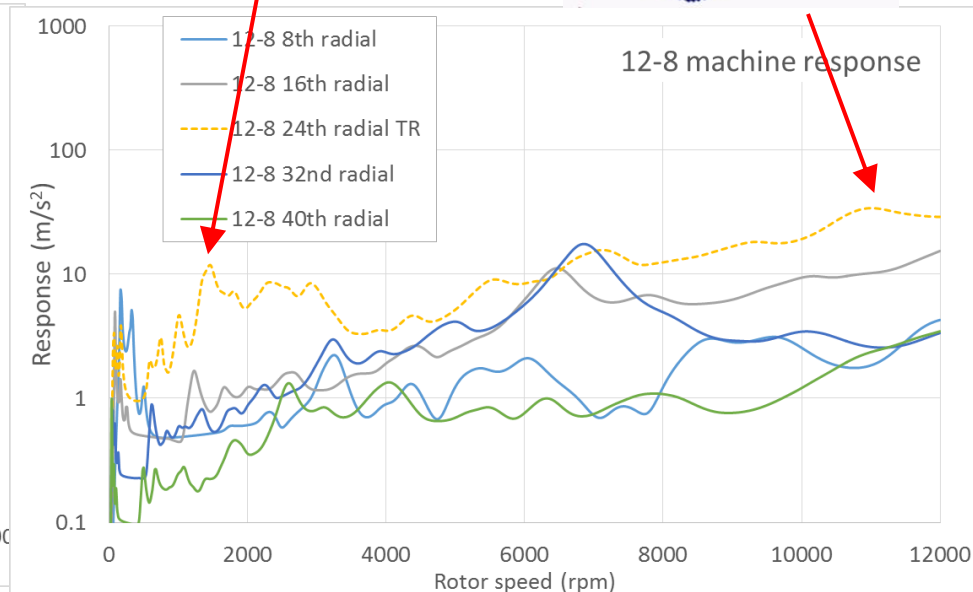
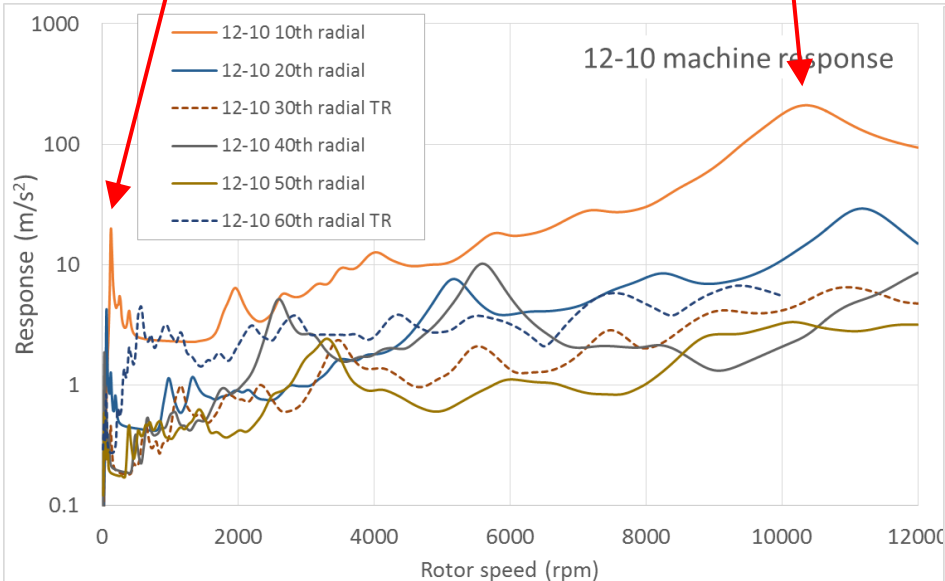
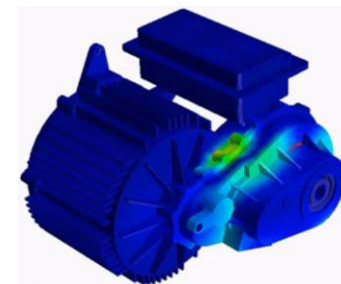
10th harmonic radial
10500 rpm



24th harmonic radial/TR
1488 rpm



24th harmonic radial/TR
11000 rpm



Summary

Comparing both traction motors using the excitation data (electromagnetic analysis alone) shows:

- **12/8** machine has highest torque ripple, particularly in field weakening region (high speed)
- **12/10** machines has slightly higher radial force magnitude, particularly in field weakening region

Using the combined Motor-CAD and RomaxDesigner solution we can identify the preferred traction motor for the drivetrain

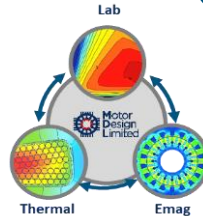
- **12/8** machine preferred candidate for NVH performance across speed range
- **12/10** machine may be preferred for performance sub-40kph

Analysis of system NVH response is required - Hard to judge based on excitation alone

Tutorial Overview

Motor Design

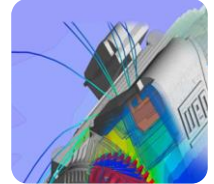
Trade-off Analysis for a BEV traction application



1. eMachine Comparison - PM, IM, Sync
2. Windings Comparison - Hairpin vs Stranded
3. Cooling Comparison - Water Jacket, Internal Air and Oil Spray

Mechanical Analysis

NVH and Mechanical Stress



4. NVH Analysis - Behaviour of Motor + Gearbox
5. **Mechanical Stress Analyses - Problem formulation and Solution**

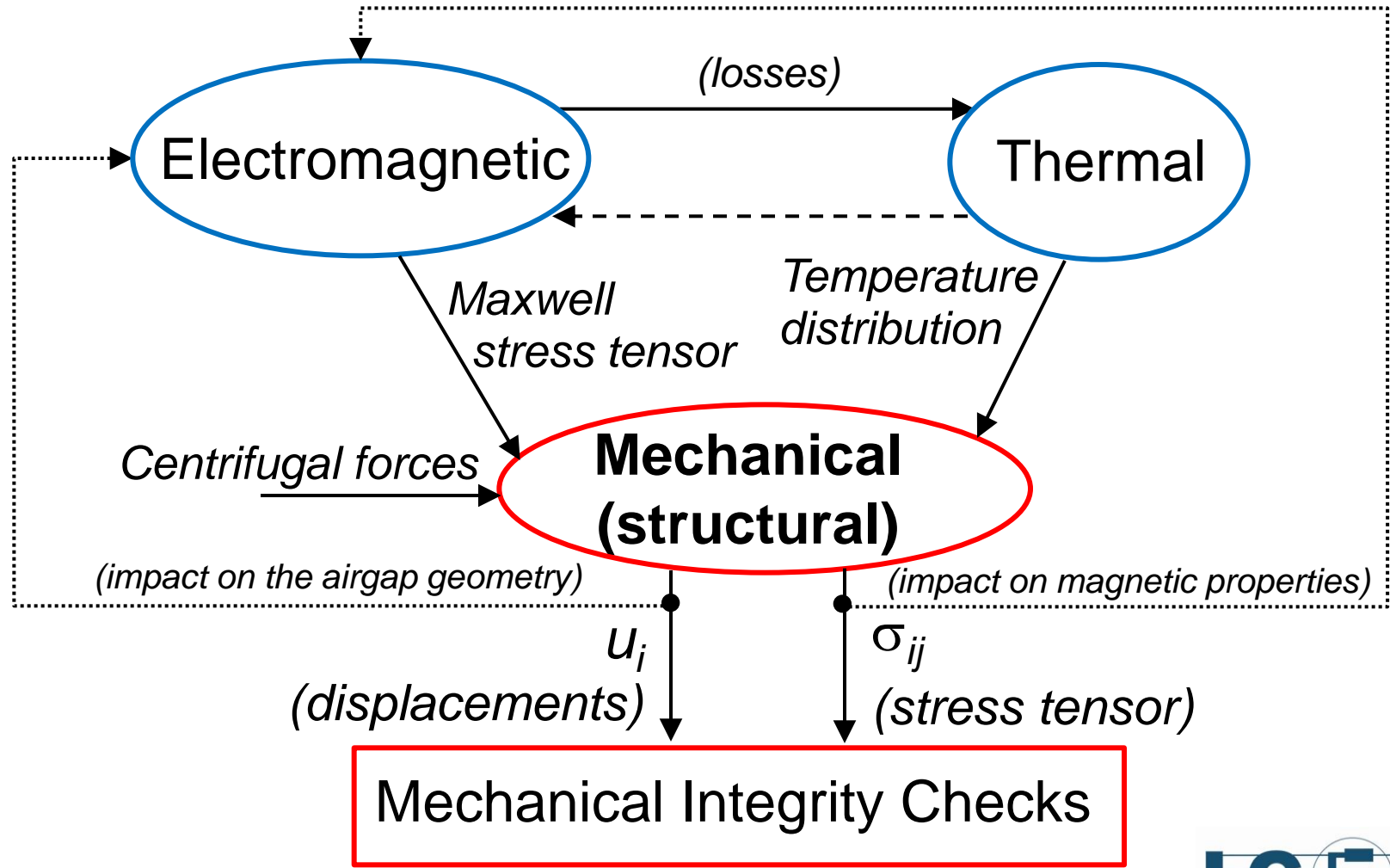
Design

Analysis

Overview

- Objectives
 - Evaluate the stress level
 - Calculate the displacements (deformation)
 - Evaluate the vibration modes
 - Verify the EM integrity against mechanical failure
 - Inspire optimised design for power density (structural mass may count for more than 50% of the overall mass)
- Formulation
 - Load and material
 - Strain – displacement
 - Boundary conditions
- Solution approach
 - Analytic
 - FE
- Post-processing
 - Checks against failure

5. Mechanical Stress Analysis Flowchart



Formulation

- General [1] (u_i =displacement, σ_{ij} = stress tensor, ΔT = temperature rise)

$$\operatorname{div}(\sigma_{ij}) + F_i = 0 \quad \text{Local equilibrium under volume force } F_i$$

$$e_{ij} = e_{ij}(u_i, \Delta T) \quad \text{Deformation model (strain definition)}$$

$$\sigma_{ij} = \sigma_{ij}(e_{ij}, \Delta T) \quad \text{Material model}$$

$$\sigma_{ij} n_j = p_i \quad \text{or} \quad u_i = \bar{u}_i \quad \text{Boundary conditions (prescribed force or displ.)}$$

- Particularisation for linear isotropic elasticity (Hooke's Law) & small displacements [2]

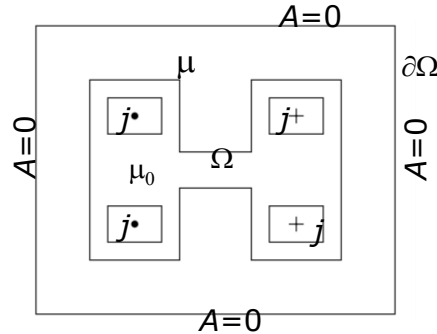
$$e_{ij} = \varepsilon_{ij} = \frac{1}{2} \left(\frac{\partial u_i}{\partial x_j} + \frac{\partial u_j}{\partial x_i} \right) \quad \text{Strain tensor}$$

$$\sigma_{ij} = \frac{E\nu}{(1+\nu)(1-2\nu)} \varepsilon_{kk} \delta_{ij} + \frac{E}{1+\nu} \varepsilon_{ij} - \frac{E}{1-2\nu} \alpha \Delta T \delta_{ij}$$

5. Mechanical Stress Analysis

Formulation: magneto-static vs linear elasticity (2D)

Magnetostatic linear 2D



Main unknowns:

$$A_z = A = A(x, y) \quad (\text{vector potential})$$

PDE formulation:

$$\Delta A = -\mu j \quad \text{in } \Omega$$

Boundary conditions:

$$A = 0 \quad \text{on } \partial\Omega$$

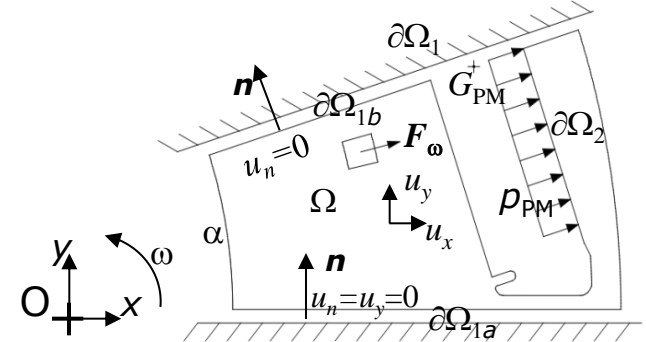
Material model:

$$H_x = \frac{B_x}{\mu}, \quad H_y = \frac{B_y}{\mu}$$

Derived quantities:

$$B_x = \frac{\partial A}{\partial y}, \quad B_y = -\frac{\partial A}{\partial x} \quad (\text{flux density components})$$

Linear elasticity 2D



$$\mathbf{u} = (u_x, u_y) \quad (\text{displacements})$$

$$\begin{cases} \frac{E}{1-\nu^2} \left\{ \frac{\partial^2 u_x}{\partial x^2} + \frac{1+\nu}{2} \frac{\partial^2 u_y}{\partial x \partial y} + \frac{1-\nu}{2} \frac{\partial^2 u_x}{\partial y^2} \right\} = F_{\omega x} \\ \frac{E}{1-\nu^2} \left\{ \frac{1+\nu}{2} \frac{\partial^2 u_x}{\partial x \partial y} + \frac{\partial^2 u_y}{\partial y^2} + \frac{1-\nu}{2} \frac{\partial^2 u_y}{\partial x^2} \right\} = F_{\omega y} \end{cases} \quad \text{in } \Omega$$

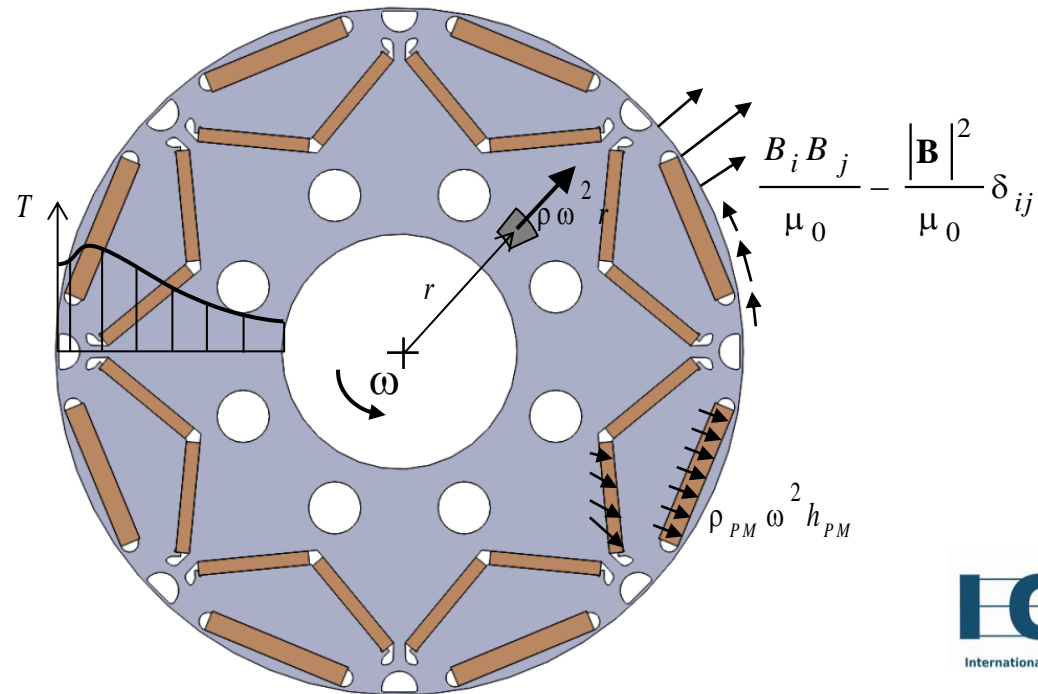
$$\mathbf{u}_n = 0 \quad \text{on } \partial\Omega_1, \quad \boldsymbol{\sigma} \cdot \mathbf{n} = \mathbf{p} \quad \text{on } \partial\Omega_2$$

$$\begin{bmatrix} \sigma_x \\ \sigma_y \\ \tau_{xy} \end{bmatrix} = \frac{E}{1-\nu^2} \begin{bmatrix} 1 & \nu & 0 \\ \nu & 1 & 0 \\ 0 & 0 & 1-\nu \end{bmatrix} \begin{bmatrix} \epsilon_x \\ \epsilon_y \\ \epsilon_{xy} \end{bmatrix}$$

$$\epsilon_x = \frac{\partial u_x}{\partial x}, \quad \epsilon_y = \frac{\partial u_y}{\partial y}, \quad \gamma_{xy} = \frac{\partial u_y}{\partial x} + \frac{\partial u_x}{\partial y} \quad (\text{strain components})$$

Loads

- Centrifugal (volume) forces $\rho\omega^2 r$
- Centrifugal (surface) forces transmitted by PMs to the core.....or contact constraints (non-linear!)
- Temperature gradients \Rightarrow thermal stresses
- Initial stresses, e.g. shrink-fit, manufacturing processes (?)
- Electromagnetic normal & tangential (surface) forces (from Maxwell Tensor)



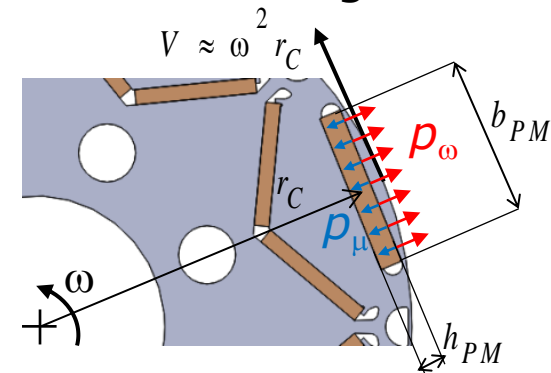
5. Mechanical Stress Analysis

Loads

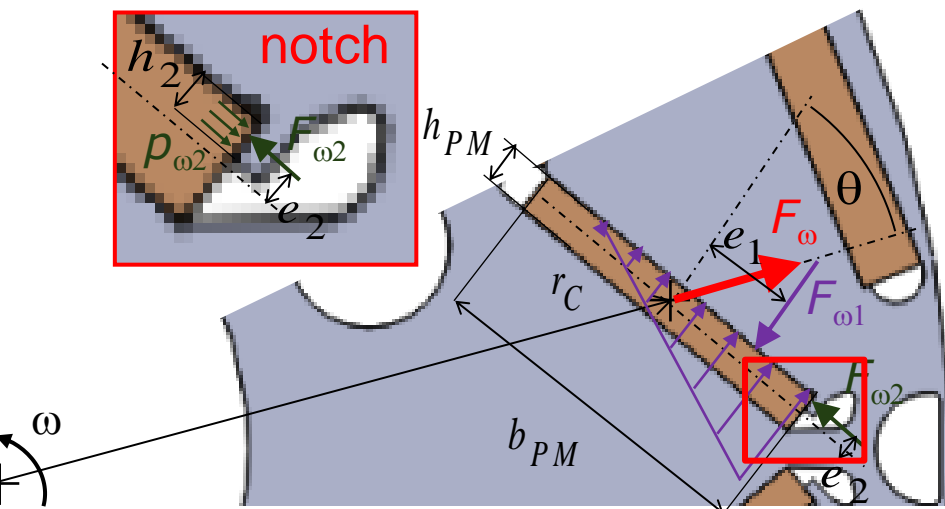
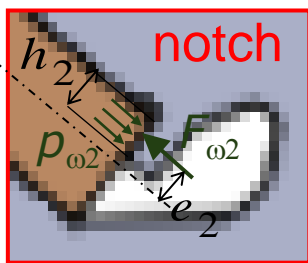
- In high-speed rotors, centrifugal forces dominate the electromagnetic forces (especially in PM pockets)

$$p_{\mu} = \frac{B^2}{2\mu_0} = \frac{1^2 \times 10^7}{2 \times 4\pi} \approx 0.4 \text{ MPa}$$

$$p_{\omega} = \rho_{PM} \omega^2 r_C h_{PM} \approx \rho_{PM} V^2 \frac{h_{PM}}{r_C} = 8000 \times 100^2 \frac{4}{70} \approx 4.6 \text{ MPa}$$



- To avoid contact formulation, PM centrifugal forces can be converted into pressure distributions on two active surfaces 1 & 2 (PM slot "roof")



$$F_{\omega} = \rho_{PM} \omega^2 r_C b_{PM} h_{PM}, \quad F_{\omega 1} = F_{\omega} \sin \theta, \quad F_{\omega 2} = F_{\omega} \cos \theta$$

$$e_2 = \frac{h_{PM} - h_2}{2}, \quad e_1 = \frac{F_{\omega 2} e_2}{F_{\omega 1}}$$

$$p_{\omega 2} \approx \frac{F_{\omega 2}}{h_2}, \quad p_{\omega 1} \approx \begin{cases} \text{triangular} & \text{if } e_1 > b_{PM} / 6 \\ \text{trapezoidal} & \text{if } e_1 \leq b_{PM} / 6 \end{cases}$$

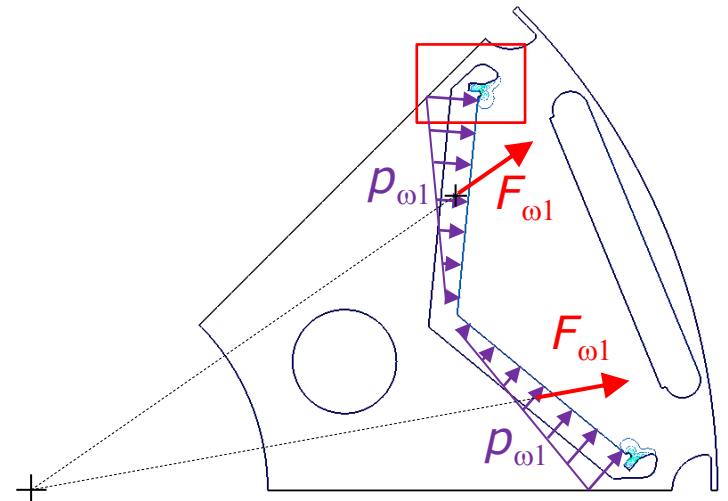
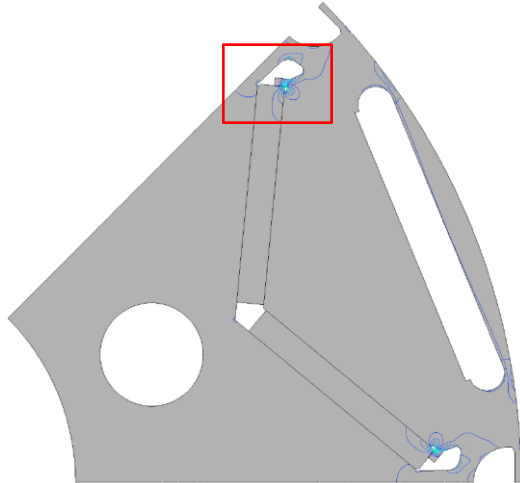
5. Mechanical Stress Analysis

PM Contact vs equivalent pressure (Nissan Leaf)

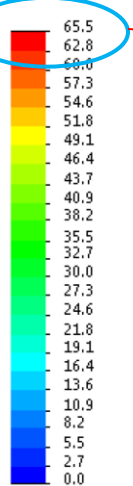
Centrifugal forces on inner PMs only, 6000 rpm

Contact constraints (Solidworks)

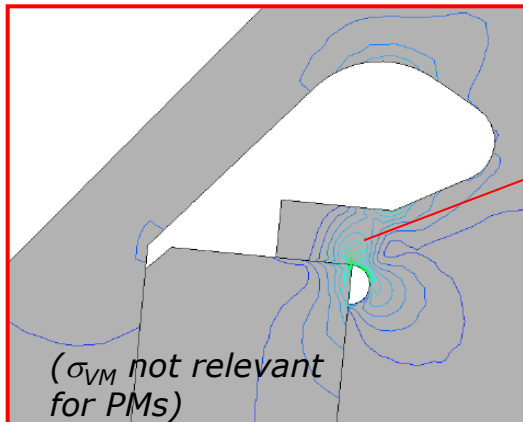
Equivalent pressure (FreeFem++)



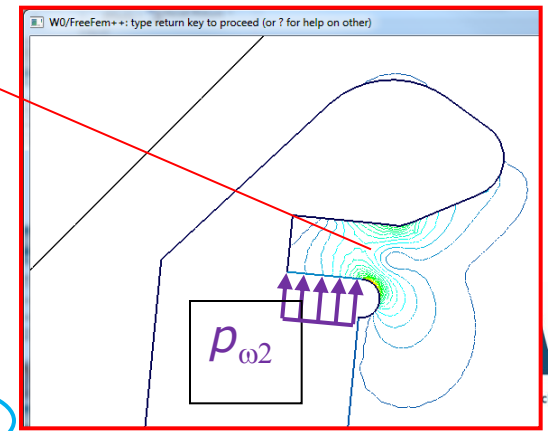
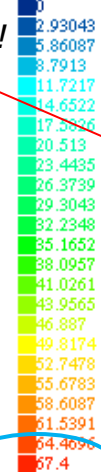
von Mises [N/mm² (MPa)]



Fairly accurate Von Mises stress σ_{VM} around the notch!



IsoValue

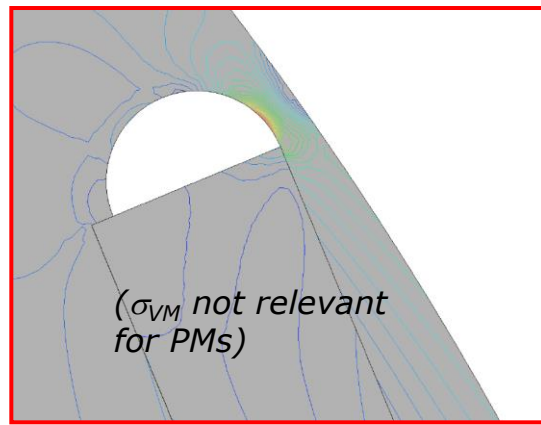
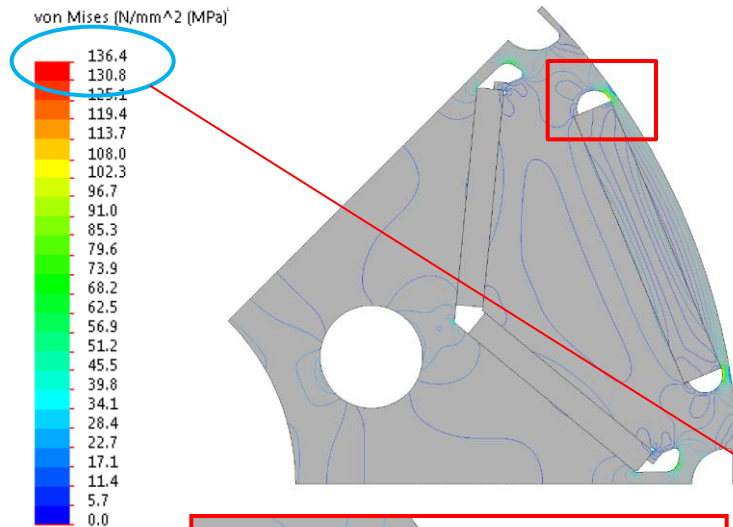


5. Mechanical Stress Analysis

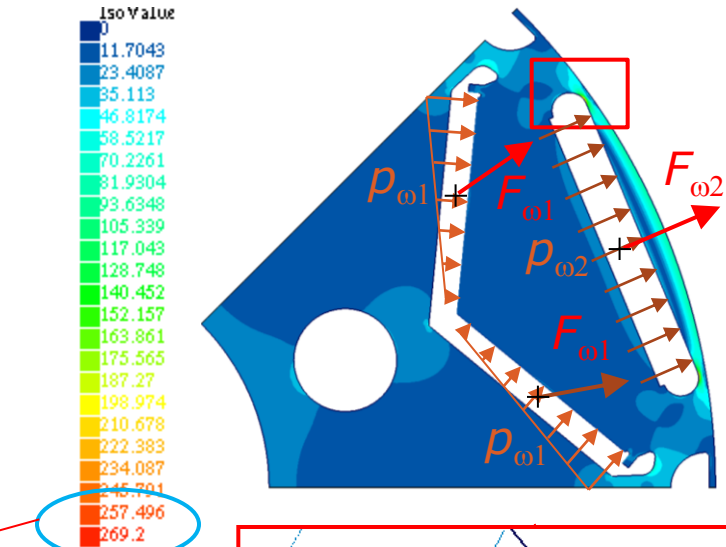
PM Contact vs equivalent pressure (Nissan Leaf)

Centrifugal forces on PMs and core, 6000 rpm

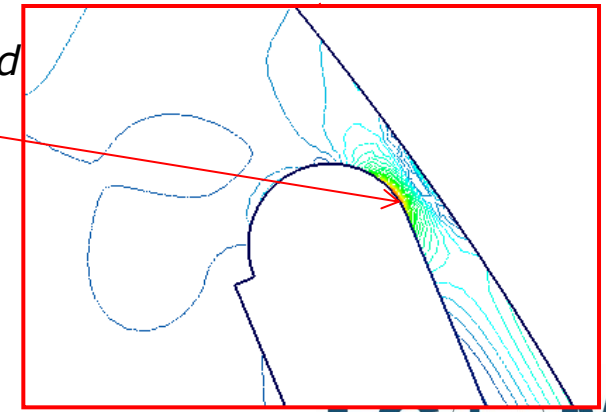
Contact constraints (Solidworks)



Equivalent pressure (Freefem++)



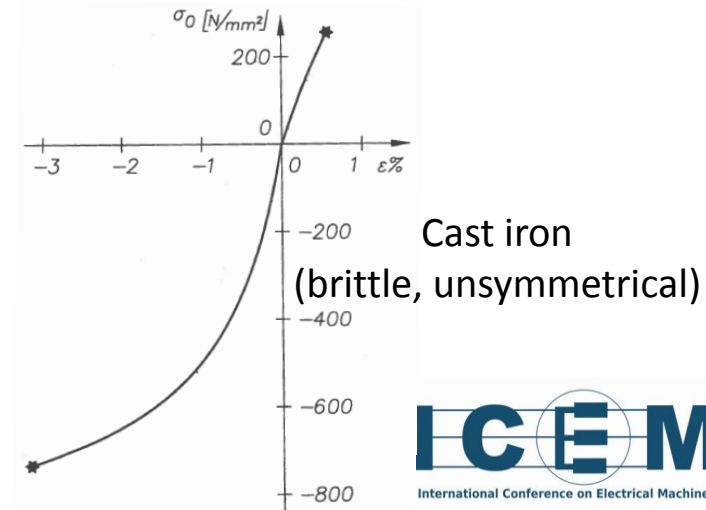
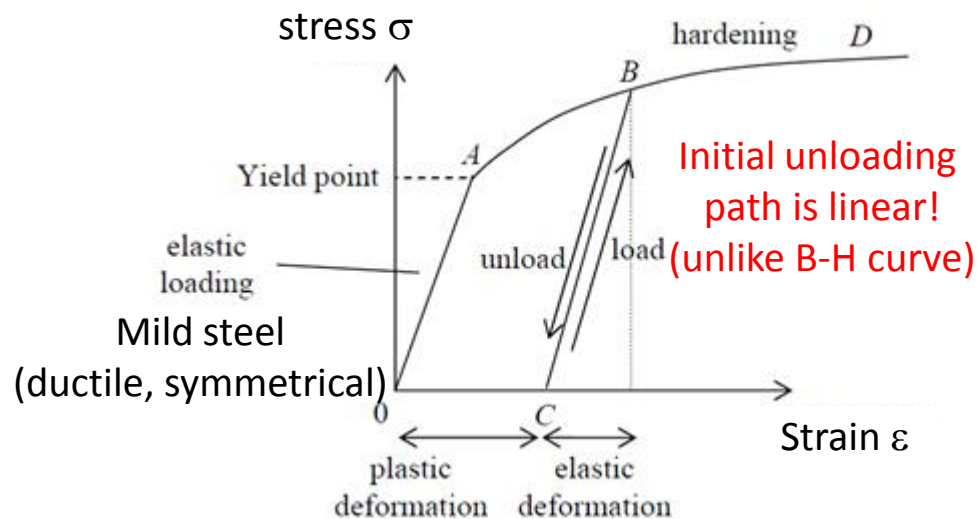
Stress overestimated on the outer fillets



- ❑ If the iron bridge is very thin, pressure distribution $p_{\omega 2}$ is not uniform!
- ❑ Need to include the contribution of the PM to the bridge stiffness to find $p_{\omega 2}$

Materials

- Linear elastic model adequate for ductile materials below the yield stress
- PM materials (brittle) may have different Young's modulus under tensile and compression stress
- Laminated cores are anisotropic....but do you know the properties along z-axis?!?
- Composite materials (fibre) require anisotropic models
- Progressive collapse analysis (if required) needs non-linear models for ductile materials (plasticity)

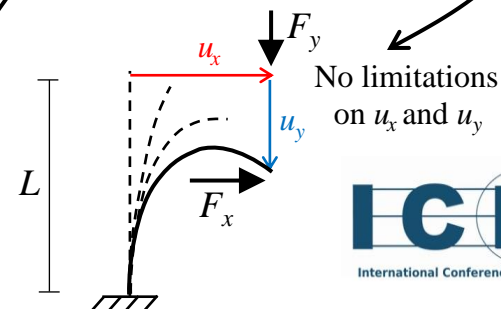
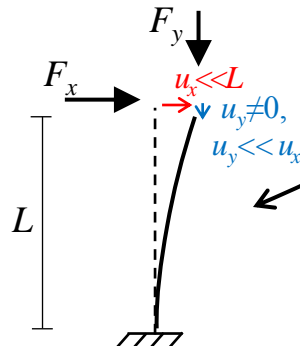
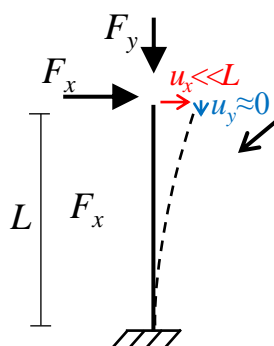


5. Mechanical Stress Analysis

Strain model and load setup

- Non-linearity (geometric) and need for iterative solution can arise from the deformation model, even with linear materials
- "Small displacements" \Rightarrow the relationship $e_{ij}(u_i)$ is linearised
- Loads can be applied to either the undeformed or deformed configuration (\Rightarrow geometric non-linearity)

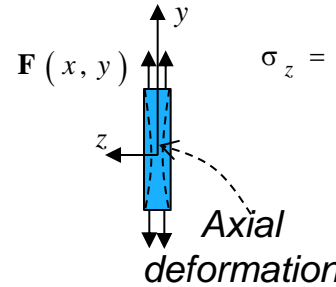
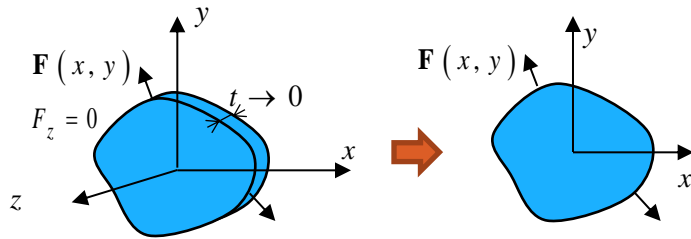
Strain model:	<i>Small displacements</i>	<i>Large displacements</i>
Loads evaluated with:		
<i>Un-deformed configuration</i>	Checks against failure in "rated" conditions (no iteration)	-----
<i>Deformed configuration</i>	Instability Contact Progressive collapse (iterative)	Instability Contact Progressive collapse (iterative)



5. Mechanical Stress Analysis

Reduction to 2D models: plane stress vs plane strain

- Plane stress: thin disc & loads only in the x-y plane $\Rightarrow \sigma_z \approx 0$

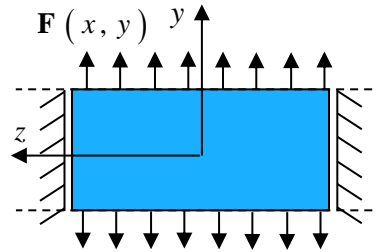
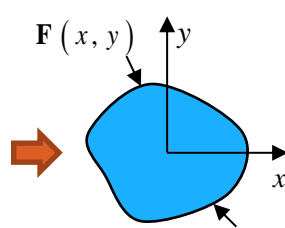
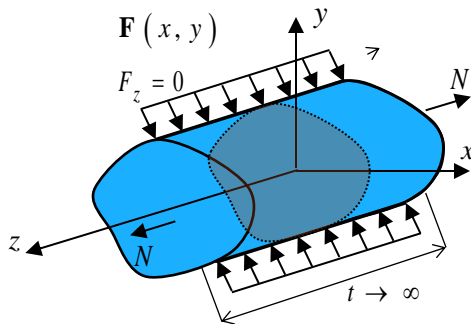


$$\sigma_z = \frac{E}{(1+\nu)(1-2\nu)} (\nu \varepsilon_x + \nu \varepsilon_y + (1-\nu) \varepsilon_z) = 0$$

$$\varepsilon_z = -\frac{\nu}{1-\nu} (\varepsilon_x + \varepsilon_y) \neq 0$$

$$u_z = \int_A \varepsilon_z dz \neq 0!$$

- Plane strain: infinitely long prisms & constant load along z $\Rightarrow \varepsilon_z = 0$

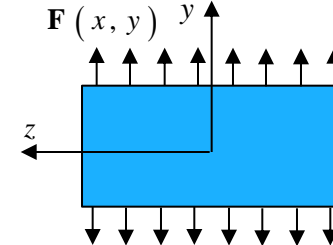
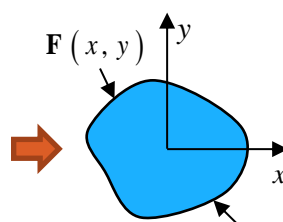
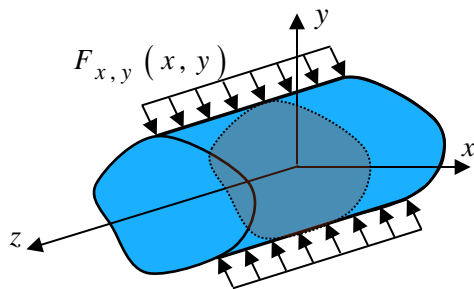


$$\varepsilon_z = \frac{1}{E} (-\nu \sigma_x - \nu \sigma_y + \sigma_z) = 0$$

$$\sigma_z = \nu (\sigma_x + \sigma_y) \neq 0$$

$$N = \int_A \sigma_z dA \neq 0!$$

- Generalised plane strain: as the previous one but with $\varepsilon_z = \varepsilon_{z0} = \text{const.}$ so $N=0$



$$\varepsilon_{z0} = -\frac{\nu}{E} \frac{1}{A} \int_A (\sigma_x + \sigma_y) dz$$

$$\sigma_z = \nu (\sigma_x + \sigma_y) + E \varepsilon_{z0} \neq 0$$

$$N = \int_A \sigma_z dA = 0!$$

The solution is accurate only in the mid section $z=0$ far away from the ends

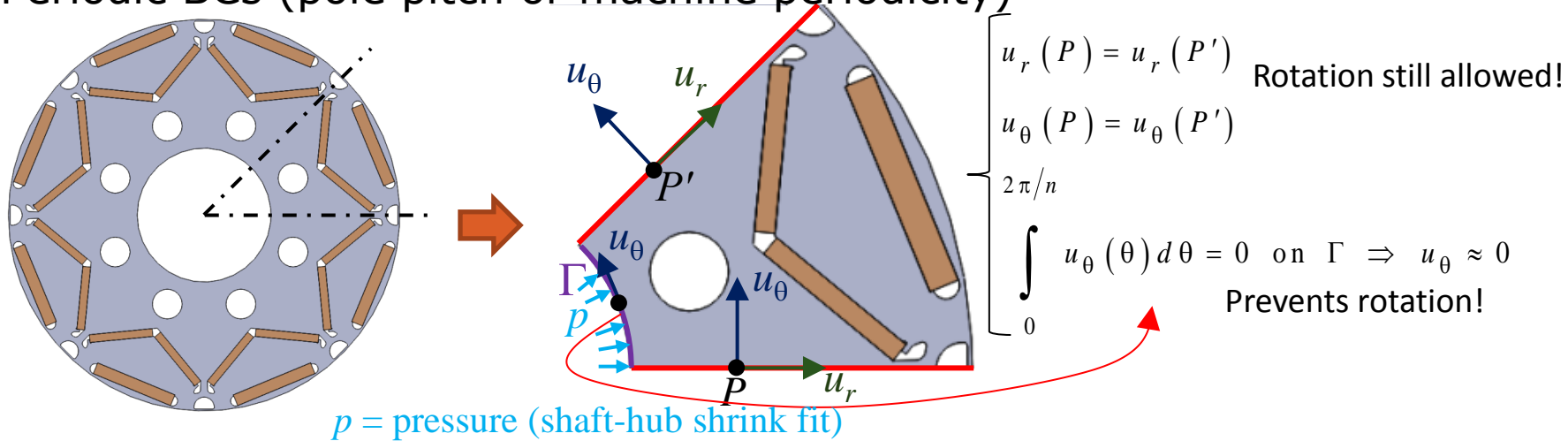
Boundary conditions

- In static models, appropriate boundary conditions (BCs) are to be set in order to stop any rigid motion (for non-singular stiffness matrix)
- BCs must represent the real constraints without introducing extra stiffness
- 2D models cannot include shaft ends and bearings & coupling, so they need alternative BCs to stop rigid movement of the rotor
 - periodic BCs + zero average tangential displacement at the inner radius (viable only if the machine periodicity is a submultiple of 2π)
 - zero average horizontal, vertical and tangential displacements at the inner radius (may be tricky to enforce!)
 - The zero average tangential displacement condition may be replaced by zero tangential displacement
 - The shrink-fit shaft/hub is represented by a constant pressure at the inner surface of the hub

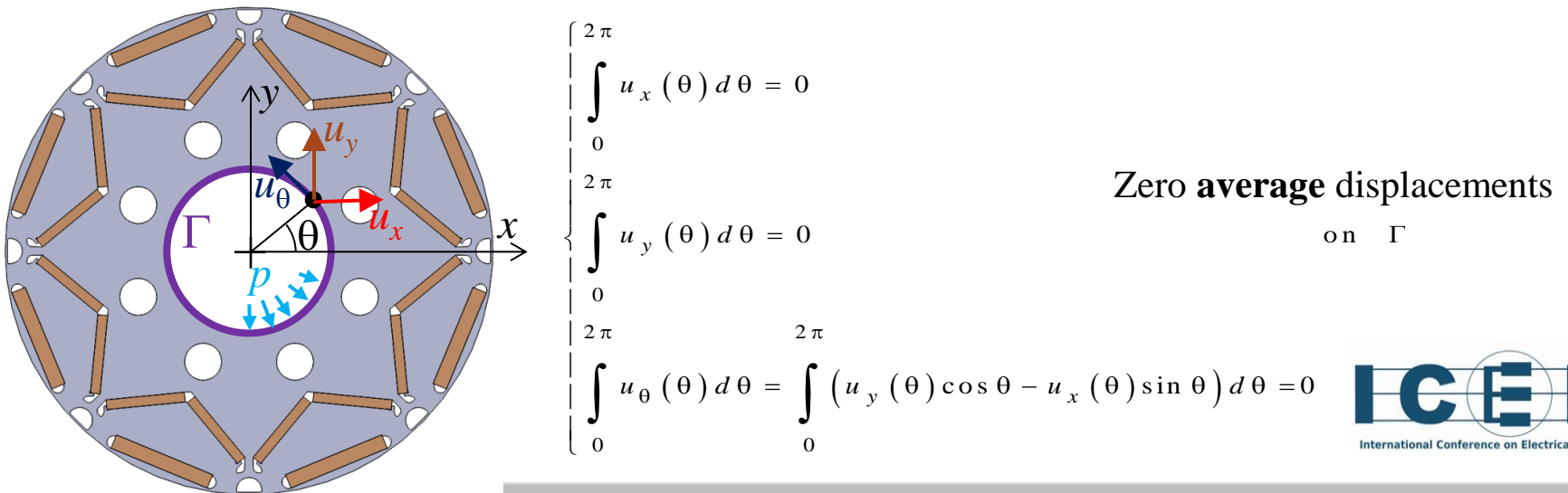
5. Mechanical Stress Analysis

Boundary conditions: 2D models

- Periodic BCs (pole pitch or machine periodicity)



- General BCs (... 2π -periodicity, e.g. machines with UMP...)



Verification of critical conditions

- Static failure
 - static loads or limited number of cycles (≤ 1000)
- Fatigue
 - Varying (periodic) loads with high number of cycles ($> 10^3$)
- Decompression / sliding in shrink fits
- Critical speeds (rotor-dynamics)
- Maximum displacement
 - Airgap clearance
- (*Instability*)
 - *Slender geometries (e.g. stators with thin back-iron depth)*
- (*Plastic collapse*)
 - *Assess ultimate strength for increasing loads*

5. Mechanical Stress Analysis

Static failure

- A generic 3D stress combination (tensor) is fully represented in terms of principal stresses $\{\sigma_I, \sigma_{II}, \sigma_{III}\}$
- Needs a criterion to compare a generic stress combination with data from standard uni-axial (1D) tensile stress tests
- Formulations depend on the behaviour of each material

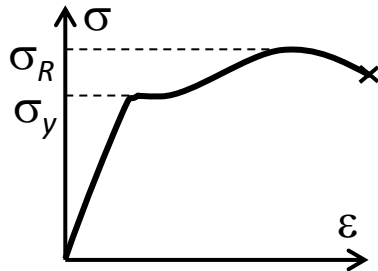
Ductile

(metal alloys - except when $\sigma_I \approx \sigma_{II} \approx \sigma_{III} > 0!$)



Von Mises:

$$\sigma_{VM} = \sqrt{\frac{(\sigma_I - \sigma_{II})^2 + (\sigma_I - \sigma_{III})^2 + (\sigma_{II} - \sigma_{III})^2}{2}} \leq \frac{\sigma_y}{\eta}$$



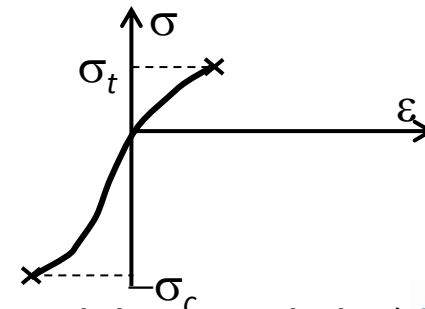
Brittle

(sintered, ceramics, metals with $\sigma_I \approx \sigma_{II} \approx \sigma_{III} > 0!$)



Rankine:

$$\max\{\sigma_I, \sigma_{II}, \sigma_{III}\} \leq \frac{\sigma_t}{\eta} \quad \& \quad \min\{\sigma_I, \sigma_{II}, \sigma_{III}\} \geq -\frac{\sigma_c}{\eta}$$



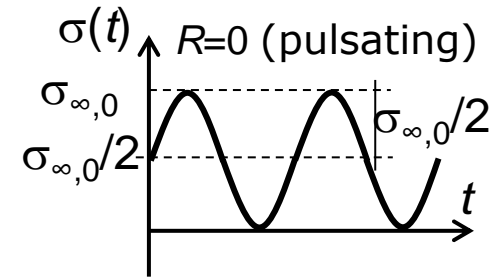
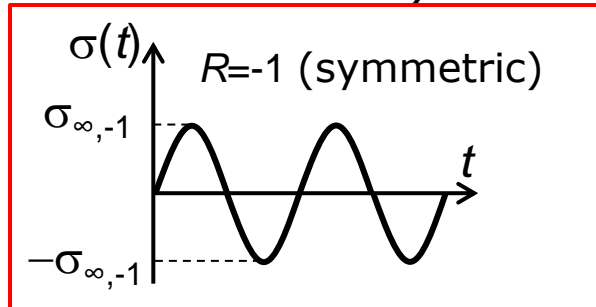
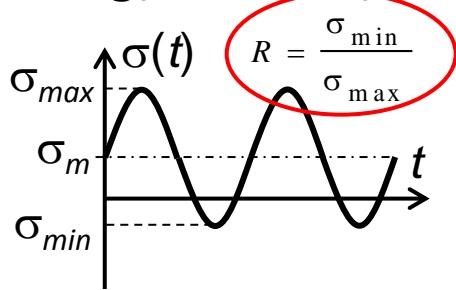
η = safety factor (depends on model and material uncertainties)

- For ductile behaviour, $\sigma_{VM} = \sigma_y$ is just a conventional limit

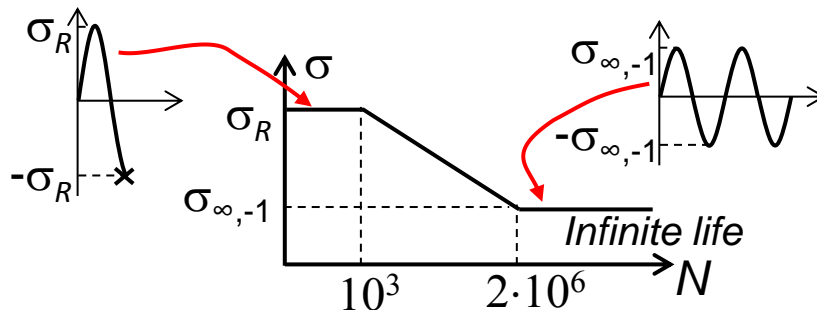
Analysis 5. Mechanical Stress Analysis

Fatigue

- Fatigue life is affected by many aspects [3]-[5] (material, surface finishing, notches, min/max stress ratio R)



- Test data refer to $R=-1$: Woehler Curve, 50% survival probability



For centrifugal forces in on-off cycles, $R=0$!

$$\sigma_{\infty,0} = \frac{2\sigma_{\infty,-1}\sigma_R}{\sigma_R - \sigma_{\infty,-1}}$$

- Classic approach based on nominal stress σ_n & concentration factor

$$K_f \sigma_n \leq \frac{\sigma_{\infty,R}}{\eta K_1 K_2 K_3}$$

K_1 surface finishing grade

K_2 dimension (thickness)

K_3 loading (stretching, bending)

K_f stress concentration (notch geometry and material)

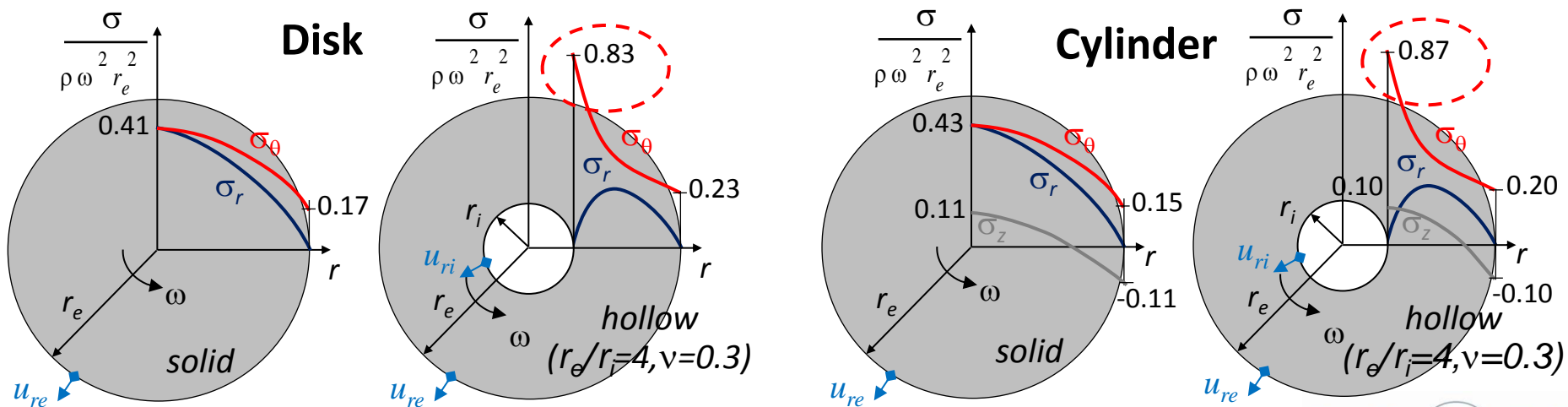
- Criteria for planar or 3D stress combinations (e.g. Sines) or based on Fracture Mechanics (Stress Intensity Factor) [5]

Analytic Models

- Features and motivation
 - Easy to integrate with magnetic lumped-parameter models
 - Useful for initial design and optimisation
 - Cross-check FE results (!!)
- Available options
 - Exact solutions for the Equations of the Theory of Elasticity are available only for simple geometries - mainly 2D and axisymmetric (IM solid rotors, SPM rotors)
 - Beam and plate theories provide additional tools [2] to set up approximate models (e.g. for iron bridges in IPM rotors)
 - Complex load configurations are treated with superposition
 - Stress concentration charts (e.g. Peterson's) are available for notches (Fatigue)

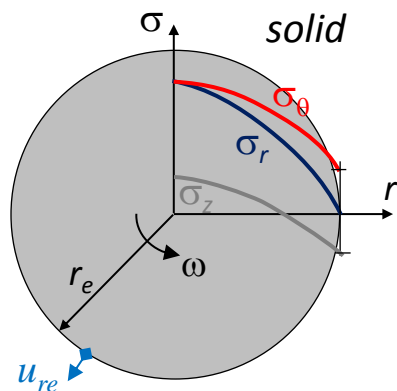
Rotating disc vs cylinder: overview

- The classic solution with $\varepsilon_z=0$ and $L=\infty$ needs a correction constant σ_{z0} to produce zero axial resultant force N at the ends
- The adjusted solution for the cylinder predicts identical displacements to plane-stress solution ($\sigma_z=0$) for discs
- Stress distributions are slightly different: the cylinder has lower σ_{VM} but higher individual principal stress values (important for brittle PMs)

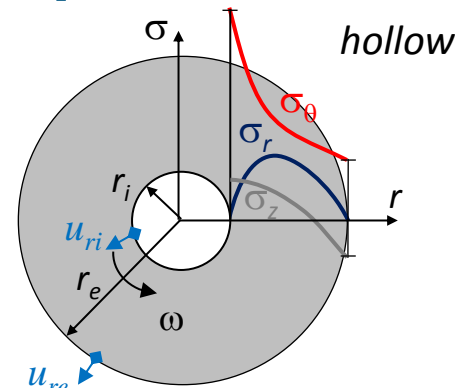


5. Mechanical Stress Analysis

Rotating disc vs cylinder: Stresses and displacements



$$a = \frac{r_e}{r_i}$$



$$\sigma_r = \frac{1}{8} \frac{3-2\nu}{1-\nu} \rho \omega^2 r_e^2 \left(1 - \left(\frac{r}{r_e} \right)^2 \right)$$

$$\sigma_\theta = \frac{1}{8} \frac{3-2\nu}{1-\nu} \rho \omega^2 r_e^2 \left(1 - \frac{1-2\nu}{3-2\nu} \left(\frac{r}{r_e} \right)^2 \right)$$

$$\sigma_z = \frac{1}{4} \frac{\nu}{1-\nu} \rho \omega^2 r_e^2 \left(1 - 2 \left(\frac{r}{r_e} \right)^2 \right)$$

Cylinder
($L < \infty$ & $N=0$)

$$\sigma_r = \frac{1}{8} \frac{3-2\nu}{1-\nu} \rho \omega^2 r_e^2 \left(1 + \frac{1}{a^2} - \left(\frac{r_i}{r} \right)^2 - \left(\frac{r}{r_e} \right)^2 \right)$$

$$\sigma_\theta = \frac{1}{8} \frac{3-2\nu}{1-\nu} \rho \omega^2 r_e^2 \left(1 + \frac{1}{a^2} + \left(\frac{r_i}{r} \right)^2 - \frac{1-2\nu}{3-2\nu} \left(\frac{r}{r_e} \right)^2 \right)$$

$$\sigma_z = \frac{1}{4} \frac{\nu}{1-\nu} \rho \omega^2 r_e^2 \left(1 + \frac{1}{a^2} - 2 \left(\frac{r}{r_e} \right)^2 \right)$$

$$u_{ri} = \frac{(1+\nu)(3-2\nu)}{4E} \left(a^2 - \frac{1-2\nu}{3-2\nu} \right) \rho \omega^2 r_i^3$$

$$u_{re} = \frac{(1+\nu)(3-2\nu)}{4E} \left(\frac{1-2\nu}{3-2\nu} + \frac{1}{a^2} \right) \rho \omega^2 r_e^3$$

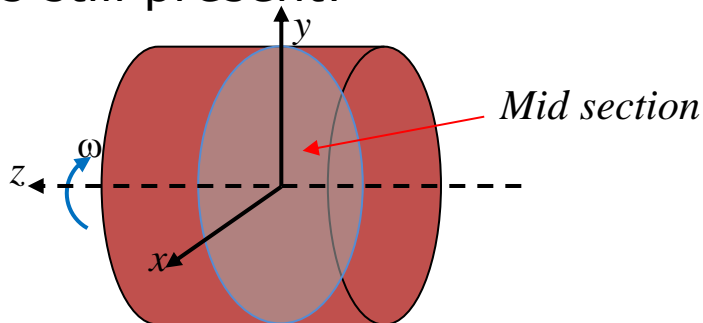
$$u_{re} = \frac{1}{4E} \frac{1+\nu}{1-2\nu} \rho \omega^2 r_e^3$$

Disc & Cylinder

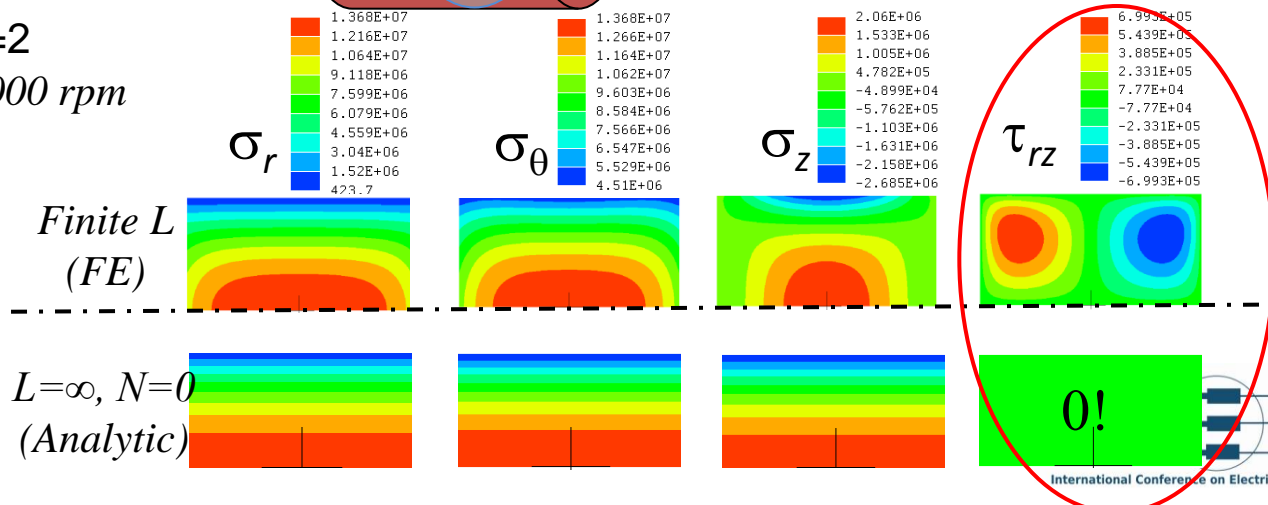
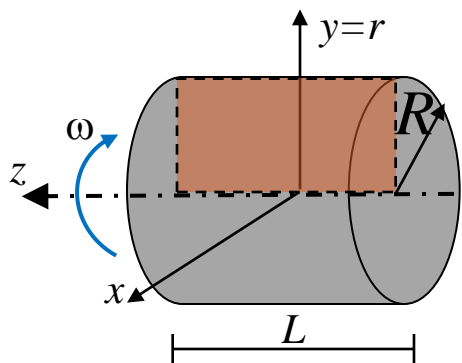
5. Mechanical Stress Analysis

Rotating cylinder: end effects

- The solution with $\varepsilon_z = \text{const}$ and $N=0$ is only valid in the mid section and for L/R aspect ratio not too small.
- End effects result in a τ_{rz} distribution that dies away far from the ends
- In "short" cylinders $L/R < 2$, the solution for σ_r and σ_θ approaches the one for discs, but $\sigma_z \neq 0$ is still present!



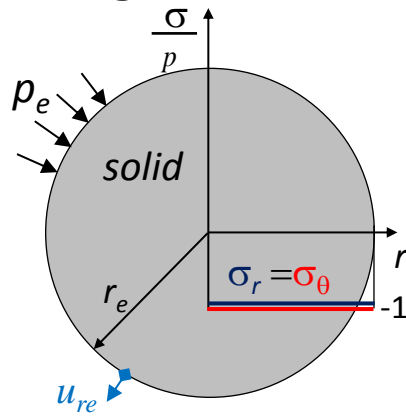
Example with $L/R=2$
(steel, $R=50$ mm, $n=12,000$ rpm)



Analysis 5. Mechanical Stress Analysis

Disc / cylinder with pressure load

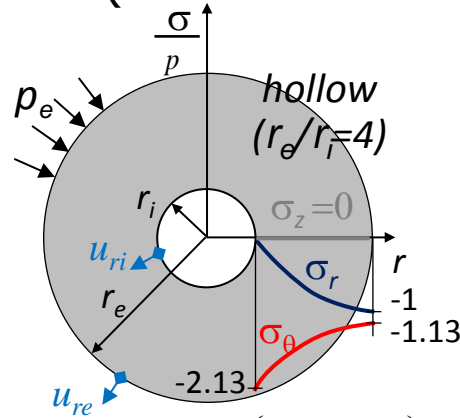
- Pressure is generated by shrink-fit or pre-stressed bandage
- Solution for discs predicts $\varepsilon_z = \text{const.}$ so it applies to cylinders of finite length too and is exact (no end effects)!



$$\sigma_r = -p_e$$

$$\sigma_\theta = -p_e$$

$$u_{re} = -p \frac{1-\nu}{E} r_e = -k_{ri} p_e$$

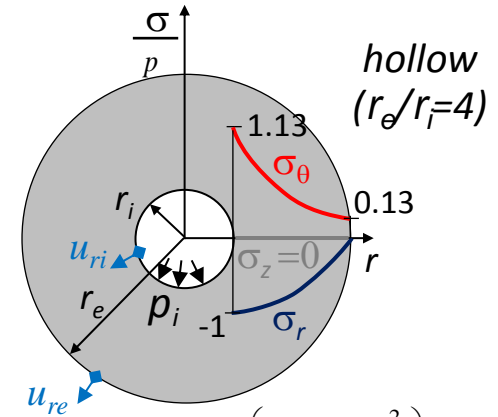


$$\sigma_r = p_e \frac{a^2}{a^2 - 1} \left(\left(\frac{r_i}{r} \right)^2 - 1 \right)$$

$$\sigma_\theta = -p_e \frac{a^2}{a^2 - 1} \left(1 + \left(\frac{r_i}{r} \right)^2 \right)$$

$$u_{ri} = -2p \frac{1-\nu}{E} \frac{a^2}{a^2 - 1} r_i = -k_{ri,e} p_e$$

$$u_{re} = -p \frac{1+\nu}{E} \frac{a^2}{a^2 - 1} \left(\frac{1}{a^2} + 1 - 2\nu \right) r_e = -k_{re,e} p_e$$



$$\sigma_r = \frac{p_i}{a^2 - 1} \left(1 - \left(\frac{r_e}{r} \right)^2 \right)$$

$$\sigma_\theta = \frac{p_i}{a^2 - 1} \left(1 + \left(\frac{r_e}{r} \right)^2 \right)$$

$$u_{ri} = p \frac{1+\nu}{E} \frac{a^2 + 1 - 2\nu}{a^2 - 1} r_i = k_{ri,i} p_i$$

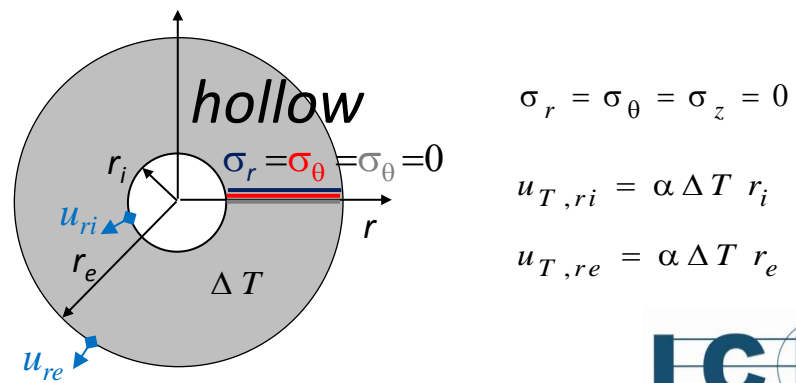
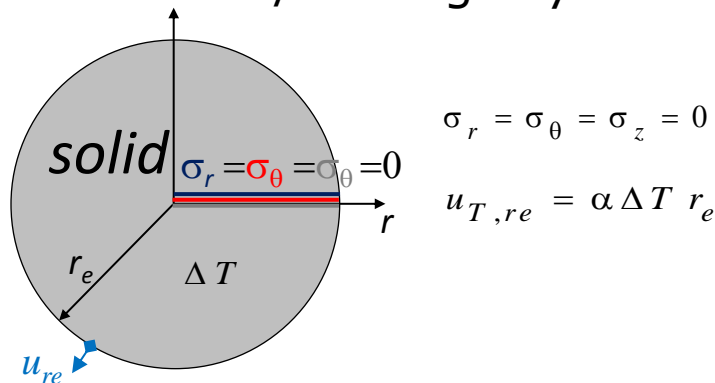
$$u_{re} = 2p \frac{1-\nu}{E} \frac{1}{a^2 - 1} r_e = k_{re,i} p_i$$

The multi-layer model requires **stiffness coefficients** k_{ri} , $k_{ri,i}$, $k_{re,i}$, $k_{ri,e}$ and $k_{re,e}$

5. Mechanical Stress Analysis

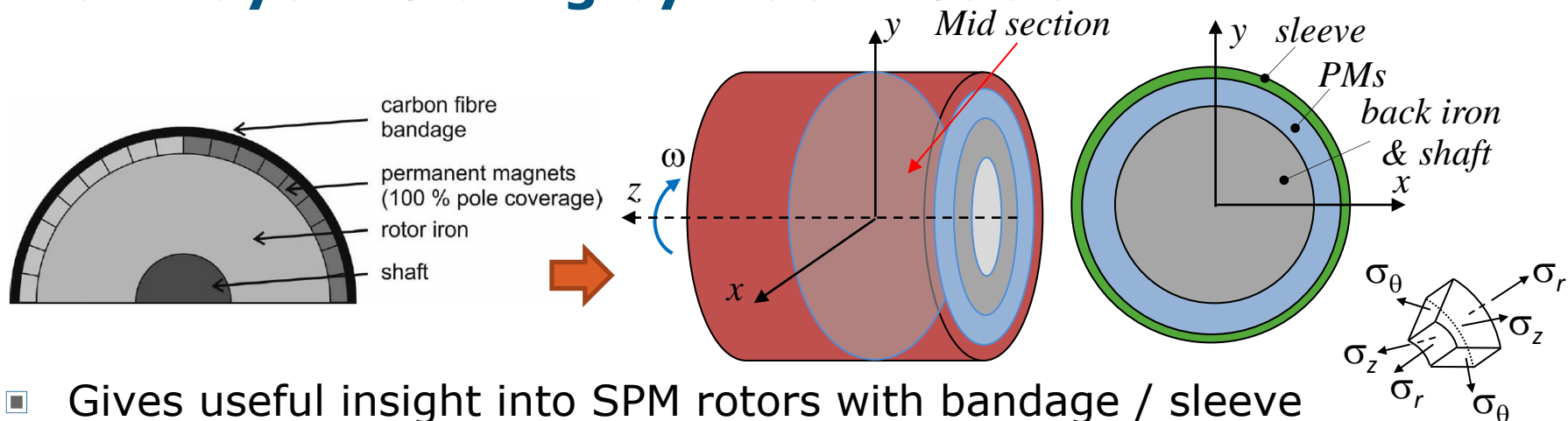
Disc / cylinder with thermal effects

- Thermal expansion is important in multi-layer models to assess the performance of a shrink-fitted sleeves
- Thermal gradients lead to additional (thermal) stresses that need to be considered
- The rotor temperature distribution may be axisymmetric but depends on z (heat transfer towards the shaft ends): 2D models set in the mid plane do not capture this aspect
- Uniform temperature rise ΔT leads to expansion only (no additional stress): this ideal scenario could be considered in the first design of the sleeve/bandage system



5. Mechanical Stress Analysis

Multi-layer Rotating Cylinder Models



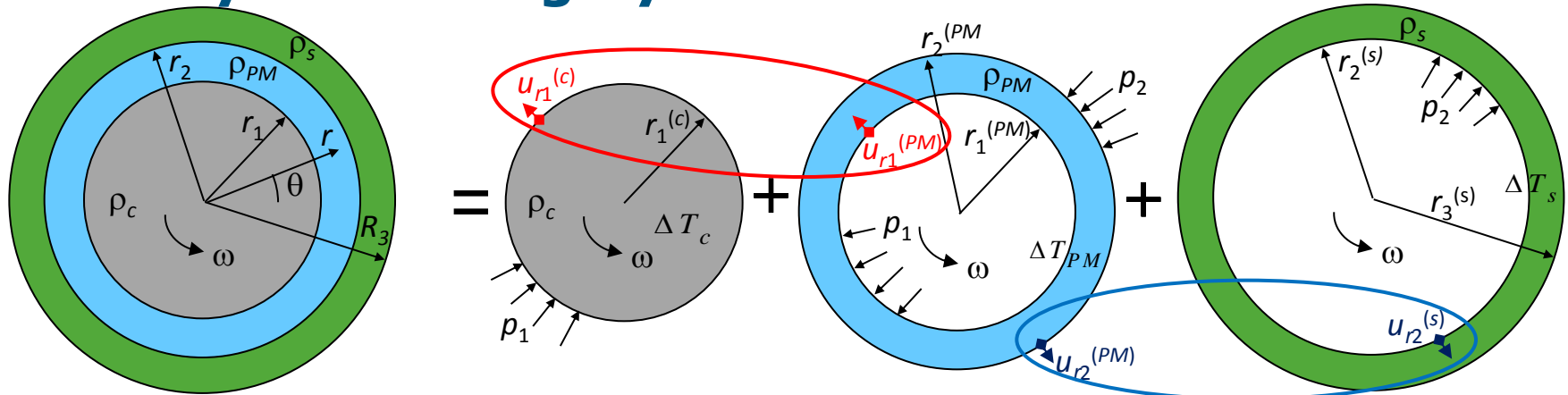
- Gives useful insight into SPM rotors with bandage / sleeve

.....**but**

- Segmented PMs can be replaced by an homogeneous layer only if the hoop stress σ_z is negative (compression, i.e. sufficient pre-stress in the bandage)
- Plane strain ($\varepsilon_z = \text{const.}$) \Rightarrow results valid on the mid section $z=0$
- Do not capture tangential stress τ_{rz} in the PM ends (potentially responsible for PM cracks)
- Do not capture stress concentration in the sleeve near pole gaps, if present

5. Mechanical Stress Analysis

Multi-layer Rotating Cylinder Models



- The model may adopt a constant piece-wise temperature profile $\{\Delta T_c, \Delta T_{PM}, \Delta T_s\}$ according to eddy current losses in each layer

- Displacement compatibility: $r_1^{(c)} + u_{r1}^{(c)} = r_1^{(PM)} + u_{r1}^{(PM)}$ and $r_2^{(PM)} + u_{r2}^{(PM)} = r_2^{(s)} + u_{r2}^{(s)}$

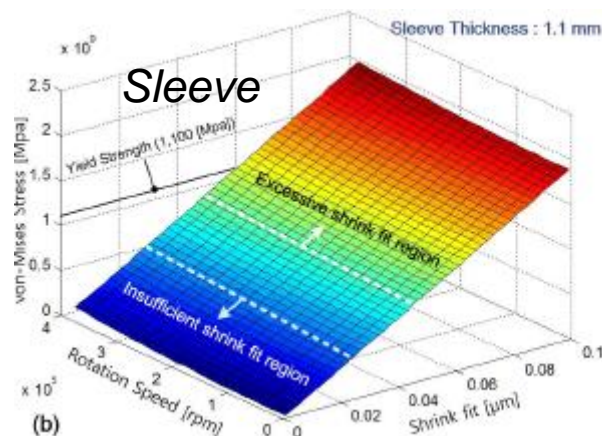
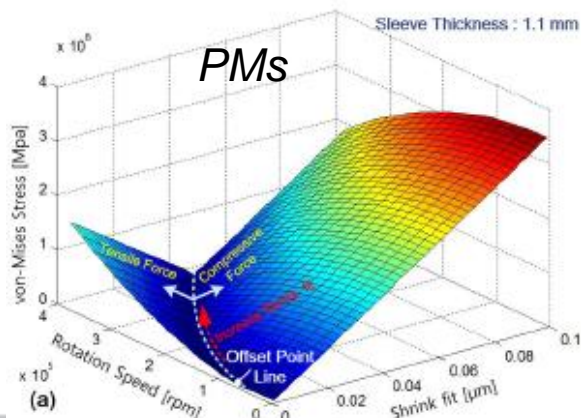
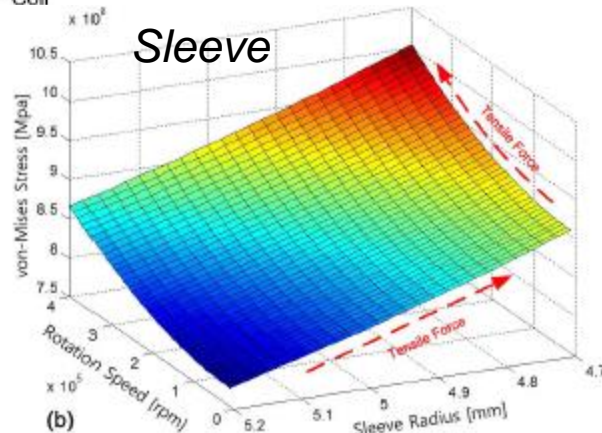
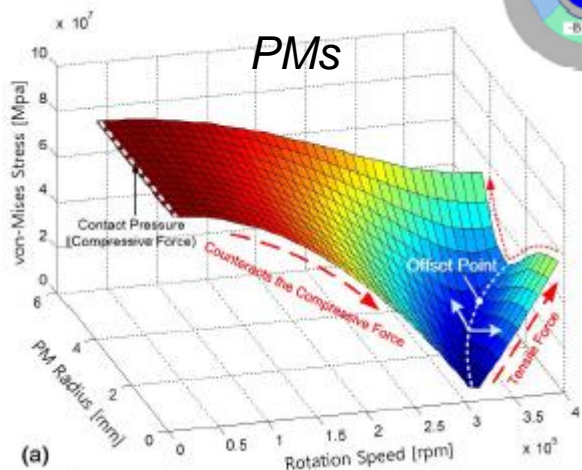
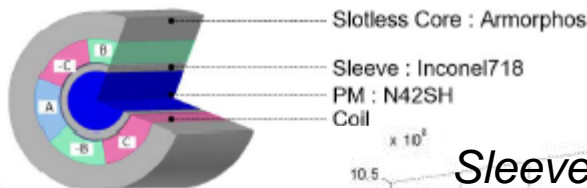
$$\begin{cases} r_1^{(c)} - k_{re}^{(c)} p_1 + u_{\omega, re}^{(c)} + u_{T, re}^{(c)} = r_1^{(PM)} + k_{ri, i}^{(PM)} p_1 - k_{ri, e}^{(PM)} p_2 + u_{\omega, ri}^{(PM)} + u_{T, ri}^{(PM)} \\ r_2^{(PM)} + k_{re, i}^{(PM)} p_1 - k_{re, e}^{(PM)} p_2 + u_{\omega, re}^{(PM)} + u_{T, re}^{(PM)} = r_2^{(s)} + k_{ri, i}^{(s)} p_2 + u_{\omega, ri}^{(s)} + u_{T, ri}^{(s)} \end{cases} \Rightarrow \begin{cases} p_1 = \dots\dots \\ p_2 = \dots\dots \end{cases}$$

- Once p_1 and p_2 are found, stress distributions in each layer are found by super-position of stress contributions from ω , p_1 and p_2
- Check different conditions (ω , ΔT_k) for the (worst-case scenario)
- **If $p_1 < 0$ or $p_2 < 0$ or $\sigma_\theta > 0$ (for segmented magnets) the solution is not valid!**

5. Mechanical Stress Analysis

Multi-layer Rotating Cylinder Models: Some Examples

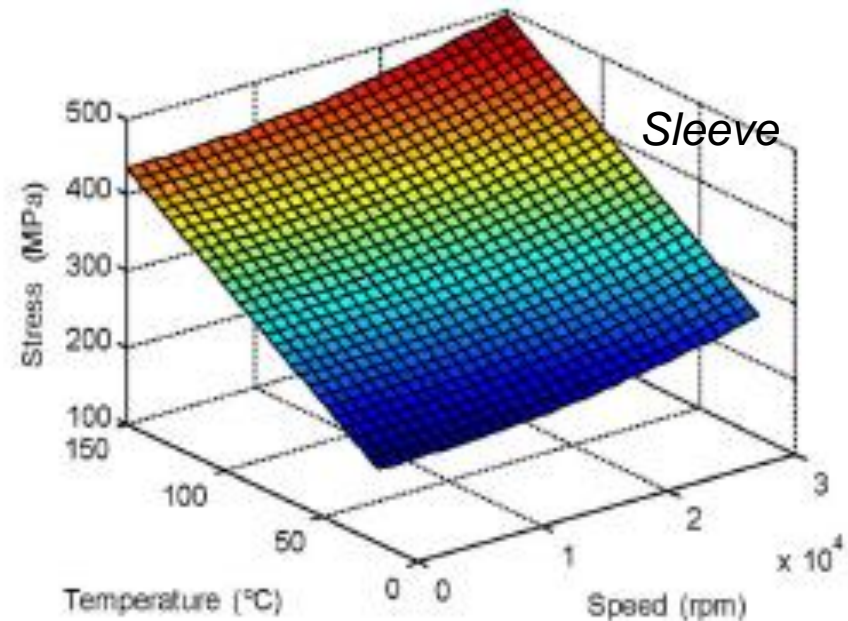
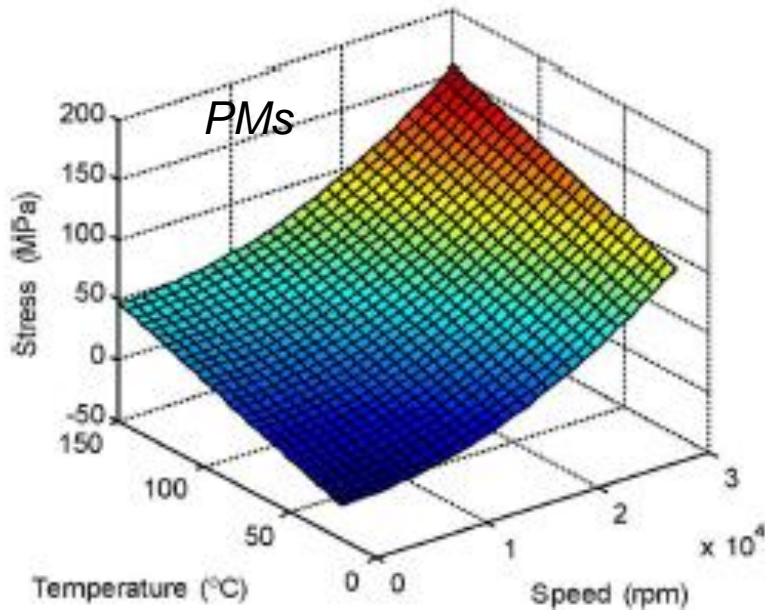
Stress sensitivity analysis in 500W, 400krpm SPM machine with $D_{PM}=9.4\text{mm}$, $D_{sleeve}=11.6\text{mm}$: impact of speed, fit interference, PM radius (from [6])



5. Mechanical Stress Analysis

Multi-layer Rotating Cylinder Models: Some Examples

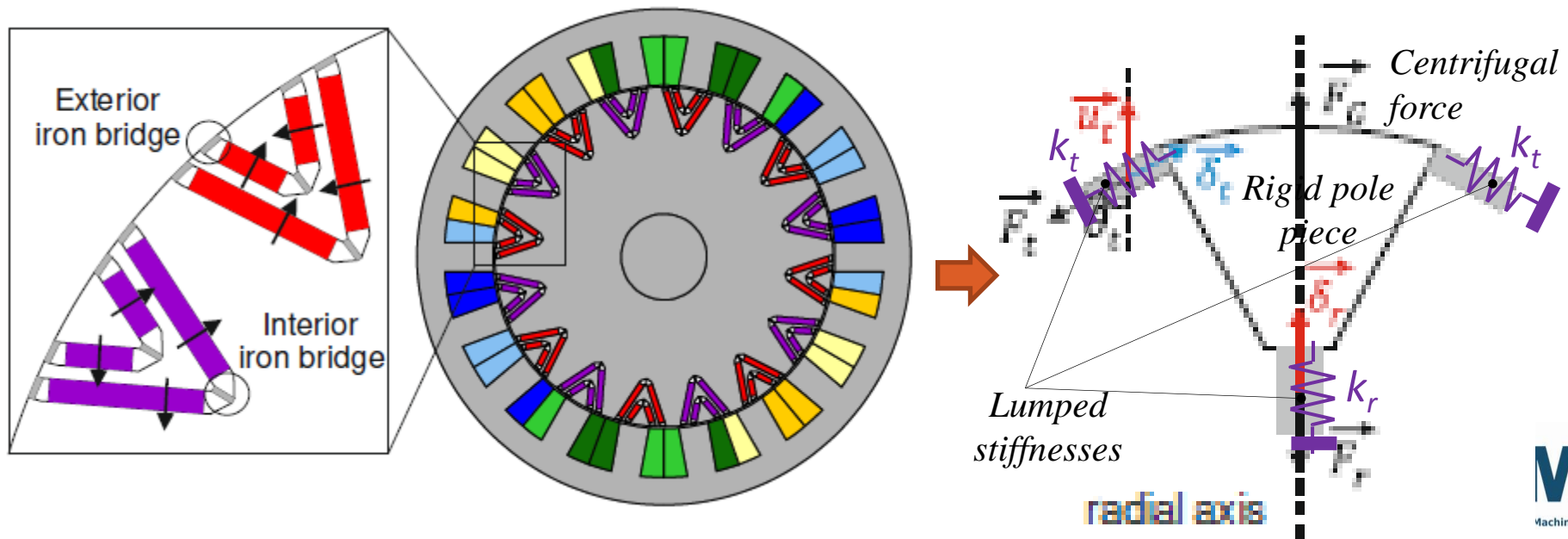
Stress sensitivity analysis in a 1.12MW, 18krpm SPM machine with $D_{PM} \approx 176$ mm, $D_{sleeve} \approx 190$ mm: impact of speed and temperature (from [7])



5. Mechanical Stress Analysis

Lumped-stiffness models (IPM rotors)

- Usually, iron bridges in different layers work in series (PMs are only in contact with the magnet slot "roof")
- The analytic model in [8] assumes rigid-body islands (pole shoes) connected with 1D stiffness elements (bridges)
- May be enhanced by considering additional bending stiffness of lateral bridges (...likely to require 2nd-order beam theory due to the interaction bending - axial resultant)



Lumped-stiffness models (IPM rotors)

- Rigid radial displacement of the pole imposes the compatibility of radial and tangential displacements in the thin bridges

$$u_t = u_r \cos \theta$$

- Stiffness coefficients

$$k_r = \frac{Et_r}{h_r}, \quad k_t = \frac{Et_t}{h_t}$$

- Radial equilibrium

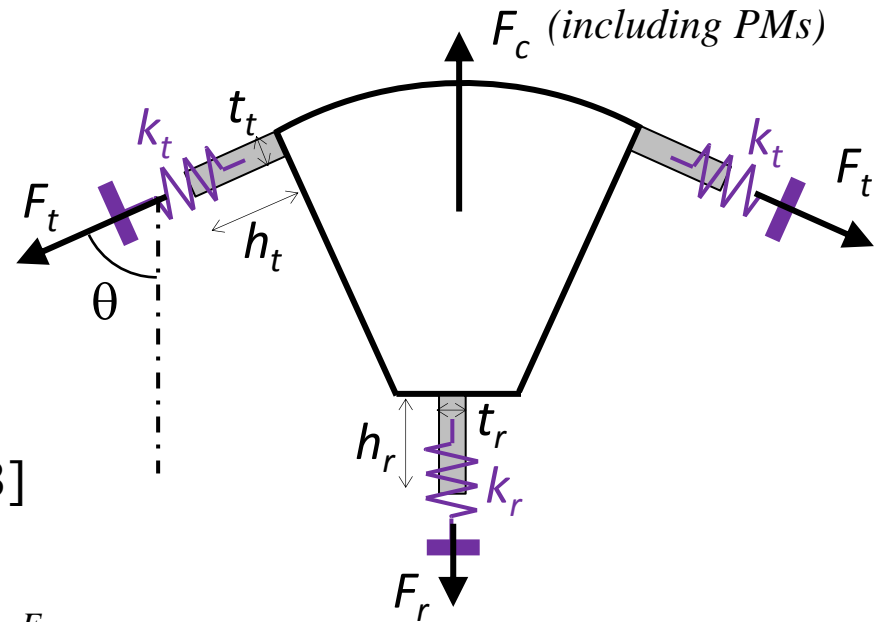
$$F_c = F_r + 2F_t \cos \theta \quad \begin{cases} F_r = k_r u_r \\ F_t = k_t u_t \end{cases}$$

- Solution for forces and stresses [8]

$$\begin{cases} F_r = \frac{F_c}{1 + 2 \frac{k_t \cos^2 \theta}{k_r}} \\ F_t = \frac{F_c \cos \theta}{\frac{k_r}{k_t} + 2 \cos^2 \theta} \end{cases}$$

$$\begin{cases} \sigma_{rn} = \frac{F_r}{t_r} \\ \sigma_{tn} = \frac{F_t}{t_t} \end{cases}$$

$$\begin{cases} \sigma_r = K_{tr} \sigma_{rn} \\ \sigma_t = K_{tt} \sigma_{tn} \end{cases}$$

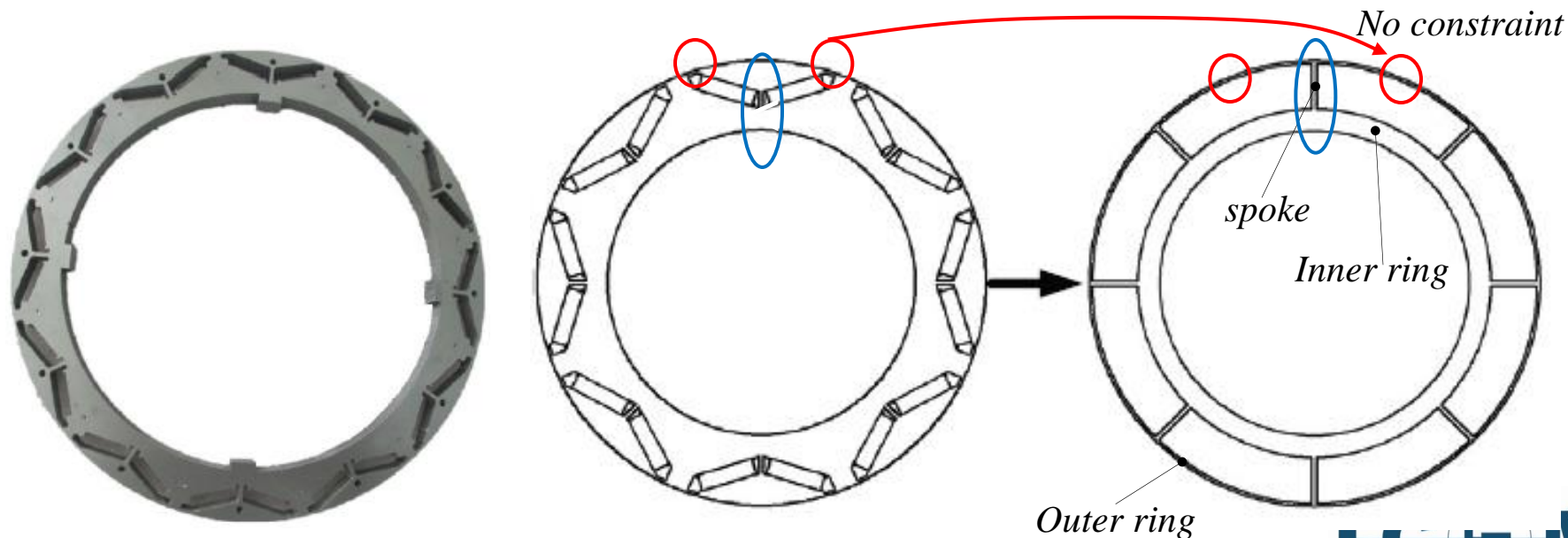


- Stress concentration factors K_{tr} & K_{tt} depend on the notch geometry

5. Mechanical Stress Analysis

Lumped-stiffness models (IPM rotors)

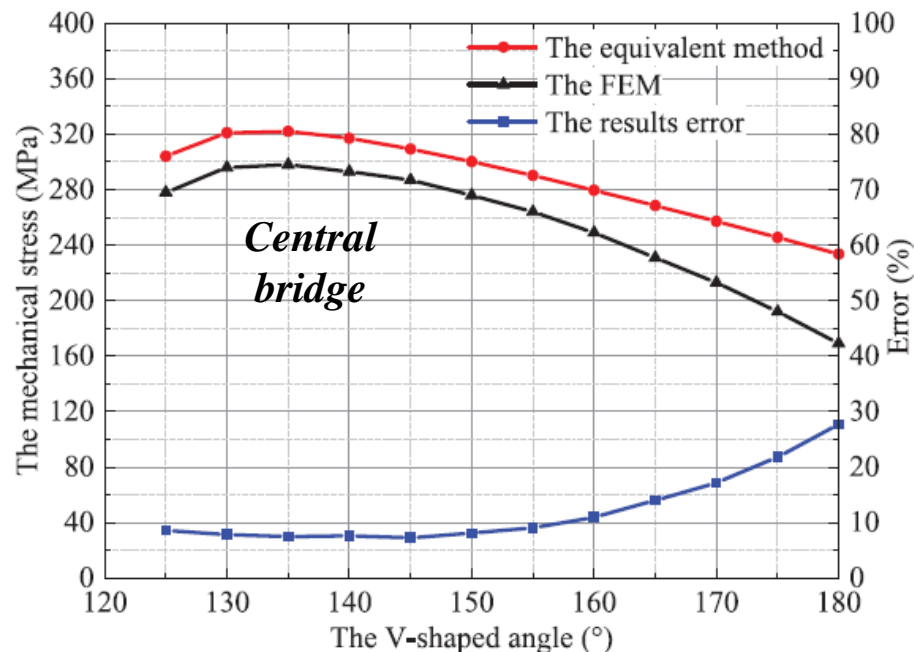
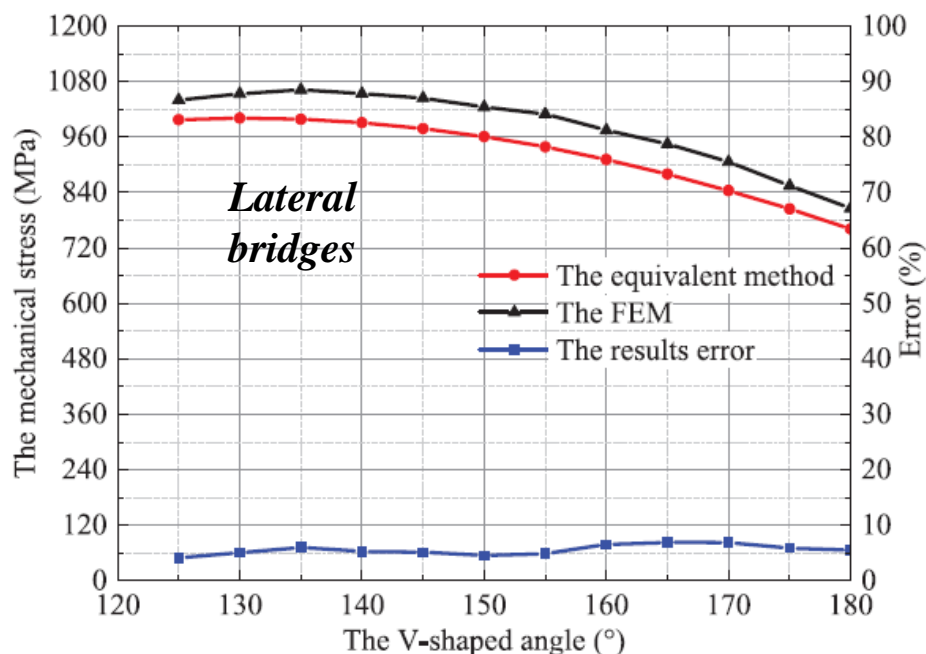
- V-shape pole shoes can be treated as part of an elastic outer ring suspended with elastic spokes to an inner ring [9]
- The shear and bending stiffness of the lateral bridges is ignored
- The set of resultant normal forces transmitted by spokes are then converted into equivalent uniform pressure on the rings
- Spokes and rings are then assumed to carry normal forces only



5. Mechanical Stress Analysis

Lumped-stiffness models (IPM rotors)

- The resulting analytic equations are convoluted (see [9])
- The model exhibits good accuracy for moderate PM angle and for the stress in the lateral bridges
- The stress in the central bridge is underestimated (the model ignores the variable moment of inertia of the pole shoe!)



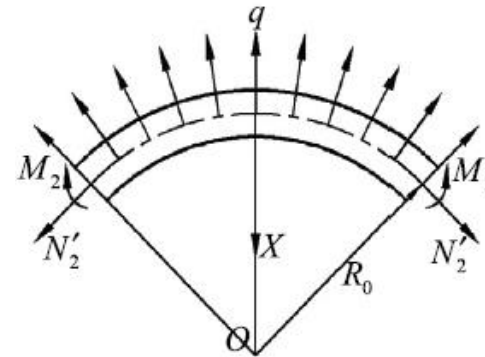
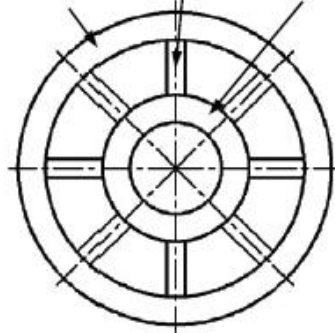
Analysis results for 2007 Toyota Camry motor (with central bridge) [5]

5. Mechanical Stress Analysis

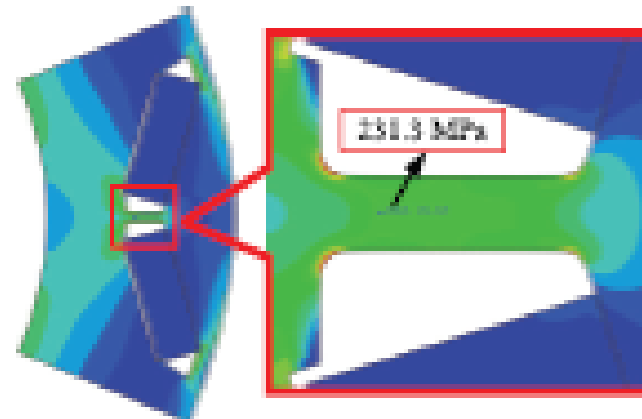
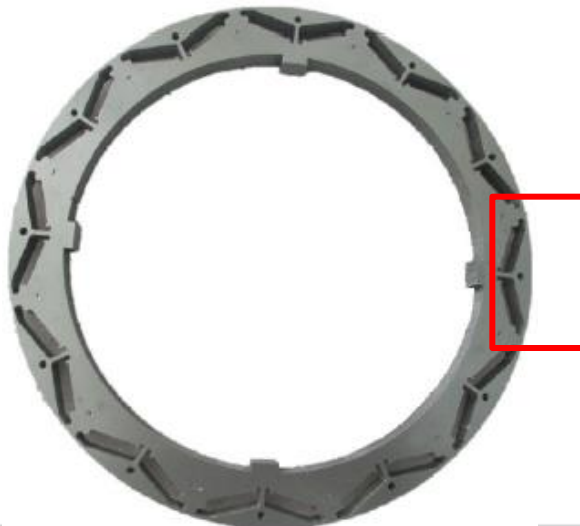
Lumped-stiffness models (IPM rotors)

- The model may be improved to include parasitic bending moments in the inner/outer rings caused by the spokes

Outer ring Spokes Inner ring



- Stress concentration around notches and fillets can be evaluated using stress concentration factors from tables [4]



5. Mechanical Stress Analysis

Conclusions

- Linear-elasticity, small-displacements formulation is the standard setup for stress analysis of EM rotors
- Interaction between PMs and rotor stack can be represented by
 - Setting non-penetration contact constraints (non-linear analysis)
 - Using equivalent pressure distributions (linear analysis): correction needed for thin iron bridges
- 2D model features
 - Results are valid only far away from the rotor ends
 - In case of 2π -periodicity (e.g. UMP), boundary conditions are not easy to set
- Verification of mechanical integrity needs appropriate stress metrics depending on
 - Material behaviour (ductile / brittle)
 - Type of loading (static / fatigue)
- Analytic models are available for SPM and IPM, with some limitations
 - Difficult to take into account pole gaps in SPM
 - In IPM rotor bridges, they only predict the average stress level
- *Cross-check FE results with an (even crude) analytic model!*

References

- [1] A Shabana, Computational continuum mechanics, 2rd Ed. Cambridge University Press, 2012.
- [2] W. C. Young, R. G. Budynas, Roark's formulas for stress and strain, McGraw-Hill, 7th Edition, 2002
- [3] M. Barcaro, G. Meneghetti and N. Bianchi, "Structural Analysis of the Interior PM Rotor Considering Both Static and Fatigue Loading," in *IEEE Transactions on Industry Applications*, vol. 50, no. 1, pp. 253-260, Jan.-Feb. 2014.
- [4] W. D. Pilker, Ed., Peterson's Stress Concentration Factors, Handbook. New York, NY, USA: *Wiley*, 1997.
- [5] N. D Dowling, Mechanical behaviour of materials, 3rd Ed. Englewood Cliffs, NJ, USA: Prentice-Hall, 2007.
- [2] J. Ahn, J. Choi, C. H. Park, C. Han, C. Kim and T. Yoon, "Correlation Between Rotor Vibration and Mechanical Stress in Ultra-High-Speed Permanent Magnet Synchronous Motors," *IEEE Trans. Mag.*, vol. 53, no. 11, pp. 1-6, Nov. 2017.
- [3] F. Zhang, G. Du, T. Wang, G. Liu and W. Cao, "Rotor Retaining Sleeve Design for a 1.12-MW High-Speed PM Machine," *IEEE Trans. Ind. Appl.*, vol. 51, no. 5, pp. 3675-3685, Sept.-Oct. 2015.
- [4] P. Akiki *et al.*, "Multi-Physics Design of a V-shape IPM Motor," *IEEE Trans. En. Conv.* doi: 10.1109/TEC.2018.2803072
- [5] F. Chai, Y. Li, P. Liang and Y. Pei, "Calculation of the Maximum Mechanical Stress on the Rotor of Interior Permanent-Magnet Synchronous Motors," in *IEEE Transactions on Industrial Electronics*, vol. 63, no. 6, pp. 3420-3432, June 2016.

Thank you for your Attention!

Dr Sara Roggia

Senior Design Engineer

Motor Design Limited

Sara.Roggia@motor-design.com



Motor Design Software by Motor Design Engineers

Dr Matteo Iacchetti

Senior Lecturer

The University of Manchester

matteo.iacchetti@manchester.ac.uk



The University of Manchester